Behaviour of Piles and Pile Groups in Marine Clay under Compressive Load at Various Stress Conditions

A Thesis Submitted
in Partial Fulfillment of the Requirements
for the Degree of
Master of Technology

by

Bappaditya Manna

to the

Department of Civil Engineering,
Indian Institute of Technology Kanpur

June, 2005

Dedicated

To

My little Pucha

CERTIFICATE

This is to certify that the work contained in the thesis entitled "Behaviour of Piles and Pile Groups in Marine Clay under Compressive Load at Various Stress Conditions", by Bappaditya Manna (Y3103014), has been carried out under my supervision and this work has not been submitted elsewhere for a degree.

June, 2005

Nihar Ranjan Patra 03/06/05

(Dr. N. R. Patra)

Lecturer,

Department of Civil Engineering

Indian Institute of Technology

Kanpur – 208 016.

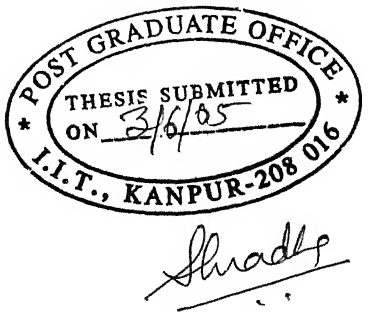

Abstract

Experimental investigations on model single piles, line pile groups (2 x 1) and square pile groups (2 x 2) subjected to axial compressive load were conducted in a specially designed triaxial cell with enlarged dimensions in marine clay at vertical and horizontal stress conditions. The variables used in this experiments were embedment length to diameter ratio (L/D= 8.93, L/D =17.5), spacing of piles in a group (4D, 5D, 6D), controlled horizontal(σ_H), vertical (σ_V) stresses (0.3 kg/ cm^2 and 0.6 kg/cm^2) and pile group geometry / configuration. Parametric study on the influence of the variables involved has been carried out on the load displacement response, tip, shaft, and total resistance and group efficiency of the pile groups.

The bearing capacity factor (N_c) value increases with increasing L/D ratio from about 9 upto a maximum of about 11. The adhesion factor (β) increases with increase in horizontal stress level and its value varies from 0.5 to 1.0. The total resistance of 2x1 pile group increases with increases in spacing from 4D to 5D and decreases from 5D to 6D for both L/D ratios and stress conditions. The spacing 5D was the critical value of spacing up to which pile and soil inside the piles acts as a one unit. For 2x2 piles group the total resistance increases with increase in pile spacing for both L/D ratios and stress conditions.

Discrete Element Method was used to simulate the experimental investigation on single pile and to get the load displacement behavior of single pile of L/D = 8.93 in both sand and clay at various stress conditions. Force generated at the side and bottom wall of pile at the time of installation were studied. The total resistance of pile in controlled horizontal stress condition (σ_H test) was more than controlled vertical stress condition (σ_V test) in both sand and clay which almost satisfied the experimental results.

A statistical Regression model, based on experimental results, is used to study the variation of efficiency of pile groups with spacing under different vertical and horizontal stress conditions. New interaction factors are proposed with varying s/D, L/D ratios and stress conditions to predict the settlement of pile groups.

Key Words: Pile Groups, Marine Clay, Axial Compressive Load, Load-Displacement Behaviour, Tip Resistance, Shaft Resistance, Total Resistance, Pile Group Efficiency Experimental Investigations, Model piles, Discrete Element Method, Regression Analysis, Interaction Factor.

ACKNOWLEDGEMENT

During the journey towards the completion of this thesis work, many people have contributed directly or indirectly. I take this opportunity to thank all of them.

I feel highly indebted to my thesis supervisors Dr. N.R.Patra who inspired and encouraged me through their invaluable guidance, constructive suggestions, critical comments and detailed instructions at every stage of my research program. The striking factor has been the freedom to work independently. He has been extremely patient and understanding. It is his whole hearted support and co-operation which has inspired me in accomplishing this undertaking.

I would like to express my deep sense of gratitude and thanks to Dr. P.K.Basudhar and Dr. S.Chandra for the overall guidance and for enriching my understanding of geotechnical engineering and also for the kind co-operation that I received throughout my degree program.

The assistance rendered by A.K.Srivastav, Gulab Chand, Parasuramji and Yadavji of the Geotechnical Engineering Laboratory are greatly appreciated and special thanks to Vivek. Also I am thankful to everyone in Central Workshop specially Mr. Srivastav and Mr. Majumder.

I am thankful to all of my friends and classmates from whom I have learnt many things and who have made my stay here pleasant and memorable.

Finally I would like to express my gratitude to my parents and family members for their encouragement to do postgraduate studies and their support at all the times.

Bappaditya Manna

June, 2005 **Bappaditya Manna**

Contents

List of Figures

List of Plates

List of Tables

List of Symbols

Following symbols are used throughout this thesis unless otherwise specified.

L	Length of the model pile
D	Diameter of the model pile
s	Spacing of pile group
s/D	Pile spacing in terms of diameter
L/D	Length to diameter ratio of pile
E_s	Modulus of elasticity of soil medium
E_P	Modulus of elasticity of pile material
γ_s	Poisson's ratio of soil
η	Efficiency of pile group
P_{ul}	Ultimate load carrying capacity in compression of the single pile
P_2	Axial compressive load carried by each pile of two pile group
PU_2	Ultimate compressive load carried by each pile of two pile group
R_A	Ratio of area of pile section A_p to area bounded by outer circumference of pile
K	Relative stiffness of pile
H	Depth of bearing stratum
ρ	Settlement of pile
α	Interaction Factor
α (s)	Interaction factor for piles at distance s
$\alpha(\sqrt{2}s)$	Interaction factor for piles at distance $\sqrt{2}s$
β	Adhesion factor

N_c	Bearing capacity factor
q_P	Tip resistance of pile
f_s	Shaft resistance of pile
σ	Cell pressure
σ_V	Stress in vertical direction
σ_H	Stress in horizontal direction
ϕ	Angle of internal friction
c_u	Cohesion of soil
m	Mass of particle
G_s	Specific gravity of soil
F_s	Spring force
K	Spring constant
C	Coefficient of damping
F_d	Damping force
x	displacement
F_x	Force in the x direction
F_y	Force in the y direction
r_i	Residual
S	Square of residual

Chapter I

Introduction

1.1.General

Pile foundations are generally used to transmit the superstructure loads to deeper strata when the subsurface soil is of inadequate strength. Extensive theoretical and experimental investigations have been carried out over the last few decades to study the behaviour of piles and pile groups subjected to compressive loads.

Due to natural hazards such as earthquake and lateral spreading and due to additional surcharge on the ground surface, stresses in the horizontal and vertical direction on the soil mass are generated. The type of foundations to be adopted for the structures constructed in the above ground conditions vary according to the suitability of the site conditions. When poor soil at shallow depth or problem of caving or water table arises, the geotechnical engineers are compelled to adopt deep foundation in the form of piles in a group.

The design of pile groups under compressive loads is, in general, based on requirements that complete collapse of pile group or the supporting structures should not occur even under the most adverse conditions and that the deflection at working loads should not be so excessive so as to impair proper functioning of the foundation or the super structure. Thus, for structures, in which deflection may not be critical, the design is governed by the ultimate resistance of the pile and pile group with a suitable factor of safety.

Generally shaft, tip and total resistance of piles and pile groups in clay depends on embedment length to diameter ratio, spacing of piles in a group, horizontal, vertical stresses and pile group geometry / configuration. Studies on pile groups under compressive load at various stress conditions are limited. No significant and systematic information on the influence of such variables on shaft, tip and total resistance of pile groups is reported in the literature. There are few experimental investigations available to predict the shaft, tip and total resistance of single pile. A good number of analytical solutions along with a large number of field and laboratory investigations are available to predict the load-deflection response of axially loaded pile groups. However, no theory is available for estimating the settlement of pile groups and hence the total resistance of pile groups under vertical and horizontal stress conditions.

Need for Experimental Investigation

From the review it is seen that systematic investigations on the quantitative and qualitative influence of the parameters such as length-to-diameter ratio, configuration/geometry of the group of piles, spacing on the behavior of the piles and pile group at various stress conditions under axial compressive loads are scanty. A trail cell of enlarged dimensions could give accurate data by conducting model tests in controlled soil condition in the laboratory with varying stress conditions. The results thus obtained could also be utilized for checking the validity of the theories and enriching the profession with data where limited information is available.

Need for Analytical Study

Analytical approaches based on the experimental observations would be helpful for predicting the load displacement behaviour and hence the total resistance of piles and pile groups under axial compressive load at various stress conditions. These approaches should reflect the effect of installation of piles and the variables as mentioned earlier.

1.2. Scope of the study

In the present study the experiments were conducted in a triaxial cell with enlarged dimensions to study the effect of axial compressive load on single pile and pile group at different vertical and horizontal stress condition. The tests were conducted in two phases. In the first phase tests were conducted by subjecting the soil to controlled vertical stress (σ_V) test and in the second type of test, soil was subjected to controlled horizontal stress (σ_H) test. By conducting σ_V test, total resistance and tip resistance of piles were determined and tip resistance and shaft resistance were determined separately by σ_H test. Total capacity were determined in terms of tip and shaft resistance for model single piles and pile group (2x1 and 2x2) of three spacing (4D, 5D and 6D) under both stress condition.

Using Discrete Element Method the results of single pile from the experiments were studied and validated. However the characteristics of the curves, which were determined by DEM, was studied and compared with the experimental curves. Total resistance of pile was determined in terms of tip and shaft resistance were determined by DEM both sand and clay.

A statistical Regression model, based on experimental results, is used to study the variation of efficiency of pile groups with spacing under different vertical and horizontal stress conditions. New interaction factors are proposed with varying s/D, L/D ratios and stress conditions to predict the settlement of pile groups.

Chapter II

Literature Review

2.1. General

A literature review discusses published information in a particular subject area and sometimes information in a particular subject area within a certain time period. Detailed survey of prevailing literature on behaviour of single piles and group piles under compressive axial loads at various stress condition has been carried out as a part of present study. This literature review consists of the experimental model on single pile and group pile embedded in clay and some analytical model to predict the behaviour of single pile and group pile in different vertical and horizontal stress conditions. The literature referenced for the current study can be reviewed in the underwritten fashion;

2.2. Axial Load Capacity of Pile in Cohesive Soil

Literature on prediction and estimation of the load carrying capacity of a pile is very extensive. Considerable work has been done to predict the pile capacity based on the soil properties. Static formulae for predicting the ultimate resistance of a pile are based on the properties of the soil. The basic equation for the pile capacity in the static calculation is:

$$Q_u = Q_b + Q_s - W_p \qquad \text{..... (2.1)}$$

where

Q_u – ultimate total resistance

Q_b – ultimate base resistance

Q_s – ultimate shaft resistance

W_p – weight of the pile

As W_p is negligible compared to equation (2.1) is modified to

$$Q_u = Q_b + Q_s \qquad \text{..... (2.2)}$$

As the behaviour of the loaded piles in cohesive soils and cohesionless soils are different and most of the work has been done either on cohesive soils or on cohesionless soils; they used to discuss separately.

As my thesis work is based on cohesive soil only the formulation for ultimate resistance of pile in cohesive soil are discussed below.

The basic equation for the ultimate resistance of a pile in cohesive soil may be considered as:

$$Q_u = c_u N_c A_b + c_a CL \qquad \text{..... (2.3)}$$

where

N_c – bearing capacity factor

c_u – undrained cohesion at the level of the base

A_b – area of pile base

C – circumference of the pile shaft

L – length of the shaft

c_a – average adhesion between pile and soil

Meyerhof (1951) had shown theoretically that the value of N_c is approximately equal to 9 provided the pile was driven to a depth of atleast 5 times the pile diameter.

Tomlinson (1957) showed that the observed adhesion expressed as a percentage of the undisturbed cohesion of the clay falls with increasing stiffness of the clay from approximately 100 in very soft clays to 20 in very stiff clays. The loss of adhesion was not related to loss of strength by remoulding, but is believed to be

due to the presence of partial gap between the pile and the soil. The gap may be formed by transverse vibration during driving and by movement of the displaced soil upwards and away from the pile.

Zeevart et al (1960) proposed the use of effective stress approach to determine the side friction in clay, which can be expressed as:

$$f_s = K \tan\delta \, \sigma_v' \qquad \ldots\ldots\ldots\ldots\ldots\ldots (2.4)$$

where

f_s – unit skin friction

K – lateral earth pressure coefficient

δ – friction angle between shaft and soil

σ_v' – effective vertical stress at any depth

Whitaker and Cooke (1965) investigated on bearing capacity of large bored piles in London clay and showed that the maximum shaft resistance was reached at a displacement less than 1% of the shaft diameter, while the maximum base resistance was reached at a displacement of the order of 10% of the diameter of the shaft.

Williams and Coleman (1965) suggested a relation between the ultimate resistance and the lower limit of the undrained shear strength, c_{ud} at any depth L as:

$$Q_u = C \int_0^L \alpha \, c_{ud} \, dL + \pi \, R_b \, 9c_{ub} \qquad \ldots\ldots\ldots\ldots\ldots\ldots (2.5)$$

where

R_b – radius of pile base

c_{ud} – undrained shear strength at the pile base level

α - a factor with a value in the range 1.0 to 1.15

Whitaker and Cooke (1966) furnished an expression based on total stress analysis for ultimate resistance for bored piles, with or without enlarge base, in London clay as

$$Q_u + W_p = \pi d_s L \alpha C' + \pi R_b^2 (N_c \gamma_s C_b + \gamma_s D) \quad \text{..... (2.6)}$$

where

d_s – diameter of the shaft

C' and C_b – mean shear strength obtained by laboratory tests

γ_s – unit weight of soil

D – depth of the base from ground level

Coyle and Reese (1966) suggested an analytical procedure to compute load-settlement curves for axially loaded piles. It consists of analyzing the pile as a number of elements which are considered to be in a state of equilibrium and solving for the side friction and base resistance.

Mattes and Poulos (1971) analysed elastic response and presented curves to predict the pile movement, or the movement of pile groups. A series of model pile tests were conducted in Kaoline with piles of different stiffness.

Burland (1973) suggested the use of the following relation:

$$f_s = \beta . \sigma_v' \quad \text{..... (2.7)}$$

where the values of β range from 0.25 to 0.4 which were obtained from various pile load test data on clay and an average value of 0.32 for β was obtained.

Vijayvergiya and Focht (1972) included the undrained strength, s_u in the expression by λ method to form the relation:

$$f_s = \lambda . (\sigma_v' + 2s_u) \quad \text{..... (2.8)}$$

where λ is a function of the length of the pile.

Bjerrum (1973) based on Hvorslevs' parameters φ_e and χ proposed the following equation for side friction:

$$f_s = \mu_t.(\sigma_h' \tan\varphi_e D_M + \chi P_e') \quad \ldots\ldots\ldots\ldots\ldots\ldots (2.9)$$

where

μ_t – coefficient for time rate effect

σ_h' – effective horizontal stress

D_M – mobilization factor for the frictional resistance

P_e' – equivalent consolidation pressure

Janbu (1976) introduced a relation taking into consideration the effect of the mobilized friction along with the effective stress parameters:

$$f_s = S_V.(\sigma_v' + a) \quad \ldots\ldots\ldots\ldots\ldots\ldots (2.10)$$

where

S_V – a function of friction angle and depth

a – adhesion which is equal to $\bar{c}/\tan\delta$

Flaate and Selnes (1977) proposed an equation:

$$\mu_L = (L + 20)/(2L + 20) \quad \ldots\ldots\ldots\ldots\ldots\ldots (2.11)$$

where μ_L is the reduction factor for the effects due to the pile length, L in feet. They suggested the equation:

$$f_s = \mu_L \mu_t [K \sigma_v' \tan\varphi_e + \chi.(\sigma_v' + 5S_u)] \quad \ldots\ldots\ldots\ldots\ldots\ldots (2.12)$$

where K is the coefficient of earth pressure, and φ_e and χ are Hvorslevs' parameters.

Kraft et al (1981) studied several times on axial pile capacity in clays and showed that the average frictional resistance, expressed as a fraction of the average undrained shear strength or average effective overburden pressure, decreased with increasing pile penetration. Procedures to compute shaft friction were reviewed, and the effect of pile length on the development of shaft friction on piles in clay was

examined in terms of the relative pile-soil stiffness and lateral pile movements during installation.

2.3. Experimental Study

The present study is an experimental procedure designed to obtain data regarding the behaviour of both single piles and pile groups in clay under compressive load. The behaviour of piles under compressive load is a function of a number of interacting variables; bearing capacity varies with soil shear strength, pile roughness and vertical or horizontal stress level. Some researchers have performed laboratory experiments as well as field experiments to study and quantify these variations.

Woodward et al (1961) concluded from field test in California that the maximum skin friction developed for piles driven in stiff clay is substantially less than the shear strength of the clay; reduction coefficients expressing the maximum skin friction as a proportion of the shear strength determined by the field test are somewhat higher than values previously reported.

Coyle and Reese (1966) established a correlation of the ratio of load transfer to soil shear strength versus pile movement from the field tests on instrumented piles under compressive load. The load settlement curves obtained from the field tests showed that the ratio of load transfer to soil shear strength is a function of pile movement and depth. For field tests it was possible to get ratios of load transfer to soil shear strength greater than 1.0. For soft clays, the soil shear strength adjacent to the pile was greater than the undisturbed shear strength obtained prior to pile driving.

To add to the knowledge gained from the study of field tests on instrumented piles, a series of laboratory tests were conducted using a hollow tube embedded in a clay soil. The tests were conducted in such a manner that the effect of depth could be simulated, and measurements were made for load transfer, soils shear strength and

pile movement. The clay sample was consolidated in a triaxial cell and a standard unconfined compression test was run. In the laboratory, a value of 1.0 was developed for the maximum ratio of load transfer to soil shear strength.

A relationship had been established between load transfer, soil shear strength and pile movement which could be used to compute theoretical load-settlement curves. This relationship was limited to use with steel pipe friction piles in clay soil with a depth of embedment that did not exceed 100ft.

Coyle and Suleiman (1967) established a relationship between the ratio of skin friction to soil shear strength and pile movement in sand from the field tests. The curves from the field data showed that this ratio was a function of pile movement and depth. The ratio decreased as depth increased and reached a limiting value of about 0.5. From the field data it was indicated that skin friction increased to a relatively constant value as pile movement reached values greater than 0.1in to 0.2in and skin friction decreased as depth below ground surface increased.

Some laboratory tests were conducted in a triaxial shear apparatus using a small steel pile embedded in saturated sand. The method of testing made it possible to determine skin friction, pile movement and soil shear strength under compressive load. From laboratory tests it was shown that the relationship between the ratio of skin friction to soil shear strength and pile movement decreased as confining pressure increased and reached a limiting value of about 0.5.

Dayal and Allen (1975) showed experimentally the effect of penetration rate on the shear strength of clay and sand. It was done by constant velocity penetration tests performed with various velocities upto 81.14cm/s. The clay and sand targets were of various strengths and moisture contents. Experimental results indicated that for granular soils the effect of penetration velocity on cone and sleeve friction

resistance were insignificant, whereas, for cohesive soils, the increase in penetration velocity cause an increase in the cone and friction resistances. It was found that for the cohesive soils the ratio of dynamic to static strength was directly proportional to the logarithm of the penetration velocity ratio. For the tested soils various values of the soil viscosity coefficient were proposed for different strength ranges. The validity of the analytical relationship was established for penetration velocities ranging from 0.13cm/s to 550cm/s.

Meyerhof (1976) from his investigations observed that the behaviour of pile foundations under load can only roughly be estimated from the surface conditions, type and length of the piles, method of installation, size and loading of the foundation and other factors. For piles in sand and non-plastic silt, conventional bearing capacity theory was limited to short piles of length less than about 15 to 20 pile diameter. The skin friction of piles in cohesionless soils varied within wide limits because it was dependent additionally on the stress history of the soil. For piles in saturated clay and plastic silt, conventional bearing capacity theory using the undrained shear strength of undisturbed soil represented mainly the failure condition at the pile points with some allowance for the effect of sensitivity of the soil.

Butterfield and Ghosh (1977) showed the results of 23 axial vertical load tests on 12mm diameter model piles of different lengths installed in large, homogeneous remoulded London clay. Data, measured during installation by jacking at constant rate, was provided on total loads, pile base loads and radial stresses at toe. From the results of experiment it was determined that the vertical displacement measurements on the piles were linear upto approximately half ultimate load. Elastic analysis had been used to interpret the vertical stiffness all of which were consistent with a single value of the soil shear modulus (G). It was concluded from the pile test

data that if the mean soil shear modulus was related empirically to the mean initial clay bed c_u value by $G = \beta.c_u$ then the entire test support $\beta = 154$. The use of the global G or β values was necessarily a gross approximation to the detailed response of different soil elements within the pile system.

Flaate and Selnes (1977) studied the behaviour of driven piles in soft to medium marine clay. The basis of the investigation was a large amount of data from which one had selected piles with the necessary data about load tests and routine soil investigations. The study concluded that the best estimate of side friction was obtained by an effective stress analysis. To give the best fit to the test data a formula for side friction was proposed which also took the overconsolidation ratio into account and it gave better estimate of average skin friction than estimate on the basis of undrained shear strength. The formula was applicable to both overconsolidated and normally consolidated clay. The magnitude of the side friction did not seem to depend on the pile material.

Fellenius et al (1978) studied by field test the soil disturbance due to the driving of two groups of 116 concrete piles each in sensitive marine clay on a construction project in eastern Canada. Pore-water pressures, heave and lateral movement of soil and piles, and tests of strength, compressibility, and consistency limits of the soil were observed prior to and up to 3 months after pile driving whereas observations of pore water pressures were continued for an additional 5 months. Driving of piles had little effect on the compressibility and consistency limit of marine clay, but the in situ shear strength and cone penetration resistance were reduced by about 15 and 30% respectively. Soil had within the group of piles decreased linearly with depth from a maximum of 450mm at the ground surface to about zero at the pile tips, and in volume amounted to approximately 55% of the soil

displaced by the pile. Pore water pressure generated during piling exceeded the total overburden pressure by 35-40%. The excess pore pressure dissipated in about 8 months after the piling was completed.

Blanchet et al (1980) showed by field test that pore pressure induced by pile driving was related to the preconsolidation of the clay and they were much larger for the tapered piles. The magnitude of the excess pore pressure depends on the distance to the pile but was apparently not affected by the group size. It was also examined that the full dissipation of excess pore pressure induced by pile driving required about 30days around a single pile and upto 300days in large pile groups. The total settlements of the monitored pile groups were mainly due to the reconsolidation of the clay as the driving pore pressure dissipate and to shear creep deformations in the clay close to the pile wall.

Roy and Blanchet (1981) carried out a full scale investigation with six instrumented test piles to study the behaviour of friction piles in soft sensitive clay. It was concluded from the test that the pore pressure generated near the pile tip, Δu_t, were the result of the expansion of a nearly spherical cavity in the intact clay and the pore pressure maintained along the pile wall during penetration, Δu_s, were much less than Δu_t. The reconsolidation of the clay around a single pile extended over a period of about 600hr. The vane shear test was temporarily reduced by a maximum of 30-40% close to the pile wall, and a lesser extent within a radius of 4 pile diameters. The initial vane shear strength was completely recovered after reconsolidation, i.e., 25days after driving.

Madhav and Anirudhan (1982) conducted model tests on both sand and clay by Triaxial cell accommodating with single pile to measure and estimate the shaft resistance of piles at axial compressive loading in different cell pressures. Two types

of sand and clay were used in the experiment. From the experimental results it was concluded that the peak shaft resistance was mobilized at a pile movement of 1.2 to1.5 percent of the pile diameter in case of sand but for clay it was within the range of 3.0 to 6.5 percent of pile diameter. At lower strain rates the shaft resistance mobilized was larger and rough pile gave significantly large capacities in sand.

Bengtsson et al (1983) carried out several load tests on floating piles in Sweden soft clay under axial load. From the theoretical analysis and the test results it was concluded that the failure load could be calculated as the critical shear strength times the shaft area multiplied by 0.9. The critical shear strength was obtained by using the vane shear strength corrected for time to failure. Furthermore, it was found that: the use of different correction factor depending on pile material was not justified; the longitudinal shape of the pile was important; the initial stress on the pile due to driving and heaving had little influence on the bearing capacity of a single floating pile in soft highly plastic clays.

Briaud and Garland (1985) proposed a method to predict the behaviour of single pile s in cohesive soil subjected to vertical load applied at various rates. The elementary simple shear model was made rate-dependent by introducing the time raised to a negative power n (undrained shear strength $s_u = ct^{-n}$ where, t-time to failure, c-constant, n-viscous exponent). This viscous exponent n was shown to vary from 0.02 to 0.08. correlation with undrained shear strength, water content, plasticity, the liquidity index and overconsolidation ratio were shown based on 152 laboratory tests. A program to predict the head load-head movement response of the pile using rate-dependent load transfer curve was described. A parametric analysis was introduced to show how the shearing rate varied significantly along the pile for long piles.

Azzouz and Lutz (1986) described the results of experimental investigation consisted of (1) Laboratory and in situ Piezocone tests to establish the in situ conditions and soil properties at a site in Empire, LA, where the pile load tests were performed; and (2) in situ measurements of stresses and pore pressures acting on the shaft of an instrumented model pile, the Piezo-Lateral Stress (PLS) cell, throughout the various stages in the life of a pile i.e. installation to loading.

Mochtar and Edil (1988) used a test apparatus to measure the load transfer along the shaft of a model pile inserted in clay. This apparatus allowed independent control of boundary stresses of a cylindrical clay specimen in a vertical and horizontal direction. The results based on these tests on Kaolinitic clay showed that the angle of pile-clay friction is independent of the vertical consolidation pressure in the clay and the overconsolidation ratio (both in the vertical and horizontal directions). The length of the pile-soil contact showed no influence on the pile-clay friction angle whereas the influence of the pile diameter was not clearly established within the range these parameter were varied. The magnitude of pile displacement to mobilize the maximum shaft resistance was relatively small and dependent on the length of the pile-soil contact surface. Finally, the unit shaft resistance was affected by the magnitude of the final effective horizontal stress operating at the pile-soil interface and the pile-soil friction angle.

Rao and Venkatesh (1988) proposed a new testing technique using a large triaxial chamber, for independent assessment of N_q, K and tanδ of sand had been suggested for the study of the behaviour of bored model pile. The tests ware conducted in two phase. In the first phase σ_V tests were conducted under controlled vertical stress condition to determine point resistance and N_q and in second phase σ_H

tests were conducted under controlled horizontal stress to determine point and shaft resistances.

Radhakrishnan et al (1991) investigated the load transfer behaviour of precast reinforced concrete piles driven through marine clay by field study. Strain gauges were installed along the pile shaft to monitor frequently during static loading tests and at regular intervals during and after the construction of the superstructure. Piezometers were installed in proximity to one of the piles. Pile capacities were calculated using wave equation models based on stress wave measurements during initial pile driving. Pile capacities gave consistently lower values than those of static loading tests one week later. Long term instrument readings indicated development of negative skin friction when the piles were in service. It was concluded that the downdrag increased with time, and this additional loading should be accounted for the pile design as part of the service load on the pile.

Indraratna and Balasubramaniam (1992) described the results of short-term pullout tests and long-term full-scale measurements of negative skin friction on driven piles in soft Bangkok clay. Two instrumented cylindrical prestressed concrete piles were fully equipped with two independent load-measurement systems, load cells and telltale rods. Pore pressures and ground movements in the vicinity of the piles were monitored throughout the period of investigation. The long term behaviour of driven pile was compared with the estimated value obtained from short-term pull-out tests and soil strength data. It was found that the negative skin friction could be predicted by the effective stress approach using values of β ($\tau_s = \beta.\sigma_v'$) between 0.1 and 0.2. The load-settlement and load-transfer behaviour were numerically modelled to acquire a more comprehensive understanding of negative skin friction developed on driven pile.

Rao and Venkatesh (2003) investigated the effect of various factor such as soil shear strength, stress level, pile roughness etc. on the behaviour of piles embedded in saturated clay by using large triaxial testing apparatus. The experiment was undertaken on smooth and rough buried piles of about 13mm diameter having embedded length diameter ratio of 6 to 28, using a testing methodology which enable to control over the vertical or horizontal stress level in the soil. The test results indicated that the bearing capacity factor N_c for piles buried in clay varied from 7 to 12 depending on the stress level in the soil, higher the stress level, higher being the value. The average skin friction and adhesion factor also showed their dependency on shear strength and stress level. The value of adhesion factor α was seen to vary from 0.2 to 1.0 depending on the pile roughness, soil shear strength and stress level.

2.4. Efficiency of Pile Group and Interaction Factor

The response of an individual pile in a pile group, where the piles are situated closely enough to one another, may be influenced by the response and geometry of neighboring piles. Piles in such groups interact with one another through the surrounding soil, resulting in what is called pile-soil-pile interaction, or the group action. The efficiency of pile group η_g is defined as the ratio of the actual capacity of the group to the summation of the capacities of the individual piles in the group when tested as single pile.

Several efficiency formulas have been proposed to relate the behaviour of a pile group to that of the individual piles in the group. These formulas are mostly based on relating the group efficiency to the spacing between the piles and always yield η_g values of less than unity, regardless of the pile soil conditions. A major apparent shortcoming in most of the available efficiency formulas is that they do not account

for the characteristics of the soil in contact with the pile group. The most acceptable formulas for pile groups are briefly summarized as follows:

Converse-Labarre Formula (Bolin 1941): One method of assigning a reduced bearing value to a group of piles is by the use of the following formula:

$$\eta_g = 1 - \frac{\xi}{90^0}\left[\frac{(n-1).m + (m-1).n}{m.n}\right] \qquad \ldots\ldots\ldots\ldots\ldots (2.13)$$

where

η_g – efficiency of pile group

m – number of rows

n – number of piles in a row

$\xi = \tan^{-1}(D/s)$

D – pile diameter

s – centre to centre spacing of piles

Los Angeles Group-Action Formula (Bolin 1941): Bolin added an additional term to the original formula of Converse to include the influence of diagonal piles. As per this formula:

$$\eta_g = 1 - \tan^{-1}(D/2s).\left[\frac{(n-1).m + (m-1).n}{90.m.n}\right] - \tan^{-1}(D/2\sqrt{2}\,s).\left[\frac{(n-1).(m-1)}{45.m.n}\right] \ldots(2.14)$$

Since the tangent of small angles is practically equal to the angle in radians, Equation (2.14) can be simplified to:

$$\eta_g = 1 - \frac{D}{\pi s m n}\left[(n-1)m + (m-1)n + \sqrt{2}(m-1)(n-1)\right] \qquad \ldots\ldots\ldots\ldots (2.15)$$

This is the form in which it appears in the city of Los Angeles Building Code.

Masters (1943) Method: Another method of determining reduced bearing values, which may give considerably greater reductions, particularly in the case of long piles is proposed by Masters in which the vertical shear values on the soil around

each pile in the group are computed and their effects on each of the other piles in the group are calculated by means of Boussinesq equation. In this method lengths of piles embedded in frictional load carrying strata are taken into account. Masters made use of Boussinesq equations for the transfer of load to a soil in a vertical line as with a pile.

Feld (1943) Method: Field proposed a rule of thumb to determine the efficiency of pile group. In this method, the capacity of a pile group is defined as the summation of the capacities of the individual piles in the group multiplied by a factor ranging between 0.72 and 0.94 according to the number of piles.

Seiler and Keeney (1944) Method: This is an attempt to modify and extend the Converse-Labarre and Masters formulae. An attempt was made to fit a formula which would give curves following the general shape of the Converse-Labarre curves but would fall in the range of Masters' value for the smaller groups. This formula reads as follows:

$$\eta_g = 1 - \left[\frac{11s}{7(s^2-1)} \cdot \frac{m+n-2}{m+n-1}\right] + \frac{0.3}{m+n} \qquad \text{..... (2.16)}$$

where s is centre to centre spacing of piles in feet.

Terzaghi and Peck (1948) Method: One of the most widely used means of estimating group load capacity is that given by Terzaghi and Peck, where the group capacity is the lesser of (a) the sum of the ultimate capacities of the individual piles in the group; or (b) the bearing capacity for the block failure of the group. For a given length and number of piles in a group embedded in clay, there was a critical value of spacing at which the mechanism of failure changes from block failure to individual pile failure. For spacing closer than the critical value, failure is accompanied by the formation of vertical slip plane joining the perimeter piles, the block of the clay

enclosed by the slip planes sinking with the pile relative to the general surface of the clay. For wider spacing piles penetrate individually into the clay. Shear force acting around the periphery of the pile group were taken into account.

Poulos and Davis (1968) analyzed the settlement behaviour of single axially loaded incompressible cylindrical pile in an ideal elastic soil mass using Mindlin's equation. Pile was considered as a number of uniformly loaded cylindrical elements together with a uniformly loaded base; solutions were obtained for distribution of shear stress along the pile and displacement of pile. Influence factors were given for settlement of a pile in semi-infinite mass and in a finite layer, and the effects of length to diameter ratio of the pile, Poisson's ratio of soil and depth of soil were examined. The elastic analysis was extended to include the effect of local shear failure.

Poulos (1968) proposed an analysis for settlement interaction between two identical piles in an elastic mass and expressed the increase in settlement of each pile due to interaction in terms of an interaction factor α. For symmetrical pile groups the increase in settlement due to interaction was obtained by superposition of values of α for the individual piles in group. Behaviour was analyzed for the case of a rigid pile cap (equal settlement of each pile) and flexible pile (equal load in all piles). For rigid pile caps the values were obtained for the ratio of settlement of group to settlement of single pile carrying the same load (the group reduction factor R_G) and load distribution within the group. For flexible pile caps values of maximum settlement and maximum differential settlement were specified. The influence of pile spacing, pile length, type of group, depth of layer and Poisson's ratio of layer were considered on the settlement behaviour of pile group.

Poulos and Mattes (1969) analyzed the behaviour of single axially loaded end bearing pile in an ideal elastic soil and provided the solutions for load distribution

within the pile and the top and tip movements of the pile for a wide range of parameters. Length to diameter ratio, the stiffness of pile to surrounding soil and relative stiffness of bearing stratum influenced the pile behaviour to great extent. Very slender piles were observed to act effectively as floating or frictional piles.

Poulos and Mattes (1971) derived the interaction factors for two identical equally loaded piles in a homogeneous semi-infinite elastic half space for end bearing as well as frictional piles using Mindlin's solution. Each pile was divided into n cylindrical elements and a circular uniformly loaded base. The pile and soil displacements at centre of each element may be equated assuming no slip or yield occurred at soil-pile interface. Interaction factors were functions of length to diameter ratio (l/d) of pile, spacing to diameter (s/d) ratio, relative pile stiffness (K). Charts had been drawn for interaction factor for different variation of l/d, s/d and K for both end bearing and floating piles separately. The interaction factor was observed to decrease with increase with spacing. Interaction factor decreased as l/d and K increased, i.e. as pile became more slender or stiffer interaction between two piles decreased. Settlement analysis for pile group was performed using the interaction factor values.

Poulos and Davis (1980) Method: In order to obtain more realistic estimate of the ultimate load capacity of a group, the following empirical relationship was suggested:

$$\frac{1}{P_G^2} = \frac{1}{n^2 P_1^2} + \frac{1}{P_B^2} \qquad \text{..... (2.17)}$$

where

P_G - ultimate load capacity of group

P_1 - ultimate load capacity of single pile

n – number of piles in group

P_B - ultimate load capacity of block

The above Equation (2.17) may be expressed as follows:

$$\frac{1}{\eta_g^2} = 1 + \frac{n^2 P_1^2}{P_B^2} \qquad \text{..... (2.18)}$$

$$= 1 + \frac{1}{\eta_T^2} \qquad \text{..... (2.19)}$$

where

η_g - efficiency factor

$$\eta_T = \frac{P_B}{nP_1}$$

It was stated that η_g was a function of the spacing, length of pile, size i.e. the number and arrangement of piles of the group.

Madhav and Poorooshasb (1985) proved that the method of superposition was valid for engineering analysis. The efficiencies for three and four pile group were written as a function of interaction factor:

$$\eta_3 = \frac{1}{1 + 2\alpha(s)} \qquad \text{..... (2.20)}$$

$$\eta_4 = \frac{1}{1 + 2\alpha(s) + \alpha(\sqrt{2}.s)} \qquad \text{..... (2.21)}$$

where

$\alpha(s)$ - interaction factor of pile for spacing s

$\alpha(\sqrt{2}s)$ - interaction factor of pile for spacing $\sqrt{2}s$

The above equations (2.20) and (2.21) are the efficiencies of three and four pile group respectively.

Madhav and Budkowska (1986) introduced the ultimate load capacity P_G of the pile group of size MxN by estimating the reduction in the pile capacity of each pile. The efficiency of the pile group η and $\eta_{i,j}$ of pile A(i, j) were respectively:

$$\eta = \frac{P_G}{M.N.P_{u1}} \qquad \text{..... (2.22)}$$

$$\eta_{i,j} = \frac{P_{i,j}}{P_{u1}} \qquad \text{..... (2.23)}$$

where

P_G - the capacity of pile group

$P_{i,j}$ - individual pile load on pile A(i, j)

P_{u1} - the capacity of a single pile

Madhav, Basudhar and Kumar (1987) introduced a simple and rational method for predicting the efficiency of free standing groups of floating and end bearing piles in clay using the interaction factor of pile group. Two models were proposed and studied to predict efficiency. In model-1 the load carrying capacity of each pile was assumed to be affected by the presence of all other piles in the group while in model-2 assumed to be influenced only by the presence of the immediately adjacent piles.

Poulos (1988) concluded by analysis that if the soil between the piles in the group was considered to be stiffer than the soil directly adjacent to the pile, the settlement interaction between piles in a group was reduced. The extend of this reduction depends on the ratio μ of the soil mass modulus to the near-pile soil modulus, the spacing between the piles, and the geometry and relative stiffness of the piles. Significant reduction in group settlement ratio can occur if the piles are widely spaced or there are several piles in the group. This observation provides an

explanation for the tendency of conventional pile group settlement theory to overpredict group interaction effects. Comparisons with recent field data showed that the consideration of a higher soil-mass modulus between the piles leads to more realistic predictions of the settlement and load distribution in the pile groups than did the conventional analysis which assumed that the soil-mass modulus was equal to the near-pile soil modulus.

Sayed and Bakeer (1992) Method: They proposed a new formula to evaluate the efficiency of axially loaded pile groups:

$$\eta_g = 1-(1-\eta_s^{'}.K).\rho \qquad \text{..... (2.24)}$$

where

η_g – efficiency of pile group

$\eta_s = \eta_s^{'}.K$ = the load efficiency of pile group

$\eta_s^{'}$ - geometric efficiency

K - group interaction factor

$\rho = \dfrac{\sum Q_s}{\sum Q_o}$ = friction factor

Q_s - the single pile capacity

Q_o - the shaft capacity

The derivation of the formula was based on the premise that the group effect could be taken into consideration only for the load component carried by the pile shafts. The formula was applicable for pile group in both cohesive and cohesionless soils. A set of design charts based on the proposed formula was developed for the analysis of pile groups with different geometries and soil conditions.

2.5. Discrete Element Method Modelling

The Distinct Element Method (DEM), a numerical technique which treats soil as a discrete assemblage of particles. It can be used to study local yield, bifurcation behavior or nonlinear soil-structure interaction. The discrete element method treats particles numerically as a collection of particles rather than as a continuum. DEM can be used successfully in various soil mechanics problem and also soil structure interaction problem. A literature containing the modelling of soil particles and various pile-soil interaction problems are discussed below.

Scott and Craig (1980) developed a simple DEM based procedure to examine the effects of the clay structure, particle size, orientation, bonding conditions, etc. by computer. The soil was formed by a simulated sedimentation process in which particle size distribution, and bonding were varied. Stick beam-column elements were used to represent the soil. The resulting two-dimensional, essentially random structure was subjected to boundary conditions representative of equivalent one-dimensional and axial unconfined compression tests. With elastic and elastic-plastic representations of the particle contacts, the global response to loading, unloading, and cyclic stress application was analyzed and reviewed with respect to real clay behavior.

Chow (1985) analyzed the behavior of single piles subjected to torsion by discrete element method. The soil was modelled using the modulus of subgrade reaction, which was expressed in terms of the soil shear modulus and the pile radius. Discrete element matrices that could be readily implemented into a computer program were listed. The accuracy of the discrete element approach was verified by comparison with analytical and finite element solutions. The nonlinear response of the

pile-soil system was computed, and compared with two reported torsional load tests in the field.

Chow and Thevendran (1987) studied the optimization of pile group by using an optimization technique in conjunction with the discrete element method for pile group settlement analysis. They demonstrated that it was possible to optimise the performance of pile groups by minimizing the load differentials between piles and/or differential settlements. This could be achieved by apportioning the lengths of the group piles to meet the requirement of their positions in the group. Numerical examples were presented to illustrate this principle.

Ting et al (1989) used discrete numerical model for various soil mechanics problems. A two-dimensional disk-based implementation of the DEM was validated using numerical simulations of standard geotechnical laboratory tests, such as one-dimensional compression, direct simple shear, and triaxial tests. These test results indicated that the two-dimensional DEM could simulate realistic nonlinear, stress history-dependent soil behavior appropriately when individual particle rotation was inhibited. Modeling of large-scale problems was accomplished by constructing a reduced-scale model, then applying the geotechnical centrifuge scaling relationships in order to reduce the number of particles simulated and to ensure stress-strain-strength similitude between the model and prototype. Full-scale simulations, including bearing capacity and lateral earth pressure tests, indicated that the DEM can accurately simulate real geotechnical problems, including those possessing large local yield zones.

Hakuno et al. (1989) modified the Cundall's Distinct Element Method by adding secondary springs which represented the mechanical properties of clay

between particles. The collapse of underground structures such as a foundation, a retaining wall and a tunnel was simulated by the modified DEM. Normal force distribution, ground assembly model, wave propagation, particle movement during driving, and bearing force was calculated in case of shallow foundation. For pile foundation particle size segregation, velocity distribution and normal force distribution with time after penetration were determined by DEM and the penetration depth with time curves were also plotted. Structural foundation under sinusoidal loading, dynamic nonlinear angular response, and the relationship between moment and response angle were clearly presented for foundation and tunnel.

Chang and Chao (1991) presented a method of analysis based on DEM for estimating bearing capacity of foundations. Soil mass in the present model was treated as comprising of blocks which were connected by elasto-plastic Winkler-springs. By considering the conditions of compatibility, the boundary stresses on the failure surface and the ultimate bearing capacity of shallow foundations could be obtained. The computed boundary stresses from the present method satisfied equilibrium conditions and did not exceed the material strength. Formulation of the method was presented. Examples were shown to demonstrate the applicability of the method to the analysis of bearing capacity of shallow foundations. Effects of stiffness of Winkler-springs and mesh pattern on the computed results were investigated. The method was a useful tool for analyzing bearing capacity of foundations with unusual geometry and loading conditions.

Ting and Corkum (1992) presented the design of an integrated suite of three computer programs that implement the discrete element method using two-dimensional ellipse-shaped particles and allow for computer-assisted-drafting (CAD) style graphic preprocessing and postprocessing. A preprocessing program—Front End

Generation (FEGEN) allowed interactive generation of a particulate system for starting the system simulation. Output from a simulation program Particle Simulation with Ellipses (PARSE) could be analyzed and graphically interpreted by a postprocessor. As a result, a novice to discrete element method modeling could specify a test system, generate the appropriate simulation parameters, run the simulation, and view the results with relative ease.

Anandarajah (1994) simulated the behaviour of cohesive soil by adding the mechanical forces, physicochemical forces between the particles in DEM and there was significant bending of individual particles. The repulsive force was modeled approximately based on a recent study on the double-layer repulsive force between inclined particles and the attractive force between particles was not considered. Dividing each particle into a number of interconnected discrete elements, bending of particles was simulated as part of the overall analysis. By employing suitable force-displacement laws for the mechanical contacts, formation of new contacts, deletion of existing contacts, and slip between particles were modeled. The preliminary results presented here showed the potential of the method for carrying out fundamental research into the stress-strain behavior of cohesive soils.

Hoit, et al. (1996) used a three-dimensional discrete element for modelling the materially and geometrically nonlinear behaviour of pile. A model had been incorporated into the computer program—Florida-Pier to model combined nonlinear behaviour of prestressed or reinforced concrete piles subjected to a variety of loading. The analysis included a highly accurate model of the structural foundation system and the soil interactions.

Jensen et al (2001) investigated the effect of particle shape on interface shear behaviour of granular materials. The discrete element method (DEM) using clusters to

model rough particles were used. Seven new cluster shapes of varying degrees of roughness were presented herein, and numerical experiments simulating ring shear tests were made using these clusters. From these simulations, the effect of particle shape on void ratio (e) and interface angle of friction between soil and structure surface (δ) was reported. Particle shape characteristics included roundness, angularity, and surface roughness. Simulation results showed that the void ratio of a particle mass increased as the angularity or roughness of the particles increased. They also showed an increase in interface shear strength between perfectly round DEM particles and the more angular cluster shapes. The simulations also successfully reflected the relationship between interface friction angle and structure surface roughness as demonstrated in recent physical experiments.

Fortin et al. (2002) proposed a new algorithm on the contact dynamics approach. It involved two stages i.e. local stage and global stage. In the first one (local stage) for each particle, forces were computed from the relative displacement using an interaction law, which modeled frictional contact and shock and in the second stage (global stage) Newton's second law was used to determine, for each particle, the resulting acceleration which was then time-integrated to find the new particle positions. This process was repeated for each time step until convergence was achieved. The two distinguishing features of the present algorithm were the local integration of the frictional contact law and the convergence criterion.

Asmar et al. (2002) introduced a discrete element model to validate the tests on vibrating cohesive particles system. A DEM program was introduced for cohesive particle vibration to show simple simulation. This method simulated the individual dynamics of all particles in an assembly by numerically integrating their acceleration resulting from all the contact forces. It was concluded that these 'mathematical tests'

on artificial situations can uncover bugs in programs that appeared to be running correctly, even if they appeared to simulate real experiments reasonably well. These tests were published with the aim of helping others validate their programs in similar applications. The paper also discussed the widely used simplification of particle–particle interactions by Hooke's law and suggested that its validity depends upon the application.

Anandarajah and Yao (2003) developed a three-dimensional discrete element method based on cuboids particles and implemented into a computer program for the numerical analysis of an assembly of clay particles. In this method interparticle forces such as mechanical, double-layer repulsive, and van der waals attractive forces, had been employed. Efficient search algorithms had been employed. The computer program had been used to simulate one-dimensional compression of kaolinite clay and the results presented and discussed. The results indicated the validity of the method, and provided valuable macroscopic and microscopic results concerning the behavior of clays. By examining these results, the macroscopic behavior was explained from a microscopic point of view. The numerical results agreed reasonably well with measurable experimental data such as the pressure versus void ratio relation and the variation of fabric anisotropy with applied stress.

Groger et al. (2003) introduced a three-dimensional cohesive discrete element method to investigate the internal tensile stress and the tensile strength and shear strength of fine, cohesive granular materials. Interparticle cohesion was taken into account by modelling liquid bridges in pendular state. The influence of surface roughness was considered by a minimum separation distance of the particles with respect to liquid bridges. Spheres and more complex particle shapes had been used for shear and tensile test simulations.

Tang (2004) developed a new boundary condition and implemented into a DEM program. The new program was used to simulate the conventional triaxial consolidated drained tests. The macroscopic friction angle obtained with this new boundary condition was higher than that of periodic boundaries. Good results were obtained in the pressure range from 20 to 100 times of the confining pressure. The new boundary mechanism was used to investigate the effect of particle shape, specimen size, and void ratio. It was observed here that the friction angle was not a function of specimen size for monosize specimens as long as the coordination number was similar. The friction angle showed a decrease with increasing aspect ratio provided that the void ratios of the two specimens were the same. For two-size specimens, the specimen size had no effect on the friction angle as long as the void ratio was the same. Also, there was a linear relationship between the peak strain and coordination number. Higher initial coordination numbers yield smaller peak strains.

Onate and Rojek (2004) analyzed the dynamic geomechanics problem by the combination of DEM and FEM. Combined models can employ spherical (or cylindrical in 2D) rigid elements and finite elements in the discretization of different parts of the system. A typical example could be an idealization of rock cutting with a tool discretized with finite elements and rock or soil samples modelled with discrete elements. The FEM allowed large elasto-plastic deformations in the solid regions. Both theoretical algorithms of DEM and stabilized FEM are implemented in an explicit dynamic code. A combined numerical algorithm was described. Selected numerical results illustrate the possibilities and performance of discrete/finite element analysis in geomechanics problems.

2.6. Conclusion of Literature Review

There were lots of studies had been done by researchers on pile foundation under axial compressive load. Also lots of analysis and experiments had been performed in past to predict the behaviour of pile and pile groups in clay.

The behaviour of pile and pile groups in Marine clay under compressive load in various stress condition is a new topic. A very few researchers concentrated on group capacity of pile in Marine clay under vertical and horizontal stress condition. There is no thumb rule or any formula to determine the pile capacity in clay when the soil medium is subjected to vertical and horizontal stress condition of different magnitude.

In Discrete Element method is a new field to apply in Geotechnical Engineering. Analysis of pile foundation under axial load in both sand and clay under different stress condition by DEM is an absolutely new approach in Geotechnical Engineering.

Chapter - III

Experimental Setup and Testing Program

3.1. General

To study the effect of axial compressive load on single pile and pile group at different vertical and horizontal stress condition an experimental setup was fabricated in the laboratory. Experiments were performed using a specially designed triaxial cell with enlarged dimensions to accommodate the steel pile group. The experimental setup should be such that the different vertical and horizontal stress can be applied separately on clay sample in triaxial cell.

3.2. Experimental Setup

The experimental setup used for the work was very similar to the one used by Rao and Venkatesh (1988, 2003). Fabrication of experimental setup as a whole comprises of under written individual components:

3.2.1. Large Triaxial Cell

A cell of diameter 305mm and height 700mm was used with frictionless piston assembly. Each part of this cell was specially designed and fabricated to accommodate pile group. After fabricating all components of the cell it was assembled together by fastening and other accessories. The various components of triaxial cell are described below.

3.2.1.1. Base Plate

It was a MS circular plate of diameter 305mm and thickness 24mm. There were four tapped hole of diameter 3/8 inches of PCD 280mm at the edge of the plate to enable to be bolted with bottom plate. There were also four hole of diameter 1/4 inches along the plane of the plate to apply cell pressure and to allow drainage. Two

holes among the four were extended upto the centre of plate for cell pressure and others two of them were drilled upto a little depth for the purpose of drainage. A O-ring of outer diameter 270mm and thickness 6mm was fitted with this plate so that it could be tightly fitted with the bottom plate. The detailing of base plate is shown in Fig. 3.1. and the pictorial view is laid down in Plate 3.1.

3.2.1.2. Bottom Plate

It was a MS circular ring of outer diameter 305mm, inner diameter 249mm and thickness 20mm. Four holes were made at the edge of the plate of diameter 11mm at PCD 280mm to connect with base plate. There were four tapped hole of 1/4 inches BSW at PCD 280mm and depth 15mm to connect with the top plate by four SS circular rod. To connect the circular Perspex cylinder with the bottom plate a 8mm wide groove were made. The detailing of bottom plate and the pictorial view are shown in Fig. 3.2. and in Plate 3.2.

3.2.1.3. Top Plate

It was a MS circular plate of diameter 305mm and thickness 16mm which was connected with two hollow cover plate (diameter – 70mm, thickness- 5mm) and hollow cylindrical bar (diameter – 70mm, height – 70mm). There was a hole of diameter of 14mm in all the plates to accommodate a loading plunger. A groove of depth 10mm was made to fit the Perspex cylinder with it. Two hole of 6mm diameter at PCD 118mm was provided to make the provision to fill the cell by water. Another four holes of diameter 6.5mm at the edge of the main plate were provided to connect with bottom plate by SS circular rod so that no load would be carried by the Perspex cylinder. The detailing of top plate is shown in Fig. 3.3 and in Plate 3.3.

3.2.1.4. Perspex Cylinder

Two Perspex cylinders of outer diameter 265mm and thickness 4mm was used as a chamber of the triaxial cell. The heights of two cylinders were 550mm and 450mm respectively. It was tightly connected with bottom plate and top plate. After fixing the Perspex cylinder with two plates the three components i.e. bottom plate, Perspex cylinder and top plate were acted as an assembled single component. The pictorial view of the Perspex sheet is shown in Plate 3.4. All components of the triaxial cell are shown in Plate 3.5. and the picture after assembling all the components is laid down in Plate 3.6.

3.2.2. Piles and Pile Caps

Steel Piles of two different lengths (125mm and 245mm) and constant diameter of 14mm were used in experiment. Pile caps were fabricated for three different spacing (4D, 5D and 6D) for the group piles and extended from the face of pile by 10mm. Two types of group piles (2x1 and 2x2) were used in experiment. Detailing of piles and pile caps are shown in Fig. 3.4. and Fig. 3.5. and the pictorial view is shown in Plate 3.7. and 3.8. Group piles after fitting with pile cap are shown in Plate. 3.9.

3.2.3. Rubber Membrane

It was tightly fitted with clay sample of diameter195mm and length 320mm. It was fabricated (total 15nos) by using a special die of diameter 150mm and thickness 0.5mm so that it could be tightly fitted with sample. It is shown in Plate. 3.10.

3.2.4. Top and Bottom Perspex and Wooden Disc

To hold the piles and pile groups in vertical position these disc (total 14nos of each material) were used. As per pile spacing holes were made in those discs. The diameter and thickness of top disc are 195mm and 20mm and that for bottom disc it is

195mm and 18mm respectively. The various top and bottom disc are shown in Plate. 3.11.

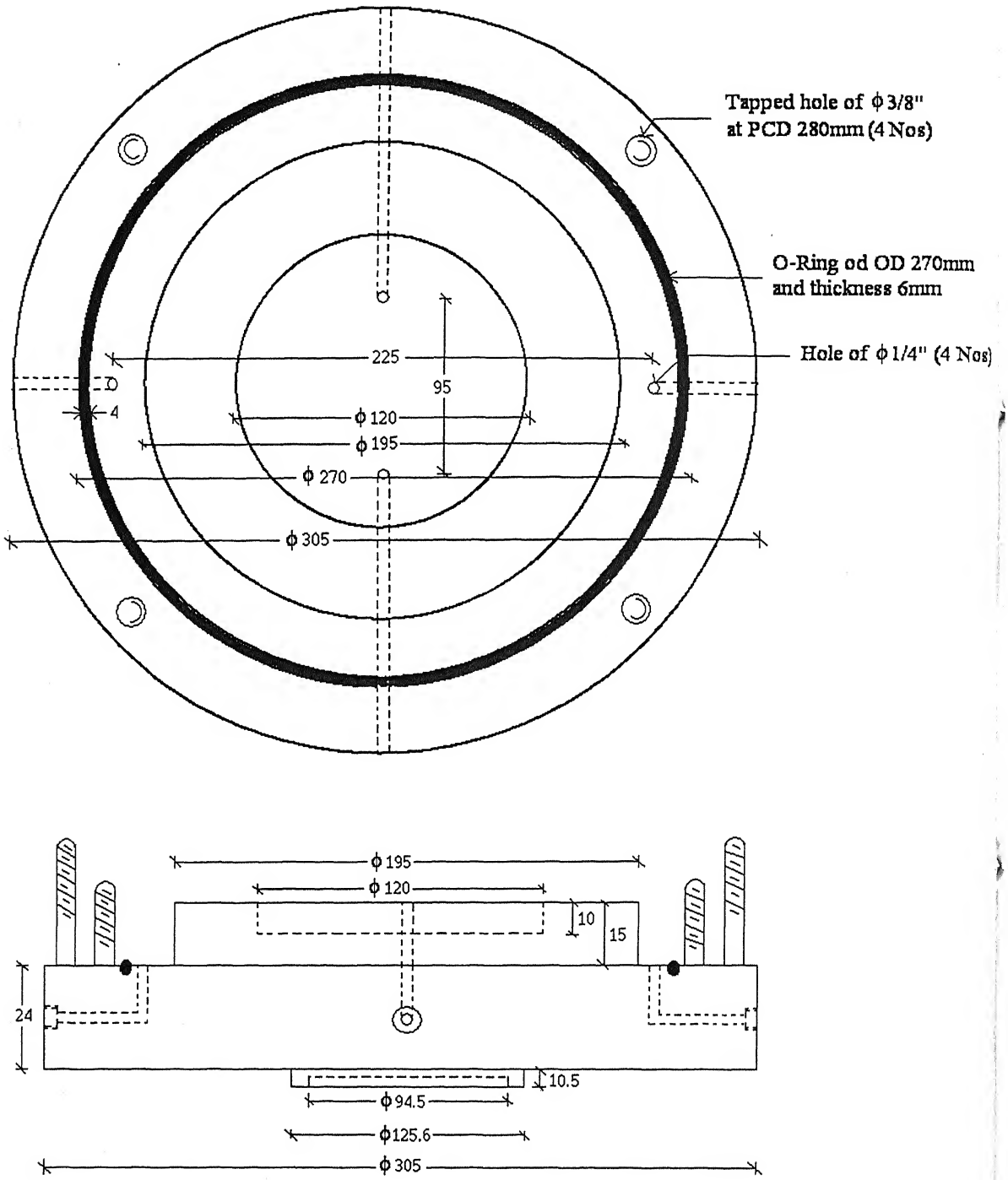

(All dimensions are in 'mm')

Base Plate

Fig. 3.1. Detailing of the Base Plate

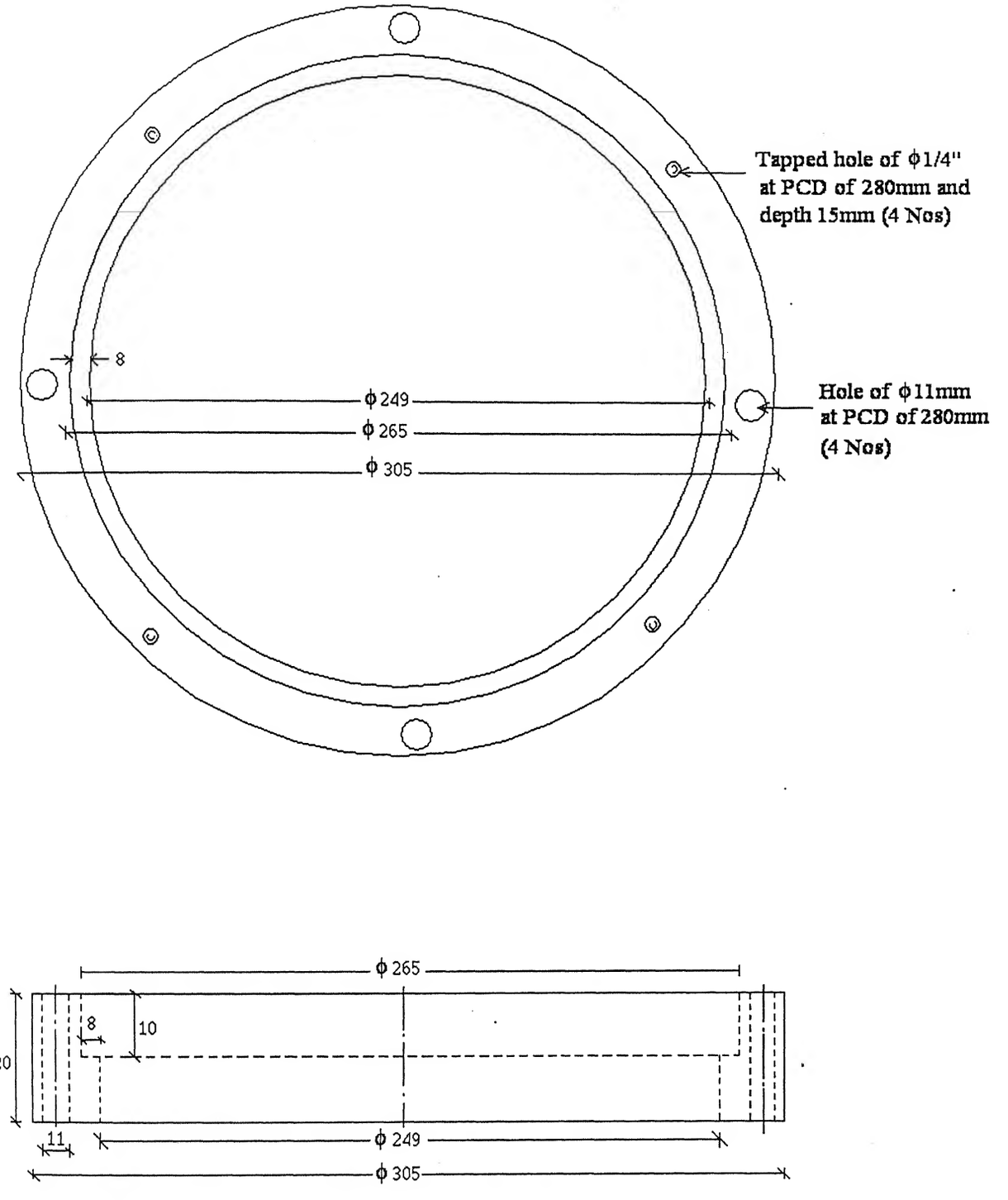

(All dimensions are in 'mm')

Bottom Plate

Fig. 3.2. Detailing of the Bottom Plate

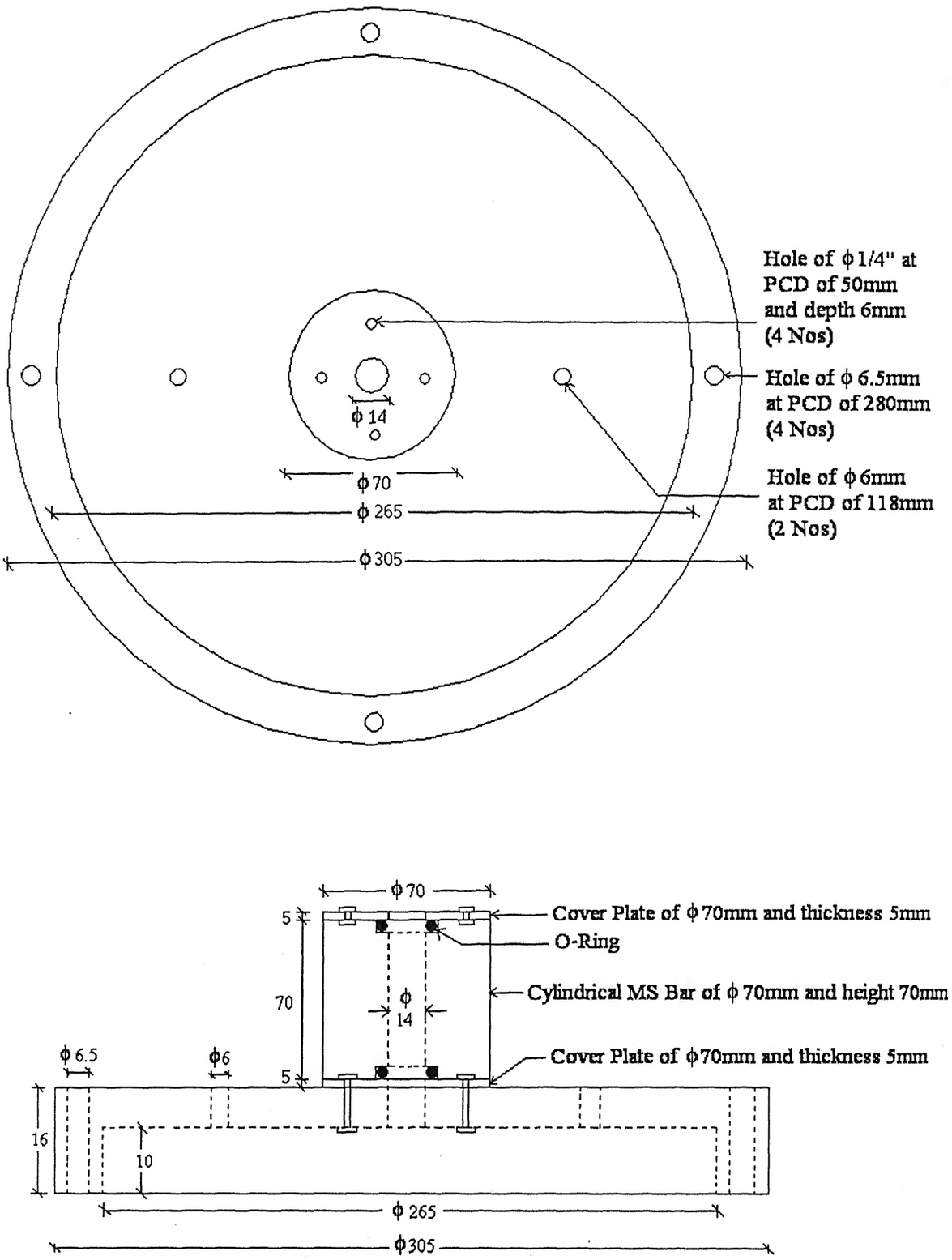

(All dimensions are in 'mm')

Top Plate

Fig. 3.3. Detailing of the Top Plate

Piles of Different L/D (8.93 & 17.5)

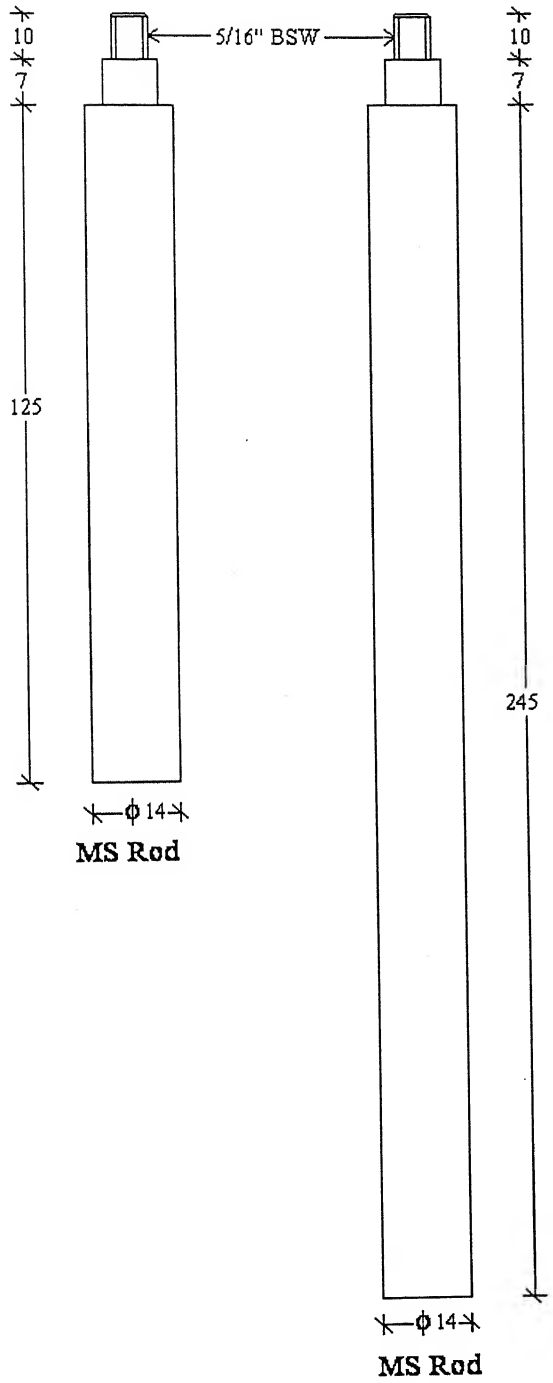

(All dimensions are in 'mm')

Fig. 3.4. Detailing of MS Piles

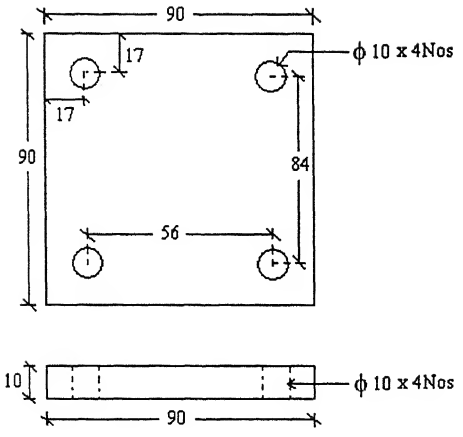

Pile Cap for 2x2 @ 4D

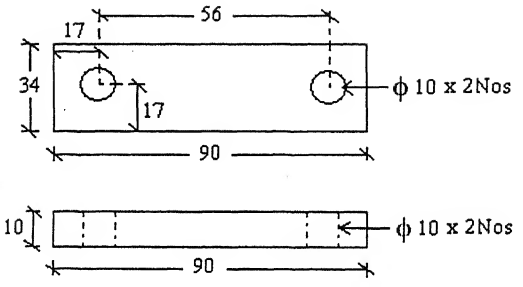

Pile Cap for 2x1 @ 4D

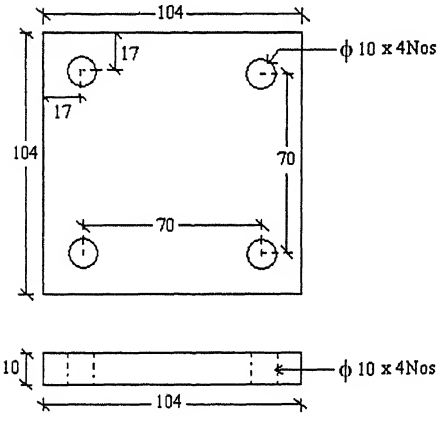

Pile Cap for 2x2 @ 5D

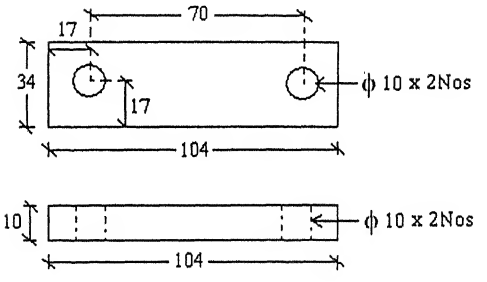

Pile Cap for 2x1 @ 5D

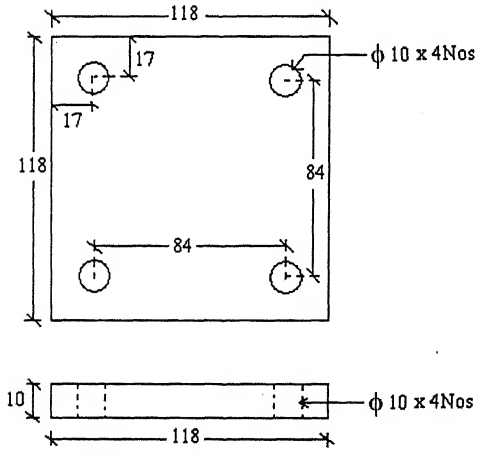

Pile Cap for 2x2 @ 6D

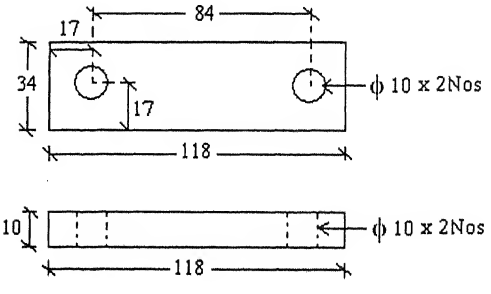

Pile Cap for 2x1 @ 6D

(All dimensions are in 'mm')

Fig 3.5. Detailing of Pile Caps at different spacing

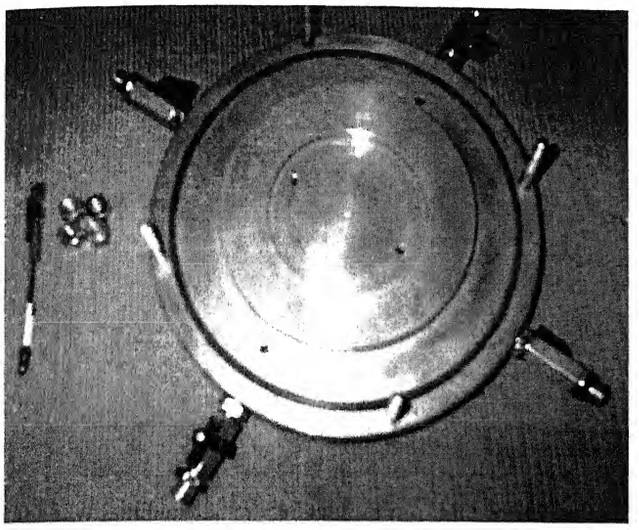

Plate 3.1. Base Plate

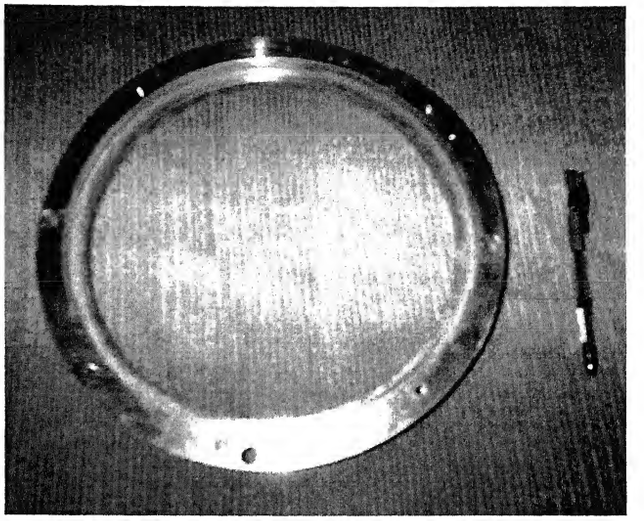

Plate 3.2. Bottom Plate

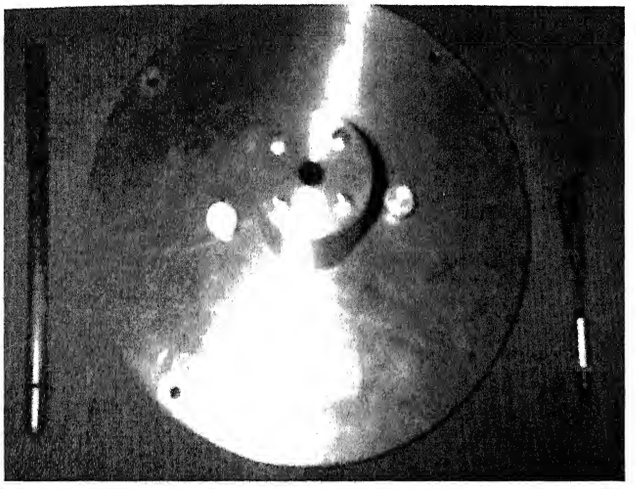

Plate 3.3. Top Plate

Plate 3.4. Perspex Cylinder

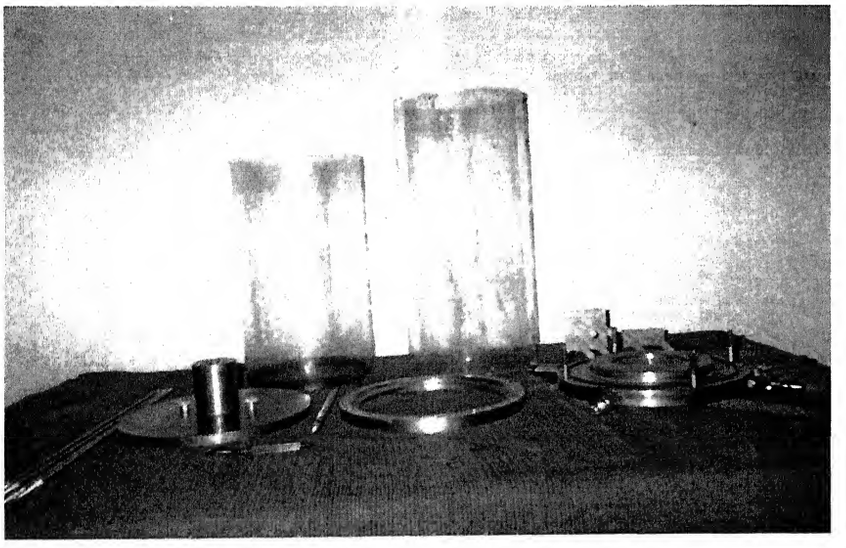

Plate 3.5. Components of Triaxial Cell

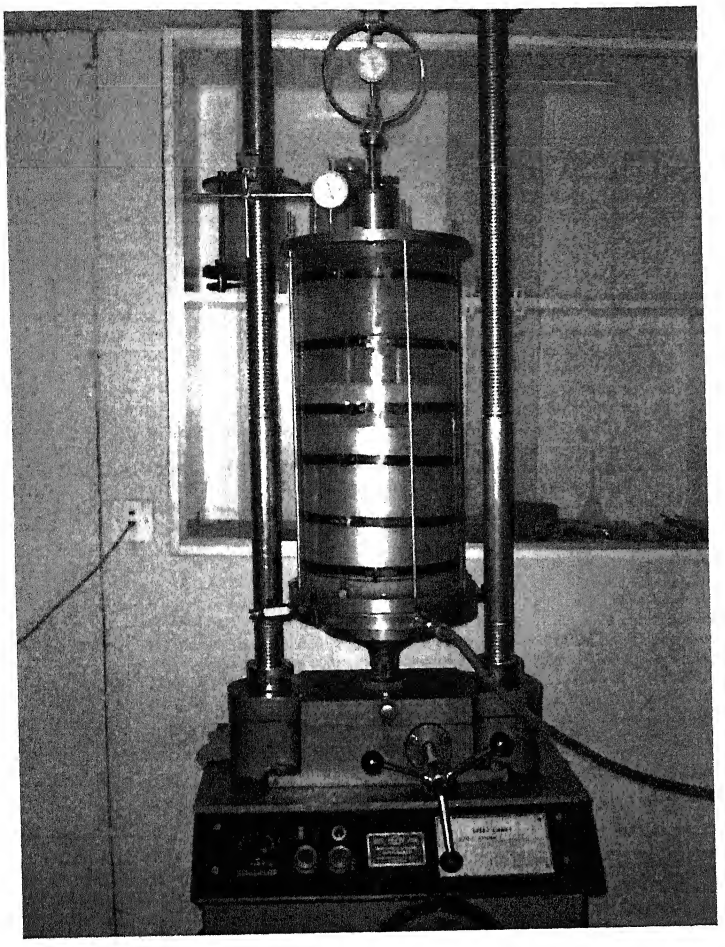

Plate 3.6. Assembled Large Triaxial Cell

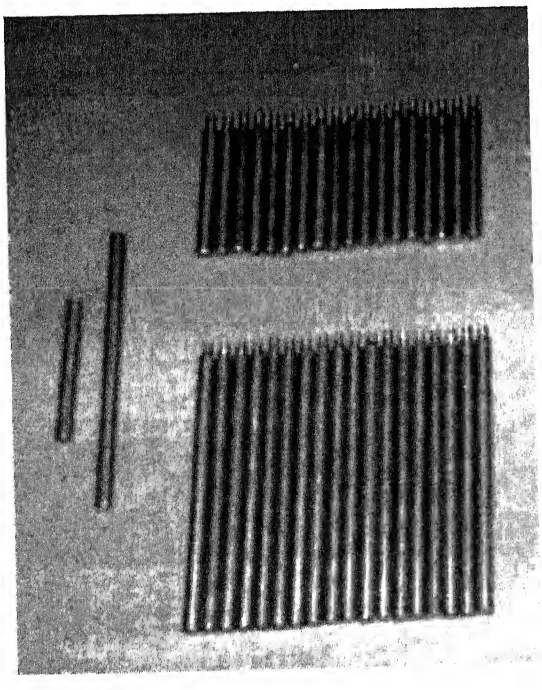

Plate 3.7. Different type of piles

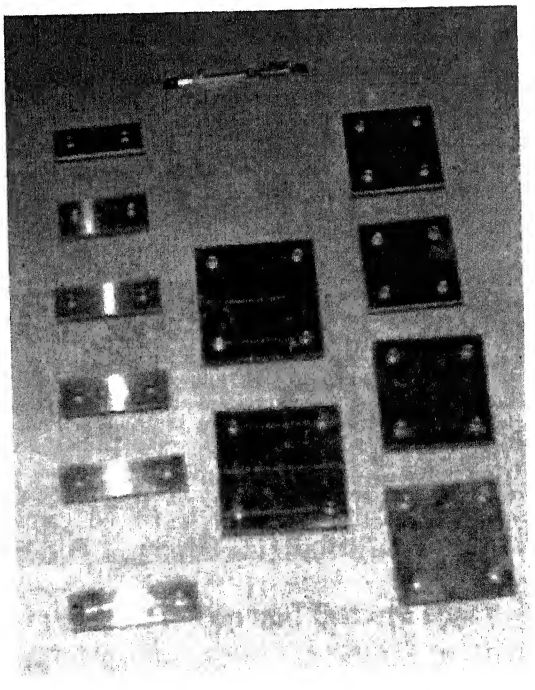

Plate 3.8. Pile cap for different spacing

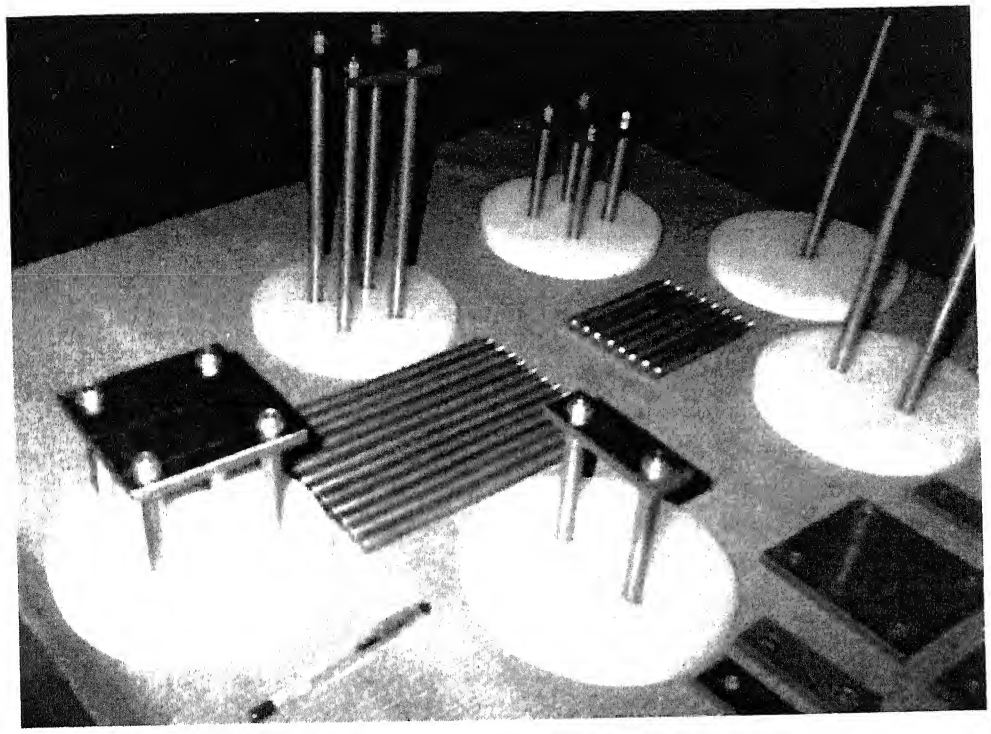

Plate 3.9. Different type of Group Piles

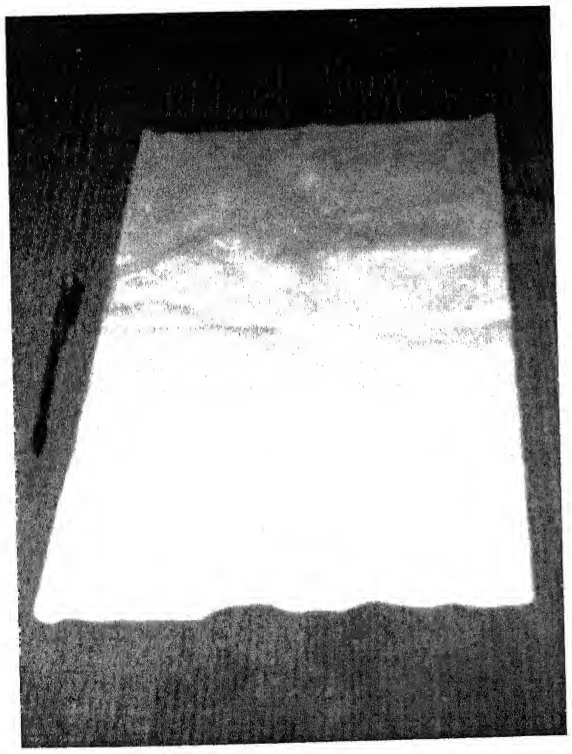

Plate 3.10. Rubber Membrane

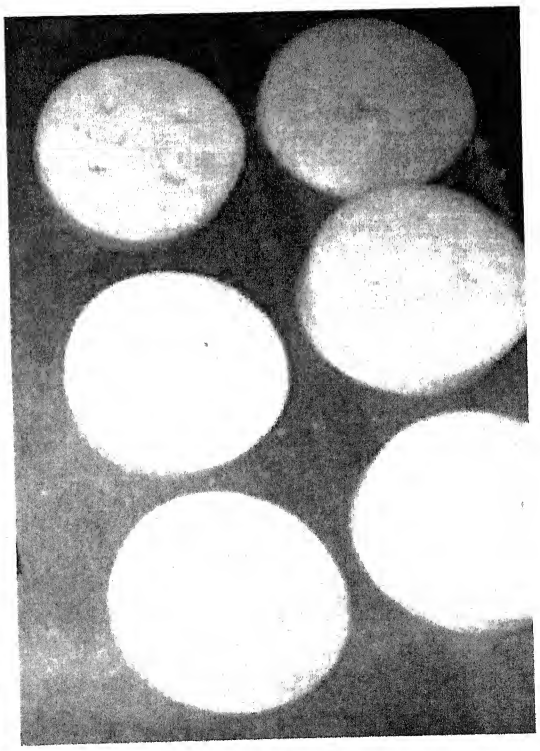

Plate 3.11. Top and Bottom Disc

In addition to above fabricated components, some pre-fabricated components were used in experimental setup. The details of these pre-fabricated components are discussed below;

3.2.5. Strain Controlled Loading Arrangement

A standard loading machine in which desired strain rate could be set was used to conduct the experiments. It consists of a fixed loading frame with a provision for proving ring to measure axial load and a base on which triaxial cell can be placed and which can be moved up and down at any rate desired using a gear and toothed wheel configuration. The compressive load was applied through a proving ring at a constant strain rate of 0.25mm/min with the help of mechanically load frame manufactured by HEICO. Compressive load was applied at the centre of pile in case of single pile and at the centre of pile cap in case of group pile by the loading plunger.

3.2.6. Self Compensating Mercury Control System

This system was used to apply and maintain the particular cell pressure during the tests. The pressure of the water in the triaxial cell results from the difference in the level between the mercury surfaces in two small cylinders connected by a thin flexible pressure tube.

3.2.7. Dial Gauge and Proving Ring

A dial gauge of 0.01mm sensitivity and 50mm capacity in conjunction with magnetic base plate was used to record the settlement of piles and pile groups under compressive load. Dial gauge was placed over the top plate of triaxial cell. A proving ring (proving ring constant 1div = 2.003N) was fitted with load plunger and loading frame to measure the axial load on the pile at the time of experiments.

3.3. Soil Considered and Conventional Test Results

The marine clay being used is from the sea bed at Vishakhapatnam, India from a depth of 30m. This marine clay passing sieve of aperture size 1.0mm was used. The liquid limit, plastic limit and specific gravity of the soil were 55.7%, 26.5% and 2.45 respectively. The optimum moisture content and maximum dry density were found to be 24.25% and 1.4gm/cc respectively. The clay samples were prepared at water content of 40% which was beyond the optimum moisture content. This soil samples were filled in mould at a density of 1.8gm/cc. The shear strength (c_u) and angle of internal friction ware 0.25kg/cm^2, and 3^0 respectively. The grain size distribution of the soil was determined by hydrometer analysis. The size of the particle varies from 0.001mm to 0.05mm and its variation is shown in Fig. 3.6.

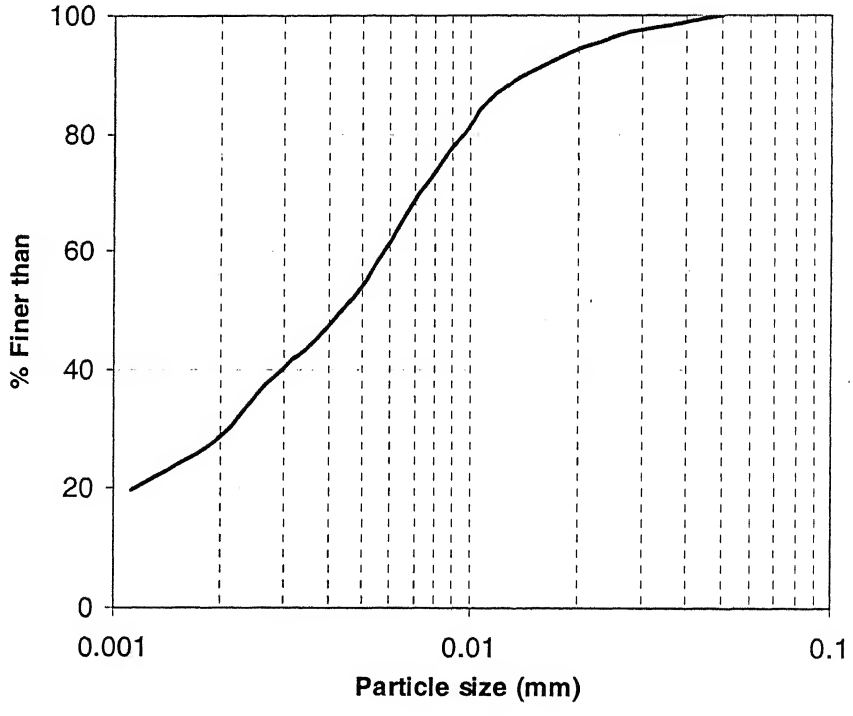

Fig. 3.6. Particle size distribution curve by Hydrometer analysis

3.4. Testing Methodology

The suggested methodology (Rao and Venkatesh 1988) involves tests in two phases. In the first phase tests were conducted by subjecting the soil to controlled vertical stress (σ_V) test. For this purpose a 195mm diameter cylindrical container with rigid walls was used to contain the soil with the embedded piles, so that the all round fluid pressure was effectively transferred to the soil in the vertical direction only. In the second phase, tests were conducted by subjecting the soil to controlled horizontal stresses (σ_H test). In this case, the soil containing the pile was enclosed by a rubber membrane and a steel frame within the soil provides the rigid ends in the vertical direction.

By conducting σ_V test, total resistance and tip resistance of piles were determined under controlled vertical stresses. The method for determining shaft resistance was not preferable owing to the difficulty of eliminating friction between soil and wall of the container. In the present study this problem was not significant because the larger diameter of the soil sample diminishes the effect of wall friction at the pile-soil interface for determination of total resistance.

In σ_H test, tip resistance and shaft resistance were determined separately under controlled horizontal stresses and ultimately the bearing capacity was separately studied in terms of tip resistance and shaft resistance.

By conducting independent test for point resistance and shaft resistance the bearing capacity factor N_c and adhesion factor β can be determined in case of single pile from the following expressions.

$$q_p = c_u N_c + \sigma_V \quad \text{.....(3.1)}$$

$$f_S = \beta c_u \quad \text{.....(3.2)}$$

In which, q_p is the unit tip resistance, f_S is average unit skin friction, c_u is the undrained shear strength of marine clay. The schematic diagram of controlled vertical test (σ_V test) and controlled horizontal test (σ_H test) are shown in Fig. 3.7. and Fig. 3.8. respectively.

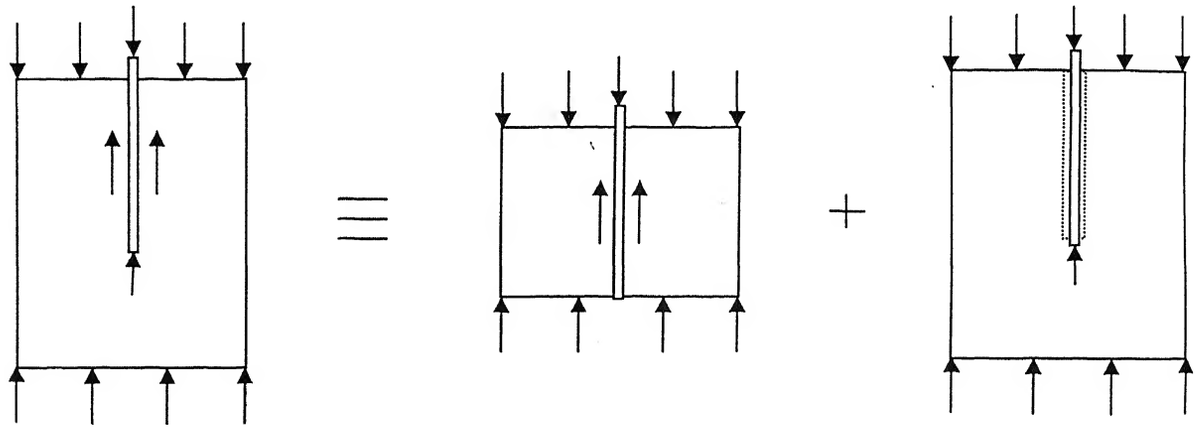

Total resistance by σ_V test | Shaft resistance | Tip resistance

(Under controlled vertical stress condition)

Fig. 3.7. Schematic diagram of σ_V test

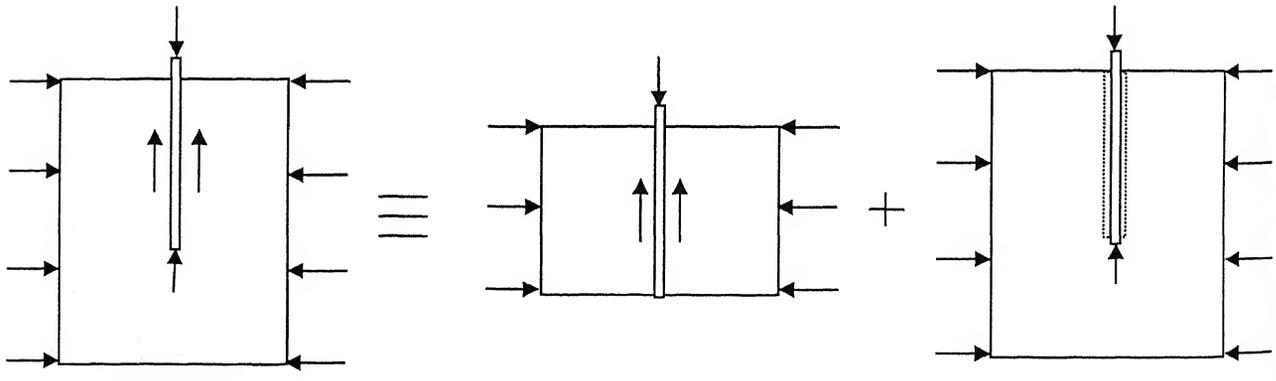

Total resistance by σ_H test | Shaft resistance | Tip resistance

(Under controlled horizontal stress condition)

Fig. 3.8. Schematic diagram of σ_H test

3.5. Testing Program

3.5.1. Controlled vertical stress test or σ_V test

For the σ_V tests, the pile testing apparatus consisted of a rigid cylinder 195mm diameter inside surface of which was coated with grease and covered by rubber membrane to minimize friction. Smooth steel piles of two different L/D ratio (8.93 and 17.5) but same diameter (14mm) were used in this experiment. The embedded length for L/D 8.93 and 17.5 were 80mm and 150mm respectively. For group piles, the spacing used was 4D, 5D and 6D. Piles were pushed into soil at a constant rate of 1.25mm/min up to the embedded length. The cylinder containing the soil and the embedded pile was housed in a large triaxial chamber (305mm diameter), so that a desired vertical stress could be applied on the soil through the fluid pressure.

In this test total resistance and tip resistance were determined separately. For total resistance the pile was directly pushed into the clay sample upto its embedded length. Then its load settlement behaviour was determined in triaxial test in two different vertical pressures of 0.3kg/cm^2 and 0.6kg/cm^2. In case of total resistance both bottom and side wall were in direct contact with clay sample so that measured load should indicate the total capacity of the pile. The experimental setup for this test was shown in Fig. 3.9.

For the tip resistance, the piles were surrounded by aluminium casings to eliminate any contact between the shaft and the soil, while maintaining a small clearance between pile and casing to eliminate friction (Fig. 3.10). The tip alone was in contact with the surface of the soil and the pile is not driven into the soil, although the point of contact is at the same depth as the embedded depth in other cases. After getting the total and tip resistance, the shaft resistance was determined by deducting those two values.

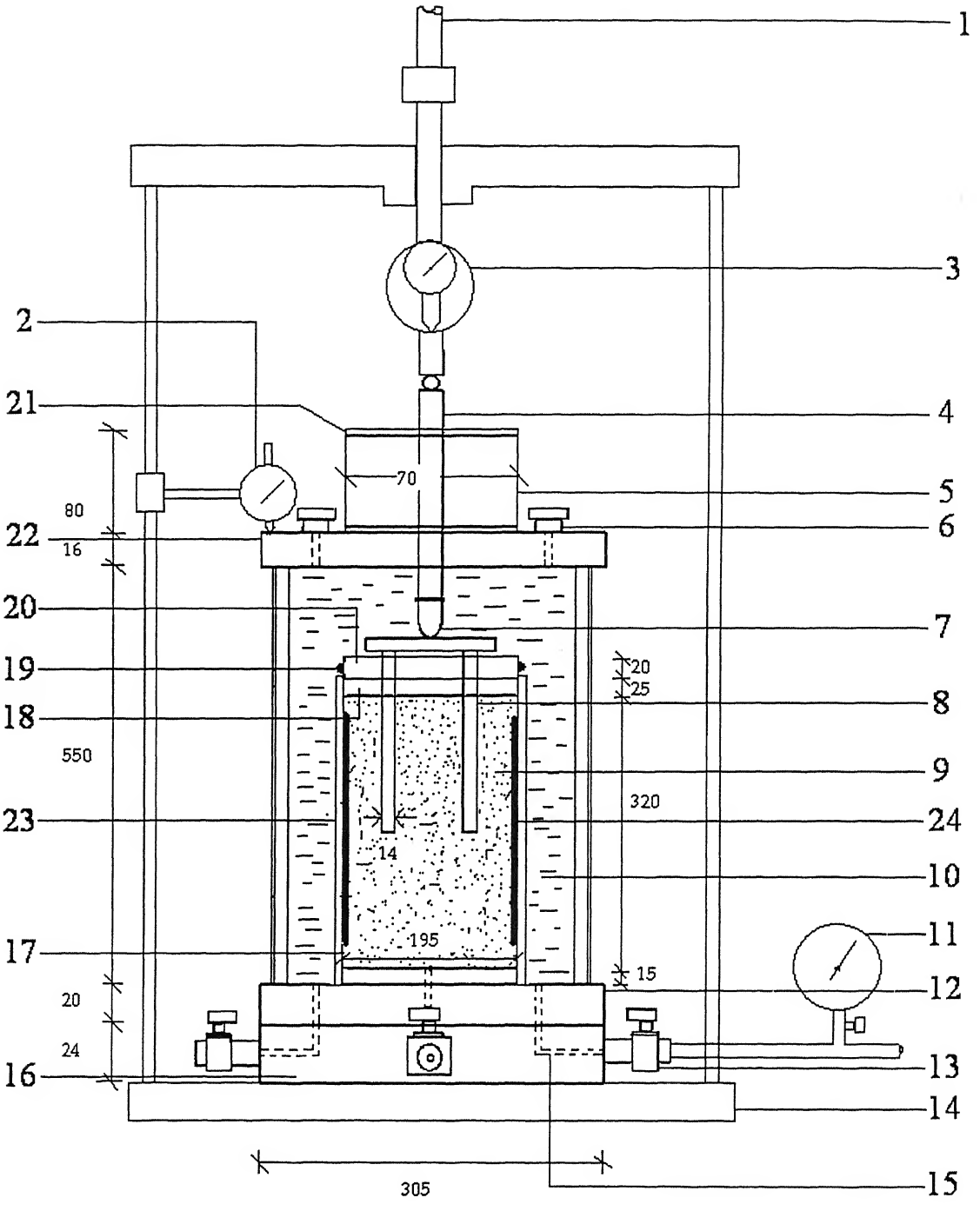

(All dimensions are in 'mm')

Fig. 3.9. σ_V Test for Total Resistance

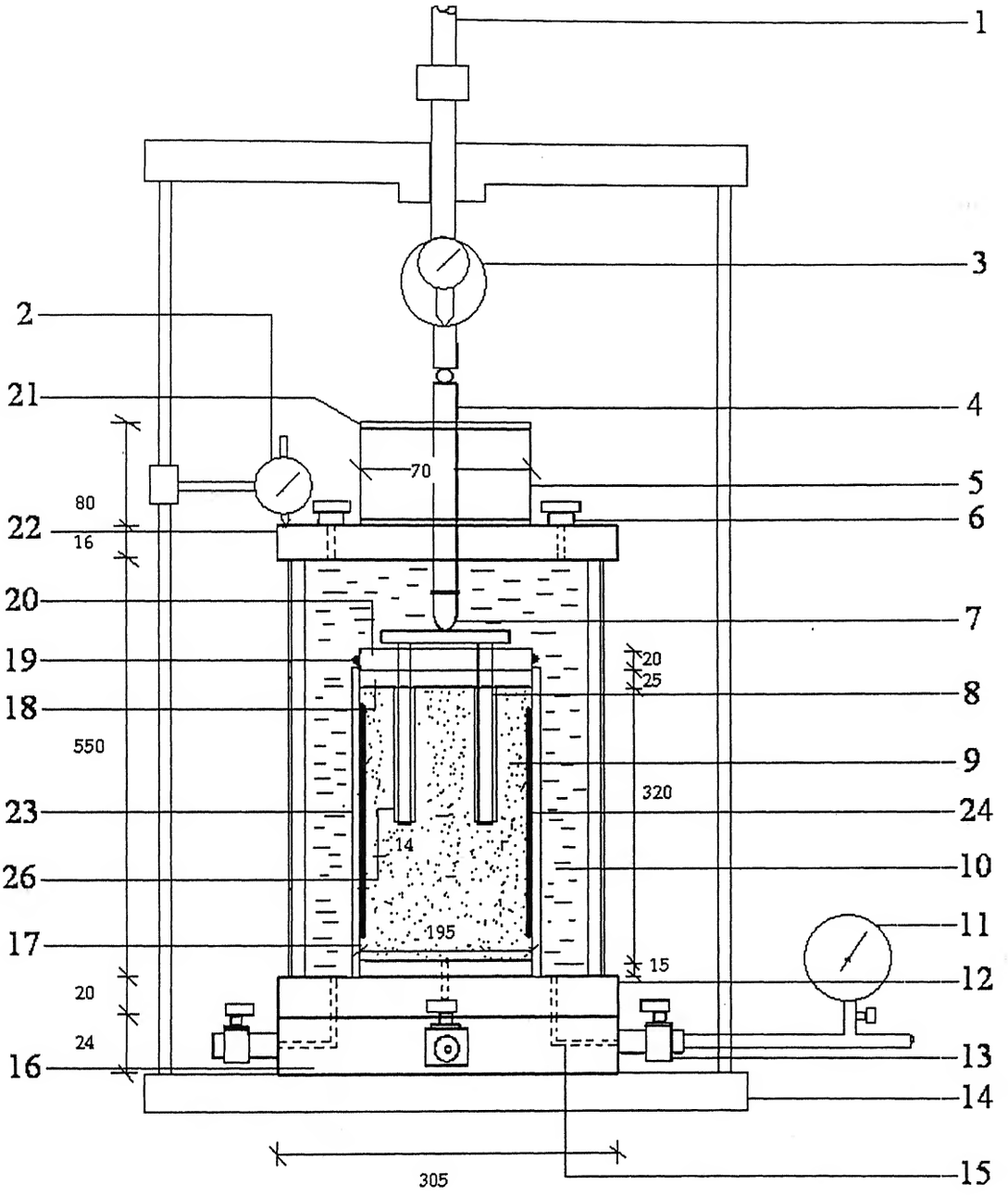

(All dimensions are in 'mm')

Fig. 3.10. σ_V Test for Tip Resistance

3.5.2. Controlled horizontal stress test or σ_H test

In σ_H tests, the rigid cylinder used for the previous test was removed and the soil was confined by the rubber membrane alone. Instead, a four-legged steel frame was provided to support two rigid discs at the top and bottom of the sample to ensure that the cell pressure was not transferred to the soil along the vertical direction. The L/D ratios, pile diameter and embedded length and strain rate were the same as for the σ_V tests.

In this test, the tip and shaft resistances were obtained separately. For the tip resistance, the setup and mechanism was same as for the σ_V test except the pressure in this case is coming from the horizontal direction. In this case only the tip of the pile was in contact with soil so that the load at the time of experiment indicated only the tip resistance at different horizontal stress. The setup for this test is shown in Fig. 3.11.

For the tests for shaft resistance, the shaft of the pile is in contact with the soil. The tip penetrates through the sample until it protrudes into a hollow space below the sample so that the tip resistance does not come into play. The length of the shaft in contact with the soil is adjusted so as to be equal to the embedded depth already mentioned. So the load coming through the pile was due to the shaft portion only as the pile tip was not in contact with soil. In this case the load indicated in the experiment was the shaft resistance. After getting tip resistance and shaft resistance, the total capacity of the piles and pile groups were determined by adding the two values. The setup for shaft resistance is shown in Fig. 3.12.

The detailing of all the experimental setup is shown in Table 3.1

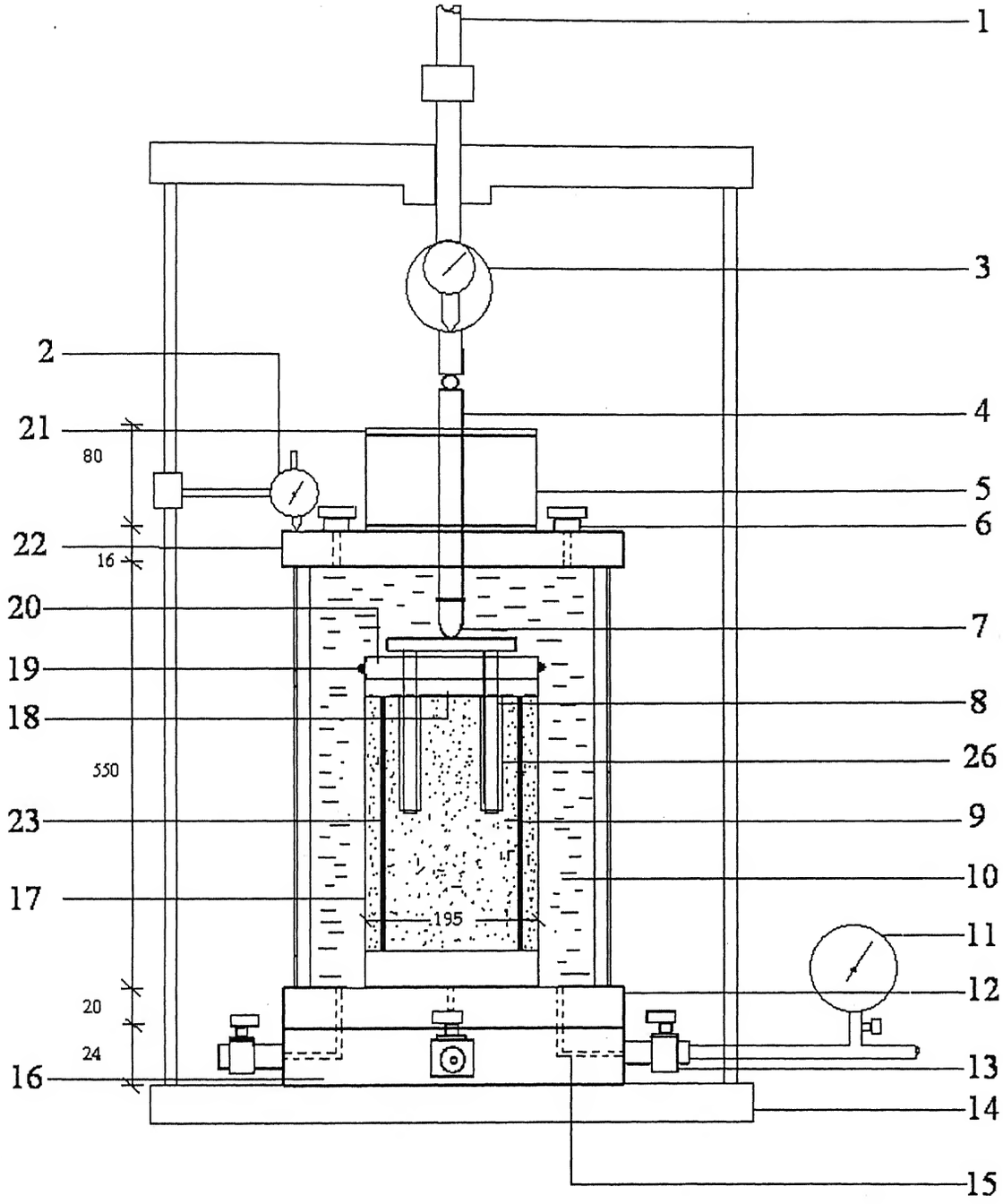

(All dimensions are in 'mm')

Fig. 3.11. σ_H Test for Tip Resistance

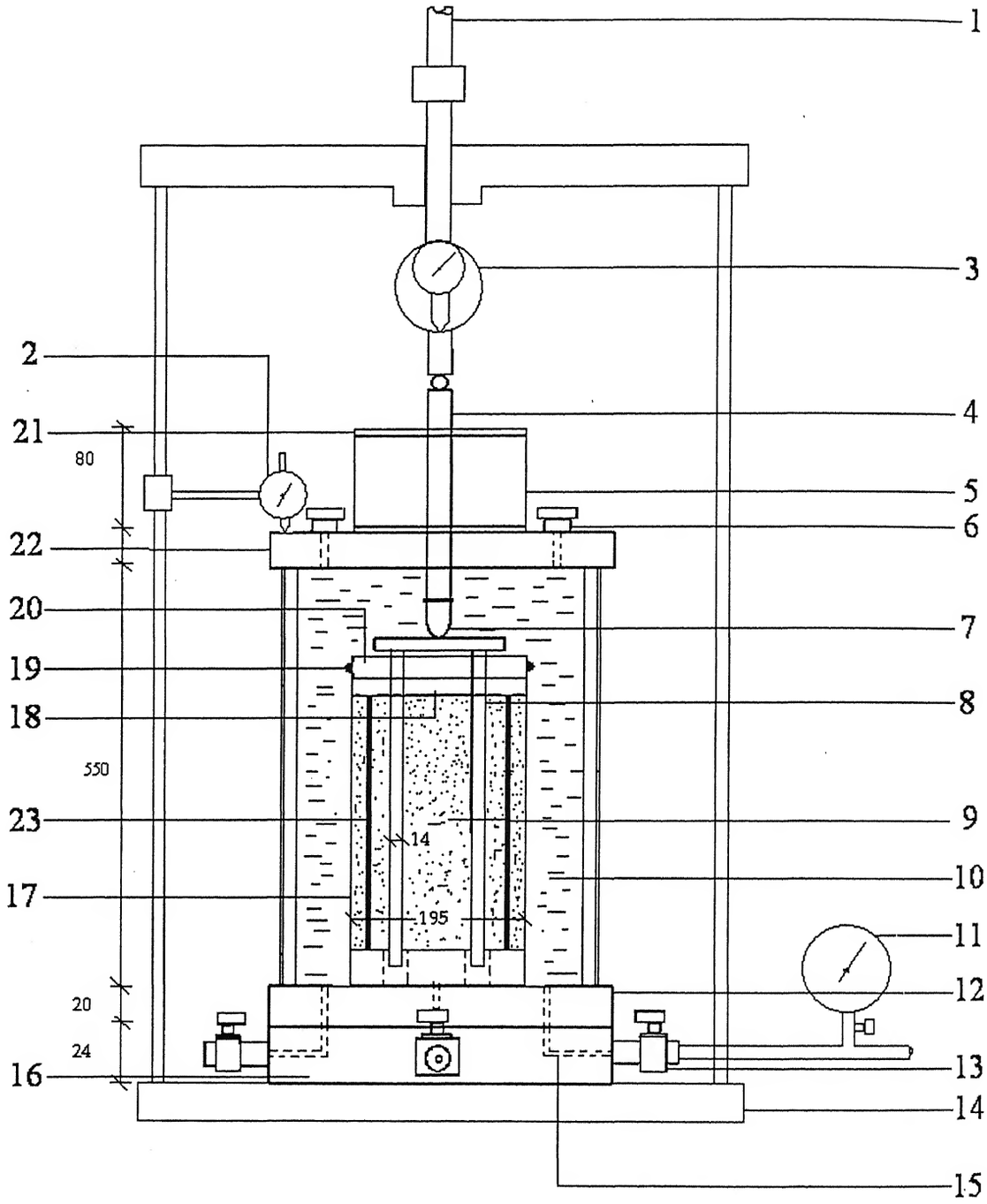

(All dimensions are in 'mm')

Fig. 3.12. σ_H Test for Shaft Resistance

Table 3.1. Detailing of experimental setup

Sl. No.	Description	Size
1	Loading Piston	Standard
2	Dial Gage	LC 1div = 0.01mm
3	Proving ring	LC 998.4divs = 2KN
4	Loading ram	Dia-14mm, Length-250mm
5	M.S. Circular Bar(Hollow)	Dia-70mm, Length-70mm
6	Air Vent Plug	Standard
7	Spherical Tip	-Do-
8	Single Pile	Dia-14mm, Length-135mm
9	Soil Sample	Dia-195mm, Length-320mm
10	Water	Normal
11	Cell Pressure Gauge	Standard
12	M.S. Ring	Dia-305mm, Thk-20mm
13	Valve	Standard
14	Base Frame	-Do-
15	Drainage	-Do-
16	M.S. Base Plate	Dia-305mm, Thk-24mm
17	Rubber Membrane	Tight fit with dia-195mm and length-400mm
18	Wooden Disc	Dia-195mm, Thk-25mm
19	O-ring	Tight fit with dia-195mm
20	Perspex Disc	Dia-195mm, Thk-24mm
21	Cover Plate	Dia-70mm, Thk-5mm
22	M.S. Top Cap	Dia-305, Thk-16mm
23	Rigid Cylinder	OD-199mm, Length-320mm
24	Rubber Membrane with grease coated wall	Tight fit with dia-195mm and length-320mm
25	Four legged frame	Length-280mm
26	Aluminium casing	As embedded length of piles

3.6. Preparation of Clay Sample for Different Tests

In σ_V test to determine the total resistance, the pile testing apparatus consisted of a rigid cylinder 195mm diameter inside surface of which was coated with grease and covered by rubber membrane. In the rigid cylinder mould clay was filled into three layers and each layer was tampered by 15 blows to achieve a constant density of 1.8gm/cc. Then pile was installed at a constant rate of 1.25mm/min upto its embedded depth. Here both shaft and tip were in direct contact with clay sample. The sample for this test for total resistance is shown in Plate 3.12.

In σ_V test for tip resistance first rigid cylinder was filled by clay at a constant density and then aluminium casings were penetrate upto embedded depth of pile into clay. Clay was taken out from these hollow aluminium casing. Then piles were penetrating through the aluminium casing so that there were a small clearance between pile and casing to eliminate side friction. The sample for tip resistance in σ_V test is shown in Plate 3.13.

In σ_H test to determine tip resistance, clay was confined by the rubber membrane alone. A four-legged steel frame was provided to support two rigid discs at the top and bottom of the sample. Other procedure and mechanism was same as in case of σ_V test for tip resistance. It is shown in Plate 3.14.

In σ_H test for shaft resistance, clay sample was prepared and confined by rubber membrane with four-legged steel frame. For this case the height of clay sample was the same as the embedded depth of pile. Then the tip of pile penetrated through the sample upto its embedded depth and the pile tip reached into a hollow space below the sample. Here only shaft of the pile was in touch with clay. The sample for this test is shown in Plate 3.15.

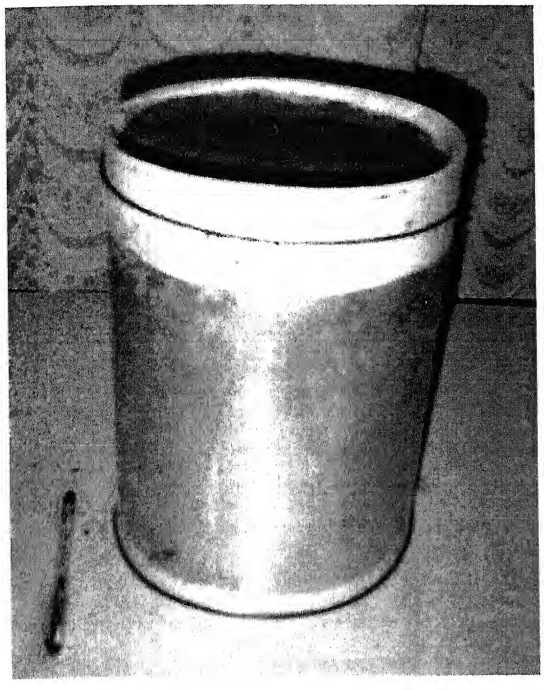

Plate 3.12. Sample for σ_V Test for Total Resistance

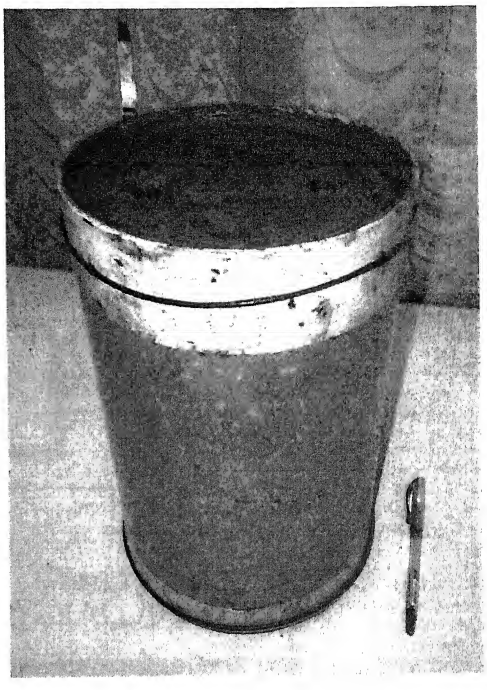

Plate 3.13. Sample for σ_V Test for Tip Resistance

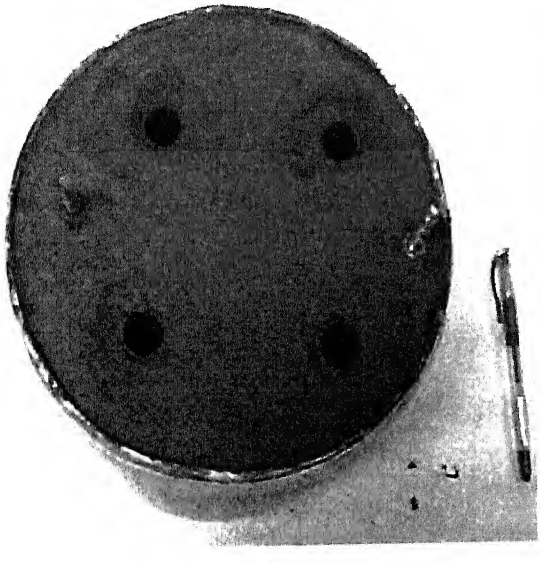

Plate 3.14. Sample for σ_H Test for Tip Resistance

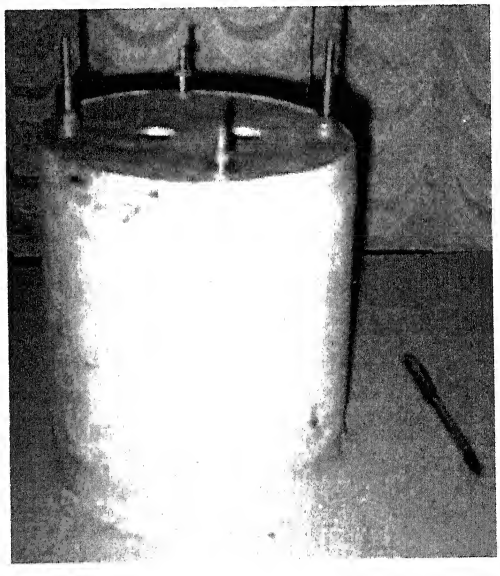

Plate 3.15. Sample for σ_H Test for Shaft Resistance

3.7. Scheme of the Testing Program

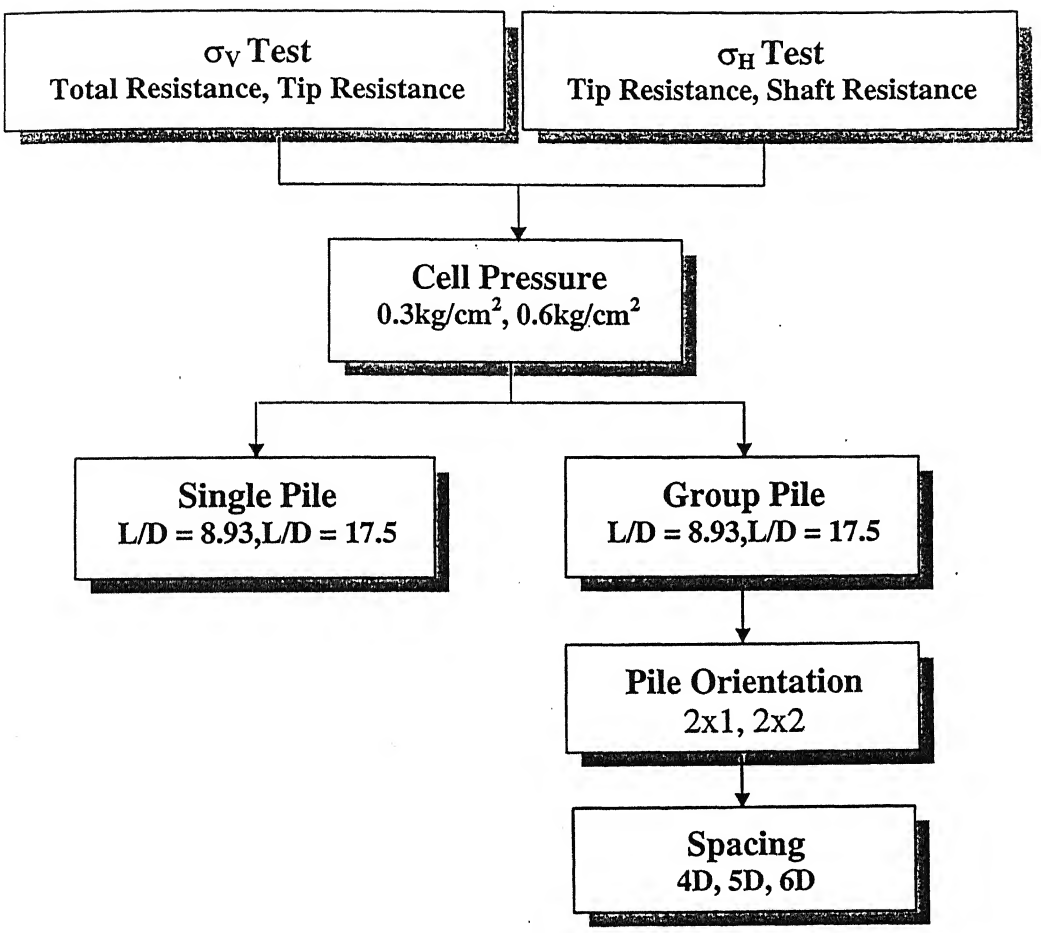

Fig. 3.13. Flowchart of the testing program scheme

Both σ_V test and σ_H test were done for two different cell pressure (0.3kg/cm^2 and 0.6kg/cm^2), two different pile (L/D of 8.93 and 17.5) and for three different pile group (spacing 4D, 5D and 6D). The total numbers of σ_V test and σ_H tests were equal and it was 56 each. So the total number of experiments that were carried out in the experimental part is 112.

Chapter - IV

Experimental Results and Discussions

4.1. General

In this chapter experimental results on the behaviour of single piles, line pile groups (2x1), square pile groups (2x2) subjected to compressive load at various stress conditions are presented. The influence of various parameters such as length to diameter ratio (L/D), configuration of pile group (line and square pile groups), spacing of piles (s), various stress conditions (σ_V and σ_H test), on the load displacement behaviour, total resistance, shaft resistance, tip resistance and efficiency of pile groups are studied. Also routine laboratory tests were conducted to determine the basic properties of Marine clay.

4.2. Test results for Basic Properties of Marine Clay

4.2.1. Determination of Liquid Limit and Plastic Limit

The percentage moisture content with number of blows is shown in Fig. 4.1.

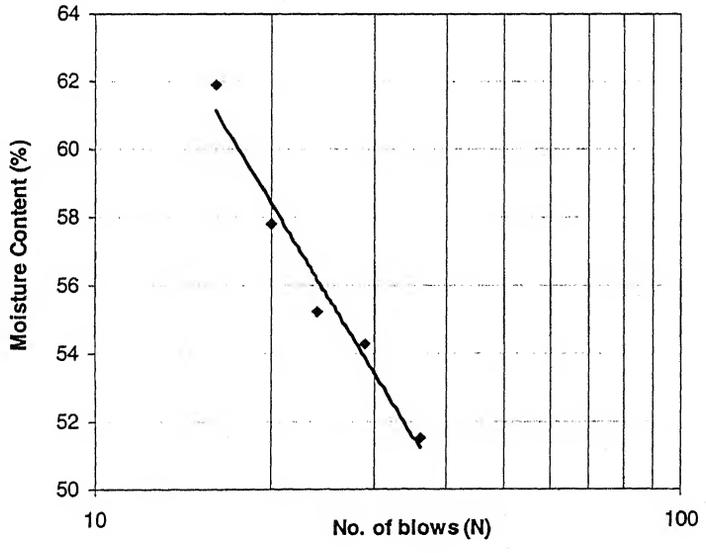

Fig. 4.1. Determination of Liquid Limit.

The moisture content corresponding to 25 blows (N) is determined from the above plot and it is 55.67%. The equation of the line is $W_L = -12.205 \log_{10}(N) + 94.961$.

From the plastic limit test the following results were obtained:

Plastic Limit (w_P) = 26.47%

Liquid Limit (w_L) = 55.67%

Plasticity Index (I_P) = (55.67-26.47) = 29.2%

Flow Index (I_F) = 12.205 %

Comments:

1) Soil is highly plastic (as I_P>17%).
2) As per IS Classification it belongs under 'CH' group (as w_L > 50 and it is above 'A' line on plasticity chart) i.e. highly compressible (H) inorganic clay (C).

4.2.2. Determination of Specific Gravity of Clay

From the laboratory test by using Pycnometer the average value of specific gravity was (G_s) 2.2.

4.2.3. Compaction Test for Determination of OMC and Maximum Dry Density

Proctor's Compaction test was done in laboratory to determine the optimum moisture content and maximum dry density of Marine clay. The moisture content vs. dry density curve is shown in Fig. 4.2. From the curve the following values were determined:

Maximum dry density = 1.398 gm/cc.

Optimum moisture content = 24.25 %.

The clay samples were prepared for the test at water content of 40% which was beyond the optimum moisture content.

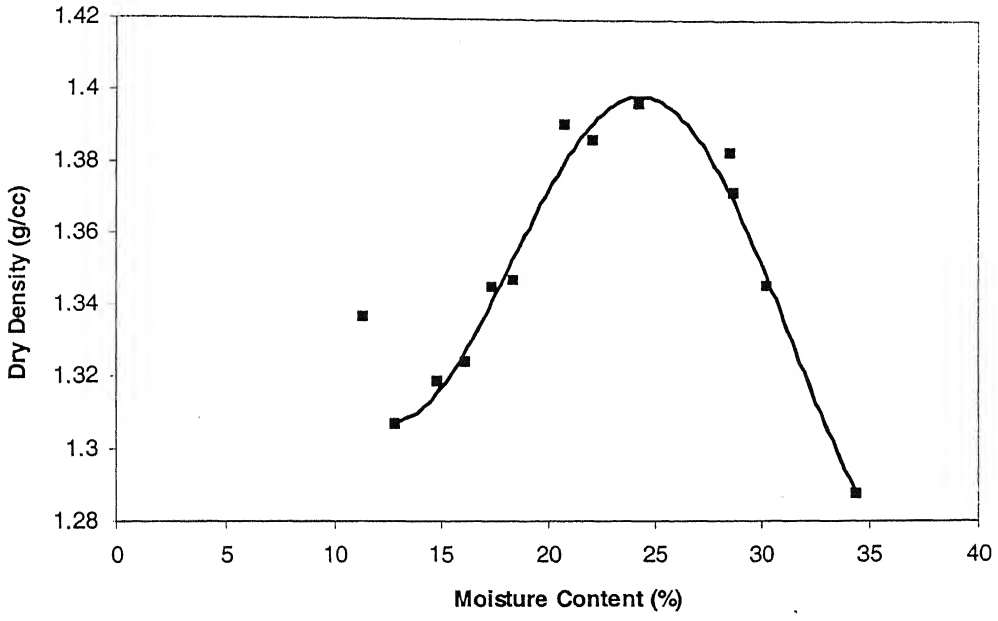

Fig. 4.2. Dry density vs. moisture content

4.2.4. Determination of Shear Strength parameter by Triaxial Test

Unconsolidated Undrained Tests were performed in the laboratory to determine undrained cohesion (c_u) and angle of friction (ϕ_u). From this test three Mohr's circle were plotted with three values of σ_1 and σ_3 as shown in Fig. 4.3.

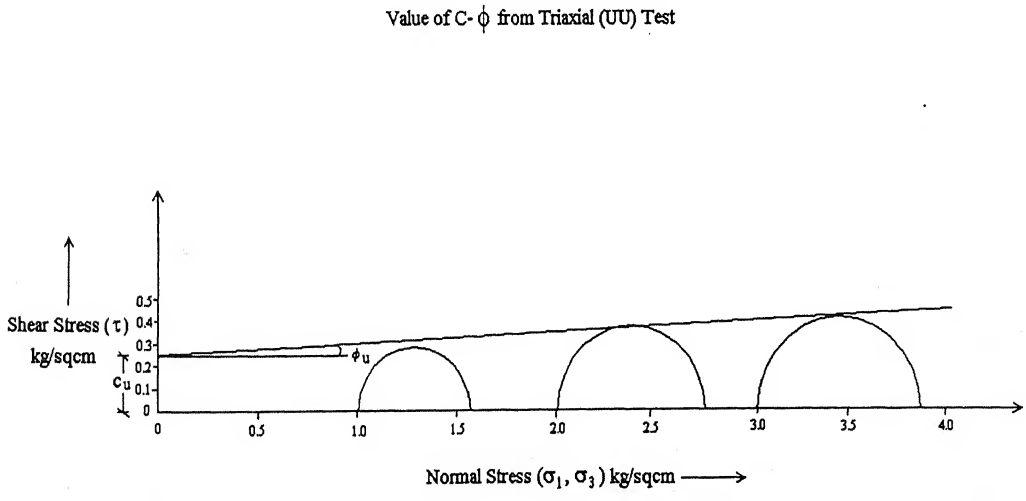

Fig. 4.3. Undrained shear strength parameters

Also shear strength envelop line was plotted and shear strength parameters were obtained as cohesion (c_u) of 0.25 kg/cm^2 and friction angle (ϕ_u) of 3^0.

4.3. Test Results of Single Piles and Pile Groups at σ_V and σ_H conditions

The experiments were conducted in a specially designed triaxial cell with enlarged dimensions (as described in Chapter III) to determine the bearing capacity of piles and pile groups under varying confining pressure. Controlled vertical stress tests (σ_V tests) were conducted to determine the tip resistance and total resistance of piles and pile groups. Similarly controlled horizontal tests (σ_H tests) were conducted to determine tip and shaft resistance separately. Load displacement diagrams were plotted for all the tests.

The general trend of all load displacement curves for all the tests was more or less same. At the initial stage of loading, the load displacement response of piles and pile groups was linear. The response gradually deviated to non-linear with increase of load and again after some load increase it regained some sort of linearity. The ultimate load of piles and pile groups were determined by single tangent when there is a definite peak and by double tangent when there is no definite peak in load displacement curves.

4.3.1. Test Results from σ_V Tests

In the controlled vertical stress tests (σ_V test) the total resistance and tip resistance of pile and pile groups of two different L/D ratios in two vertical cell pressures were determined.

4.3.1.1. Total Resistance from σ_V Tests

4.3.1.1.1. Single Pile

Load displacement behaviour of single pile for different cell pressure is shown in Fig. 4.4.

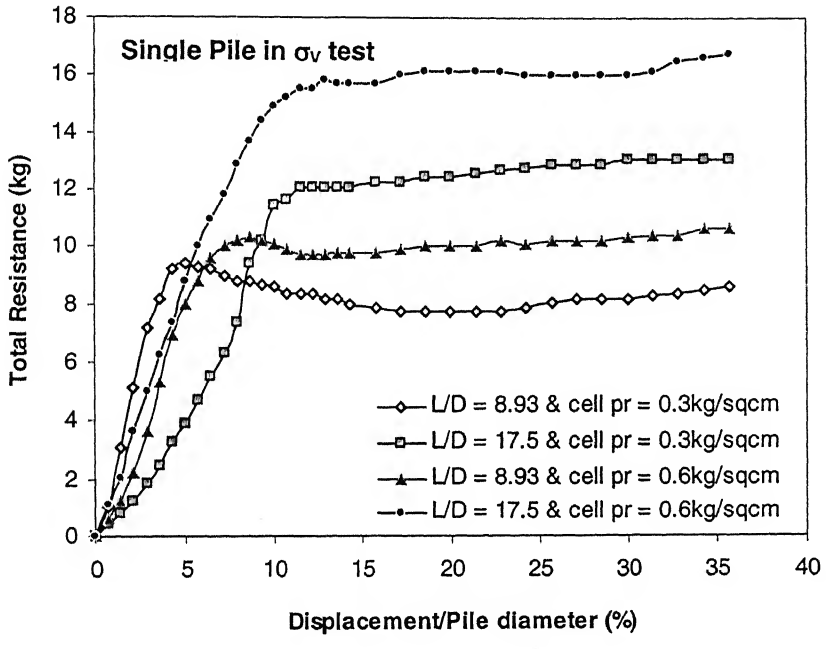

Fig. 4.4. Load displacement behaviour of single pile (σ_V test)

From the above plot it is observed that the total resistance of single pile increases with increasing cell pressure and L/D ratio. Response is linear at displacement ranging from 3 to 6% of pile diameter for cell pressure of 0.3kg/cm^2 and 7 to 8% of pile diameter for cell pressure of 0.6kg/cm^2. The mobilization of total resistance occurred at a pile head displacement of 5 to 11% of pile diameter for all the cell pressures and L/D ratios. After reaching its peak value it becomes linear. The percentage increase of total capacity at different cell pressure is about 9.57% for L/D = 8.93 and 33.33% for L/D = 17.5 respectively.

4.3.1.1.2. Line Pile Group (2x1)

The load displacement responses for 2x1 pile groups are shown in Fig. 4.5. and Fig. 4.6. for cell pressure of 0.3kg/cm^2 and 0.6kg/cm^2 respectively.

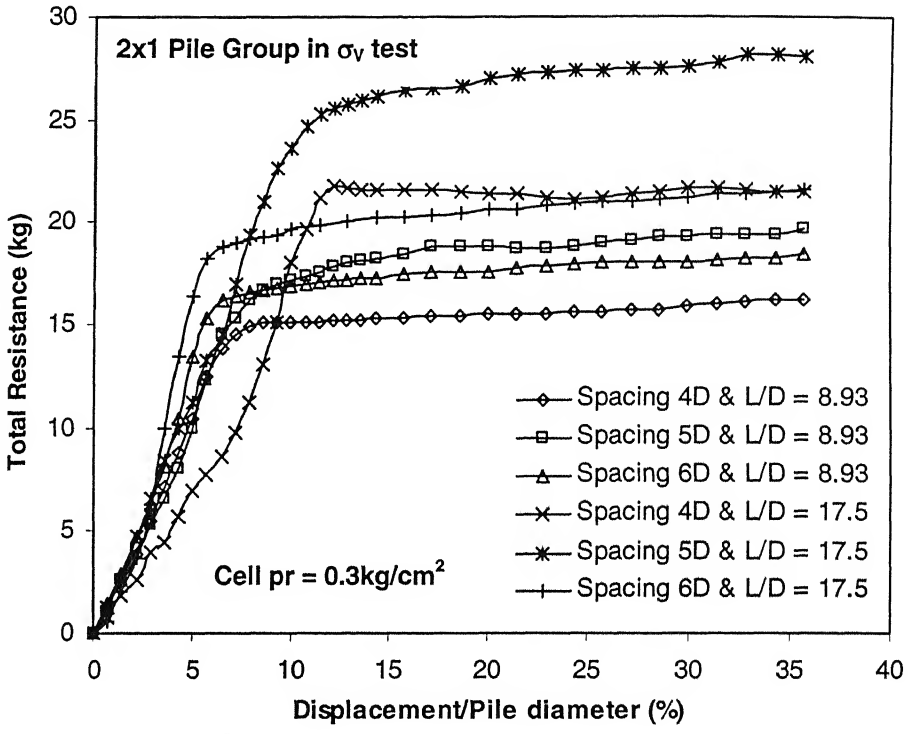

Fig. 4.5. Load displacement behaviour of 2x1 pile group for total resistance (σ_V test, cell pressure = 0.3kg/cm^2)

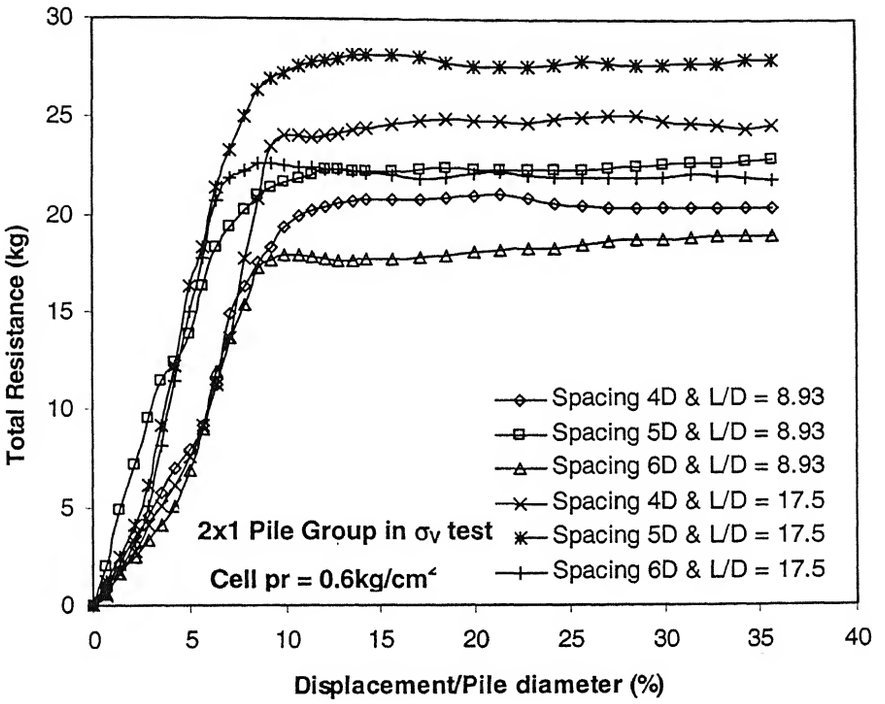

Fig. 4.6. Load displacement behaviour of 2x1 pile group for total resistance (σ_V test, cell pressure = 0.6kg/cm^2)

From the above figure it is observed that the load displacement responses are almost liner up to displacement of 4% to 10% of pile diameter and afterwards become nonlinear. The total capacity of line pile increases with increase in L/D ratio. The mobilization of total resistance occurs at a pile head displacement of 5 to 7% of the pile diameter for L/D = 8.93 and 5 to 12% of the pile diameter for L/D = 17.5.

The rate of increase of total resistance at various cell pressures is shown in Table 4.1. It is observed that the total capacity of pile group increases with increase in cell pressure for a particular value of L/D ratio. The rate of increase of total resistance is about 12% to 24 % more for L/D = 17.5 than L/D = 8.93. Again the rate of increase of total resistance is more for pile spacing of 5D and 6D.

Table 4.1. Rate of increase of total resistance with cell pressure (σ_V test, 2x1 Pile Group)

Spacing	L/D	Total Resistance (kg)		% of Increase
		Cell pr = 0.3 (kg/cm^2)	Cell pr = 0.6 (kg/cm^2)	
4D	8.93	15	18	20
	17.5	21.75	23.5	8.04
5D	8.93	17.5	19.5	11.43
	17.5	22.5	28	24.44
6D	8.93	16.5	18.5	12.12
	17.5	19	22.5	18.42

The variation of total resistance for different L/D ratios and pile spacing at cell pressure of 0.3kg/cm^2 and 0.6kg/cm^2 are shown in Table 4.2. and Table 4.3.

Table 4.2. Rate of change of total resistance with spacing (σ_V test, 2x1 Pile Group, Cell pr = 0.3kg/cm^2)

Cell pressure = 0.3kg/cm^2					
L/D = 8.93					
s/D		% of Increase	s/D		% of Decrease
4	5		5	6	
15	17.5	16.67	17.5	16.5	5.71
L/D = 17.5					
s/D		% of Increase	s/D		% of Decrease
4	5		5	6	
21.75	22.5	3.45	22.5	19	15.55

Table 4.3. Rate of change of total resistance with spacing

(σ_V test, 2x1 Pile Group, Cell pr = 0.6kg/cm^2)

Cell pressure = 0.6kg/cm^2					
L/D = 8.93					
s/D		% of Increase	s/D		% of Decrease
4	5		5	6	
18	19.5	8.33	19.5	18.5	5.13
L/D = 17.5					
s/D		% of Increase	s/D		% of Decrease
4	5		5	6	
23.5	28	19.15	28	22.5	19.64

The total resistance increases with increase in pile spacing from 4D to 5D for all L/D ratio and cell pressures. The percentage of increase is about 8% to 16 % for L/D = 8.93 and 3 to 19% for L/D = 17.5 respectively. For L/D = 8.93, percent of decrease remains almost constant from spacing 5D to 6D. However for L/D = 17.5, the total resistance decreases sharply from 5D to 6D. The percentage decrease is about 15 to 20% for cell pressure of 0.3 kg/cm^2 and 0.6 kg/cm^2 respectively.

4.3.1.1.3. Square Pile Group (2x2)

The total resistances versus displacement curves for 2x2 pile groups were plotted for spacing 4D, 5D and 6D for different L/D ratio and different cell pressure (shown in Fig. 4.7. & 4.8.).

The load-displacement response of 2x2 pile groups are almost linear upto a displacement of about 8 to 10% of pile diameter for different cell pressures. Also the ultimate value of total resistance is reached at a pile head displacement of 7 to 13% of pile diameter.

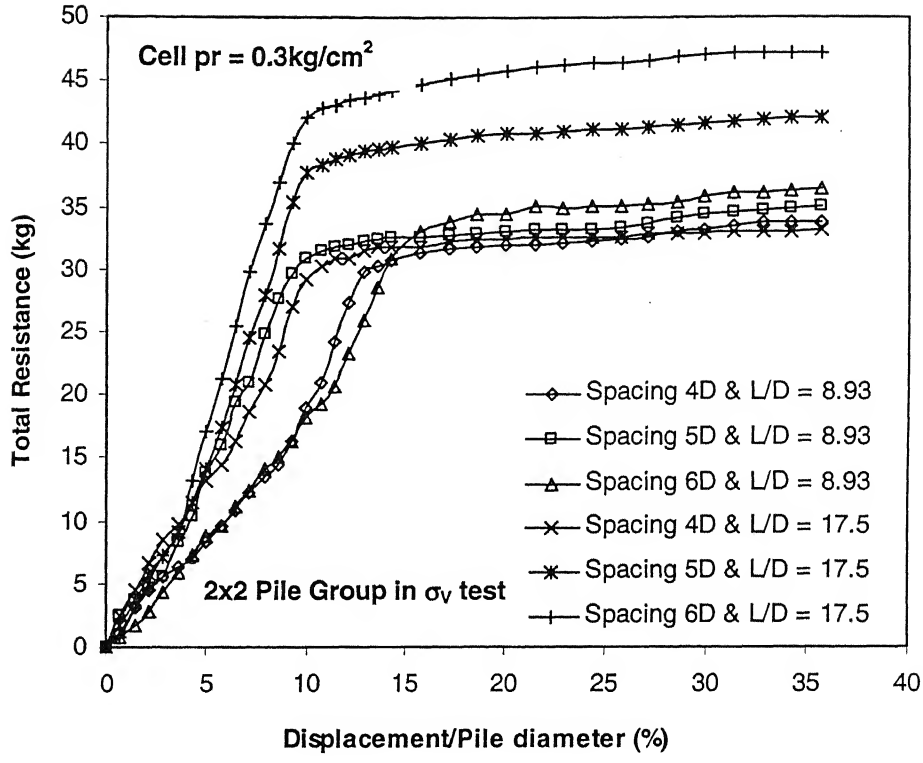

Fig. 4.7. Load displacement behaviour of 2x2 pile group for total resistance (σ_V test, Cell pr = 0.3kg/cm^2)

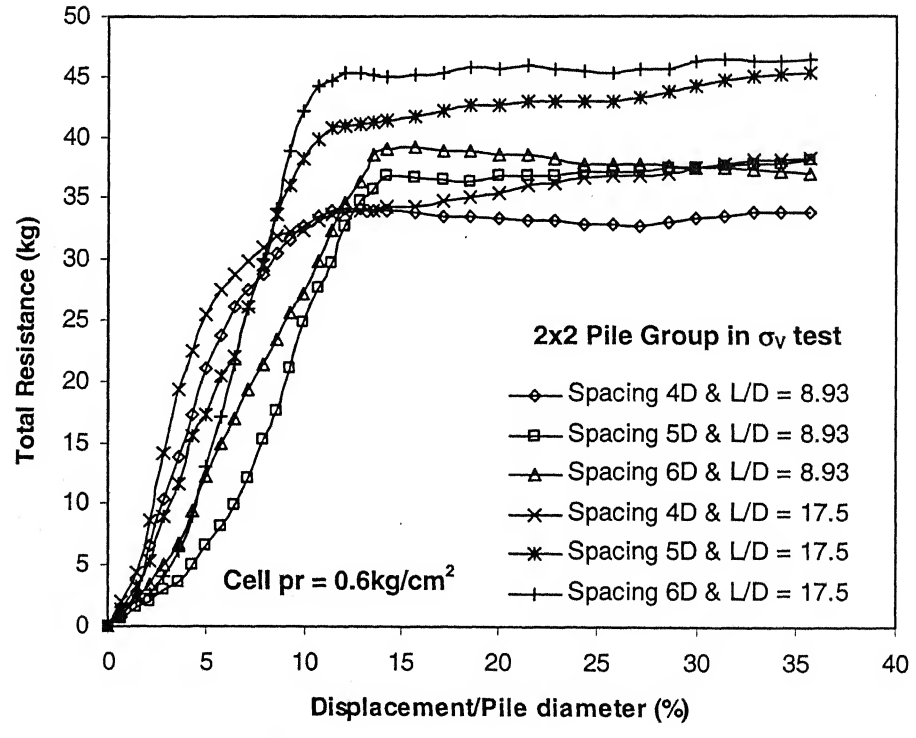

Fig. 4.8. Load displacement behaviour of 2x2 pile group for total resistance (σ_V test, Cell pr = 0.6kg/cm^2)

The rate of increase of total resistance with cell pressures is shown in Table 4.4. The total resistance increases with increase in cell pressure and L/D ratios.

Table 4.4. Rate of increase of total resistance with cell pressure (σ_V test, 2x2 Pile Group)

Spacing	L/D	Total Resistance (kg)		% of Increase
		Cell pr = 0.3 (kg/cm^2)	Cell pr = 0.6 (kg/cm^2)	
4D	8.93	30.5	34	11.47541
	17.5	31.5	35.5	12.69841
5D	8.93	32.5	36.6	12.61538
	17.5	37	38.5	4.054054
6D	8.93	34.5	39.2	13.62319
	17.5	42	43	2.380952

The total resistance increases linearly with increase in pile spacing. The percent increase of total resistance with spacing is about 6.15 to 13% for cell pressure of $0.3kg/cm^2$ and 7.1 to 11.67% for cell pressure of $0.6kg/cm^2$. It is shown in Table 4.5 and 4.6.

Table 4.5. Rate of change of total resistance with spacing (σ_V test, 2x2 Pile Group, Cell pr = $0.3kg/cm^2$)

Cell pressure = $0.3kg/cm^2$					
L/D = 8.93					
s/D		% of Increase	s/D		% of Increase
4	5		5	6	
30..5	32.5	6.56	32.5	34.5	6.15
L/D = 17.5					
s/D		% of Increase	s/D		% of Increase
4	5		5	6	
31.5	37	17.46	37	42	13.51

Table 4.6. Rate of change of total resistance with spacing (σ_V test, 2x2 Pile Group, Cell pr = 0.6kg/cm^2)

Cell pressure = 0.6kg/cm^2					
L/D = 8.93					
s/D		% of Increase	s/D		% of Increase
4	5		5	6	
34	36.6	7.65	36.6	39.2	7.1
L/D = 17.5					
s/D		% of Increase	s/D		% of Increase
4	5		5	6	
35.5	38.5	8.45	38.5	43	11.67

4.3.1.2. Tip Resistance from σ_V Tests

4.3.1.2.1. Single Pile

The load displacement curve for tip resistance for single pile has a similar trend as for single pile for total resistance in σ_V tests. The load displacement curves for single pile in this test are shown in Fig. 4.9.

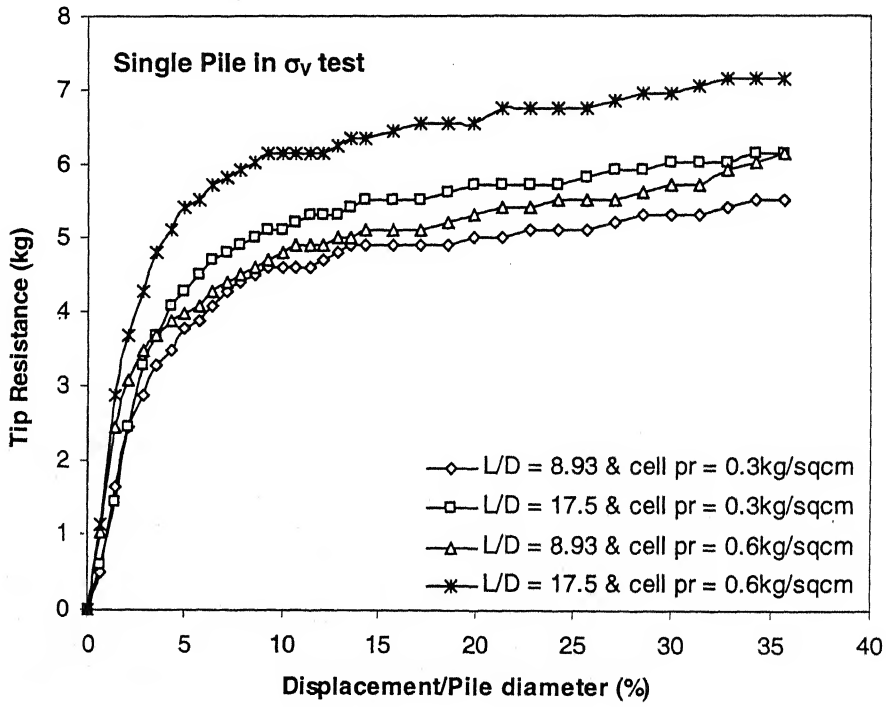

Fig. 4.9. Load displacement behaviour of single pile (σ_V test)

In all cases the curves exhibit a definite peak at pile displacement of 3 to 8% of pile diameter for all the cell pressures and L/D ratios.

4.3.1.2.2. Line Pile Group (2x1)

For 2x1 pile group load displacement curves were plotted to determine the tip resistance for pile spacing of 4D, 5D and 6D for different vertical cell pressures and L/D ratios. The load displacement curves for 2x1 pile group for cell pressure 0.3kg/cm^2 and 0.6kg/cm^2 for two different L/D ratios are shown in Fig. 4.10 and Fig. 4.11.

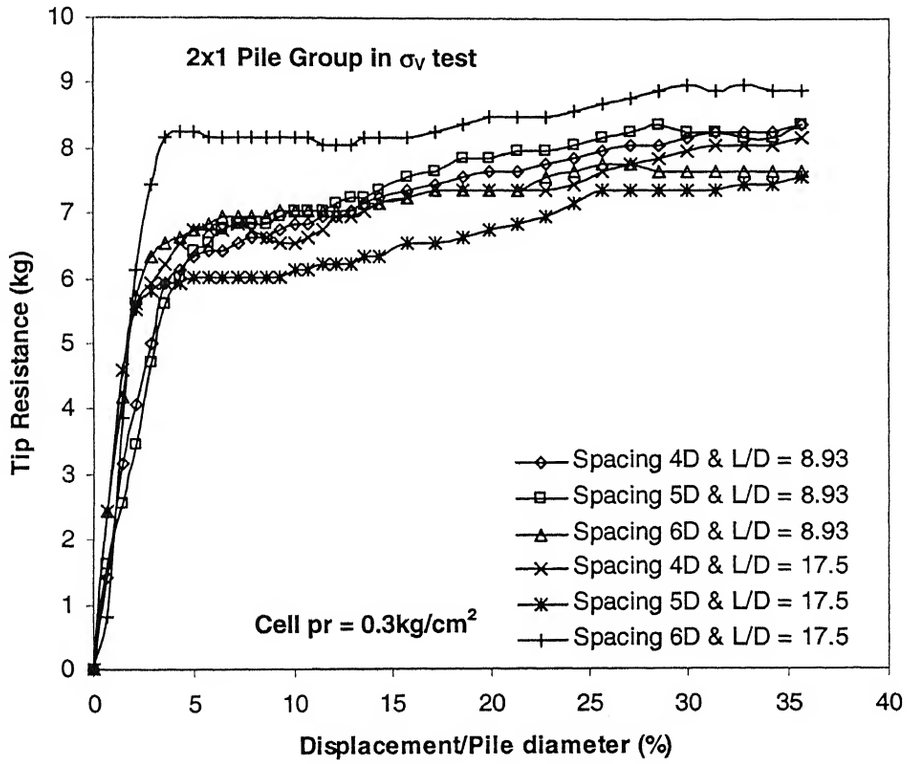

Fig. 4.10. Load displacement behaviour of 2x1 pile group for tip resistance (σ_V test, Cell pr = 0.3kg/cm^2)

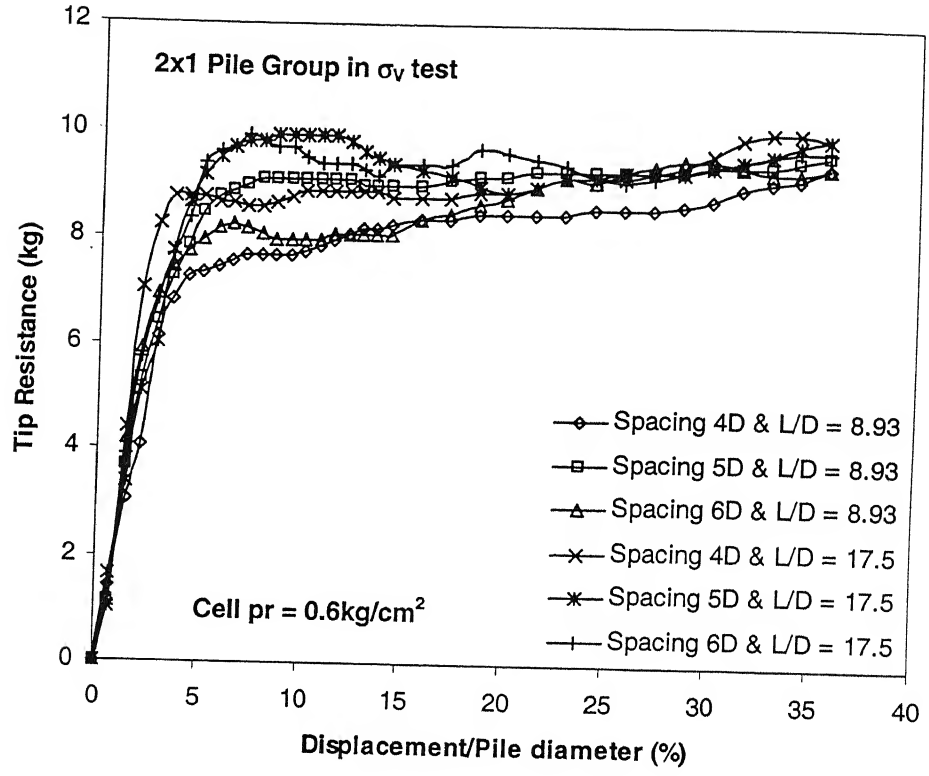

Fig. 4.11. Load displacement behaviour of 2x1 pile group for tip resistance (σ_V test, Cell pr = 0.6kg/cm^2)

It is observed from the figures that the tip resistance reaches its maximum value at a pile displacement of 2 to 5% and 3 to 9% of pile diameter at cell pressures of 0.3kg/cm^2 and 0.6kg/cm^2 respectively.

The rate of increase of tip resistance of 2x1 pile group for various cell pressures in σ_V test is shown in Table 4.7. It is observed that the tip resistance increases with increase in cell pressure for all spacing and L/D ratios. Maximum rate of increase is observed in case of spacing 5D and L/D of 17.5 and minimum is for spacing 6D and L/D of 8.93.

Table 4.7. Rate of increase of tip resistance with cell pressure (σ_V test, 2x1 Pile Group)

Spacing	L/D	Tip Resistance (kg)		% of Increase
		Cell pr = 0.3 (kg/cm^2)	Cell pr = 0.6 (kg/cm^2)	
4D	8.93	6.2	7	12.90323
	17.5	6.8	8.8	29.41176
5D	8.93	6.4	8.8	37.5
	17.5	6	10	66.66667
6D	8.93	6.8	7.2	5.882353
	17.5	8.4	9.8	16.66667

4.3.1.2.3. Square Pile Group (2x2)

The load displacement curves for 2x2 pile group for tip resistance were plotted for various spacing, cell pressure and L/D ratios. It is shown in Fig. 4.12 and Fig. 4.13 for cell pressure of $0.3kg/cm^2$ and $0.6kg/cm^2$.

The ultimate value of tip resistance is observed at a pile head displacement of 2 to 5% of pile diameter at cell pressure of $0.3kg/cm^2$ and 6 to 10% of pile diameter at cell pressure of $0.6kg/cm^2$.

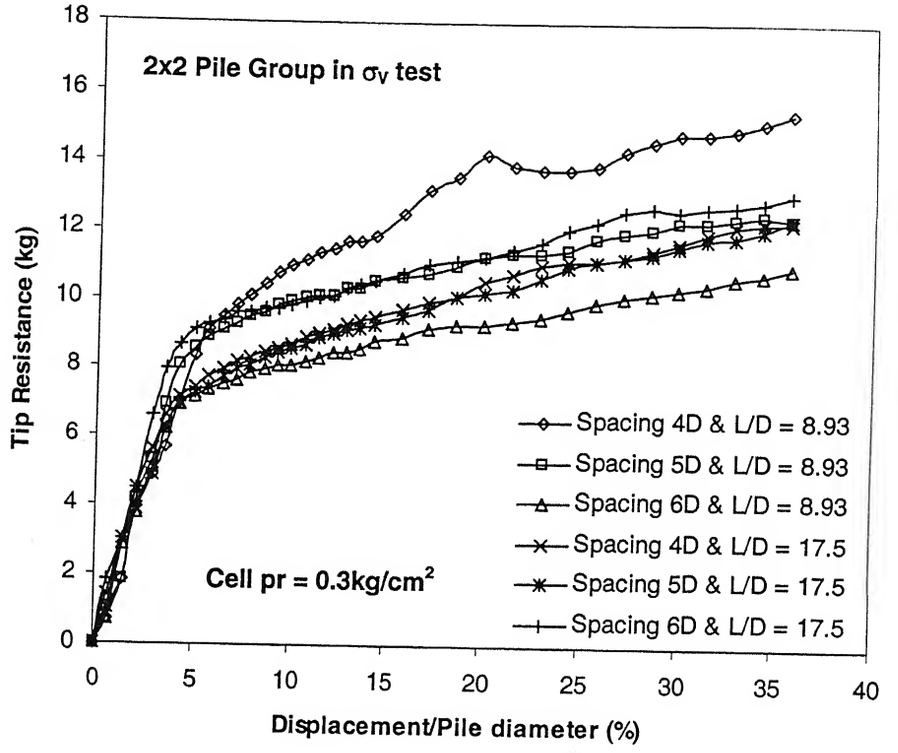

Fig. 4.12. Load displacement behaviour of 2x2 pile group for tip resistance (σ_V test, Cell pr = 0.3kg/cm^2)

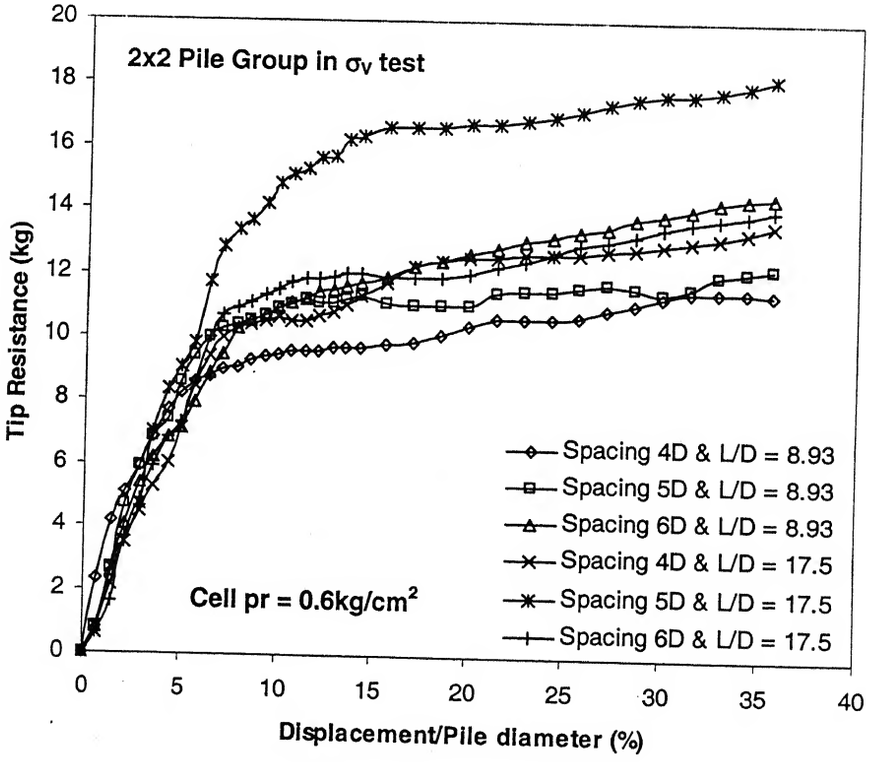

Fig. 4.13. Load displacement behaviour of 2x2 pile group for tip resistance (σ_V test, Cell pr = 0.6kg/cm^2)

The rate of increase of tip resistance of 2x2 pile group for various cell pressures in σ_V test is shown in Table 4.8. It is observed that the tip resistance increases with increase in cell pressure for all spacing and L/D ratios. Maximum rate of increase is observed at spacing 6D and L/D = 17.5 and minimum is observed at spacing 4D and L/D = 17.5.

Table 4.8. Rate of increase of tip resistance with cell pressure (σ_V test, 2x2 Pile Group)

Spacing	L/D	Tip Resistance (kg)		% of Increase
		Cell pr = 0.3 (kg/cm^2)	Cell pr = 0.6 (kg/cm^2)	
4D	8.93	5.5	7.8	41.818182
	17.5	7.5	9	20
5D	8.93	7	10.2	45.714286
	17.5	7.2	14.5	101.38889
6D	8.93	6.6	9.2	39.393939
	17.5	9.5	10.5	10.526316

4.3.1.2. Shaft Resistance from σ_V Tests

Shaft resistance in σ_V test is determined for piles under axially compressive load by the following relation:

Shaft Resistance = Total Resistance – Tip Resistance

In σ_V test the total and tip resistance are determined by experiments.

4.3.1.2.1. Single Pile

The rate of increase of shaft resistance with cell pressure is shown in Table 4.9. It is about 13.46 % and 46 % for L/D= 8.93 and L/D= 17.5.

Table 4.9. Rate of increase of shaft resistance with cell pressure (σ_V test, Single Pile)

Pile	L/D	Shaft Resistance (kg)		% of Increment
		Cell pr = 0.3 (kg/cm^2)	Cell pr = 0.6 (kg/cm^2)	
Single	8.93	5.2	5.9	13.46
	17.5	7.5	11	46.67

4.3.1.2.2. Line Pile Group (2x1)

The rate of increase of shaft resistance with cell pressure is shown in Table 4.10. It is observed that the shaft resistance increases with increase in cell pressure. It is about 5% to 25% and 5% to 19% for L/D = 8.93 and L/D = 17.5.

Table. 4.10 Rate of increase of shaft resistance with cell pressure (σ_V test, 2x1 Pile Group)

Spacing	L/D	Shaft Resistance (kg)		% of Increase
		Cell pr = 0.3 (kg/cm^2)	Cell pr = 0.6 (kg/cm^2)	
4D	8.93	8.8	11	25
	17.5	13.95	14.7	5.376344
5D	8.93	11.1	11.7	5.405405
	17.5	16.5	18	9.090909
6D	8.93	9.7	11.3	16.49485
	17.5	10.6	12.7	19.81132

4.3.1.2.3. Square Pile Group (2x2)

The rate of increase of shaft resistance with cell pressure is shown in Table 4.11. It is observed that the shaft resistance increases with increase in cell pressure. It is about 3% to 7% and 2% to 10% for L/D = 8.93 and L/D = 17.5.

Table. 4.11. Rate of increase of shaft resistance with cell pressure (σ_V test, 2x2 Pile Group)

Spacing	L/D	Shaft Resistance (kg)		% of Increase
		Cell pr = 0.3 (kg/cm^2)	Cell pr = 0.6 (kg/cm^2)	
4D	8.93	25	26.2	4.8
	17.5	24	26.5	10.41667
5D	8.93	25.5	26.4	3.529412
	17.5	25.8	26.5	2.713178
6D	8.93	27.9	30	7.526882
	17.5	30.5	32.5	6.557377

4.3.2. Test Results from σ_H Tests

In the controlled vertical stress tests (σ_V test) the tip resistance and shaft resistance of pile and pile groups of two different L/D ratios in two vertical cell pressures were determined. Total resistance of pile and pile groups are determined by adding tip and shaft resistance values.

4.3.2.1. Tip Resistance from σ_V Tests

4.3.2.1.1. Single Pile

Load displacement curves are plotted to find out the tip resistance of single pile in σ_H test. The load displacement behaviour of single pile for various L/D ratios and different cell pressure for tip resistance in σ_H test is shown in Fig. 4.14.

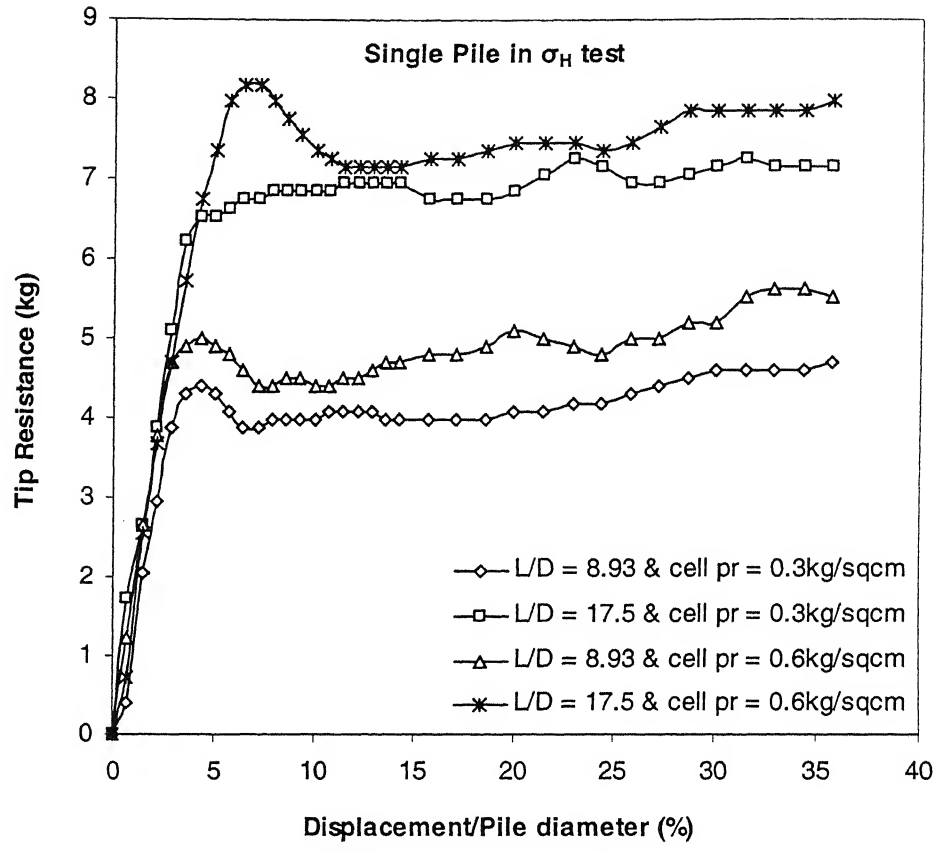

Fig. 4.14. Load displacement behaviour of single pile (σ_H test)

In all cases the curves exhibit a definite peak at a pile head displacement of 3 to 7% of pile diameter for all the cell pressures and L/D ratios.

4.3.2.1.2. Line Pile Group (2x1)

The load displacement responses for 2x1 pile group are shown in Fig. 4.15 and Fig. 4.16 for cell pressure of 0.3kg/cm^2 and 0.6kg/cm^2 respectively. It is observed from the figures that the tip resistance reaches its maximum value at displacement of 3 to 6% of pile diameter at cell pressure of 0.3kg/cm^2 and it is 4 to 7% of pile diameter at cell pressure of 0.6kg/cm^2.

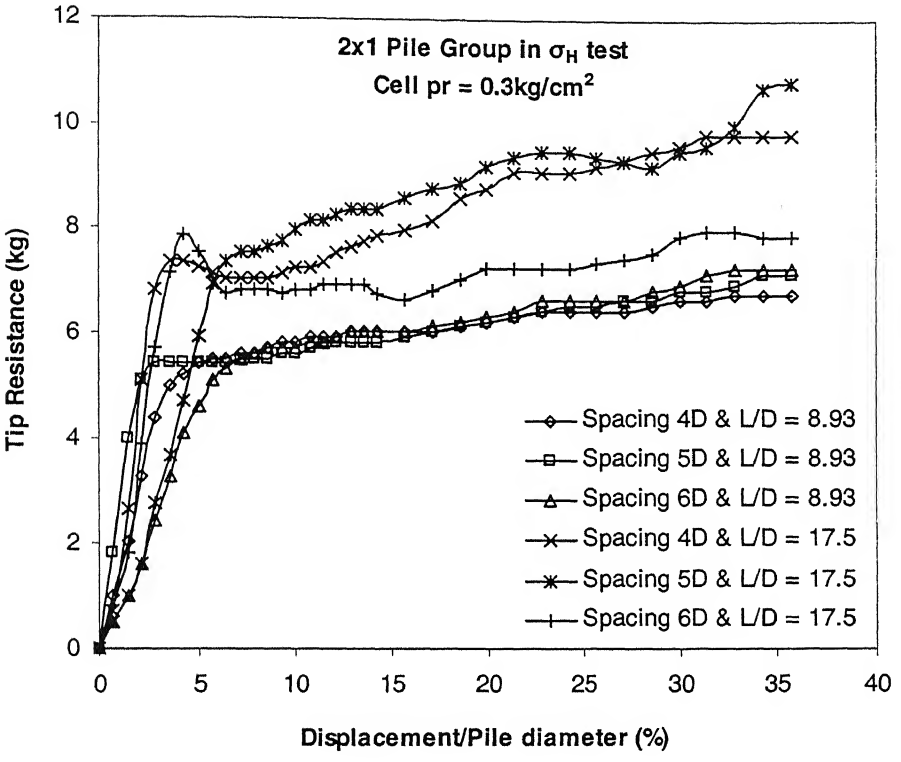

Fig. 4.15. Load displacement behaviour of 2x1 pile group for tip resistance (σ_H test, Cell pr = 0.3kg/cm^2)

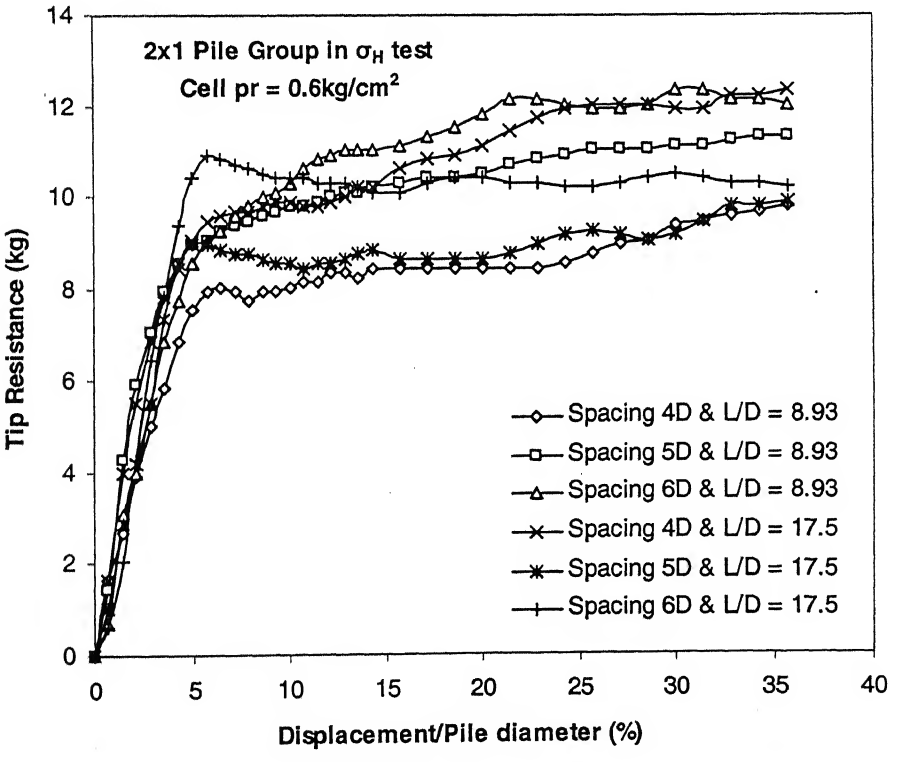

Fig. 4.16. Load displacement behaviour of 2x1 pile group for tip resistance (σ_H test, Cell pr = 0.6kg/cm^2)

The rate of increase of tip resistances of 2x1 pile groups for all cell pressures in σ_H test is shown in Table 4.12. The percentage increase in tip resistance is about 26% to 67 %. The rate of increase is more for L/D =8.93 than L/D =17.5.

Table 4.12. Rate of increase of tip resistance with cell pressure (σ_H test, 2x1 Pile Group)

Spacing	L/D	Tip Resistance (kg)		% of Increase
		Cell pr = 0.3 (kg/cm^2)	Cell pr = 0.6 (kg/cm^2)	
4D	8.93	5.4	8	48.14815
	17.5	7.4	9.6	29.72973
5D	8.93	5.5	9.2	67.27273
	17.5	7.5	9.5	26.66667
6D	8.93	5.6	8.8	57.14286
	17.5	7.9	10.8	36.70886

4.3.2.1.3. Square Pile Group (2x2)

The load displacement curves for 2x2 pile group for cell pressure 0.3kg/cm^2 and 0.6kg/cm^2 for two different L/D ratios are shown in Fig. 4.17 and Fig. 4.18. The magnitude of tip resistance increases with increase in L/D for both cell pressures. The mobilization of full tip resistance for 2x2 pile group in σ_H condition occurs at a pile movement of 3 to 8% of pile diameter at cell pressure of 0.3kg/cm^2 and it is 4 to 9% at cell pressure of 0.6kg/cm^2.

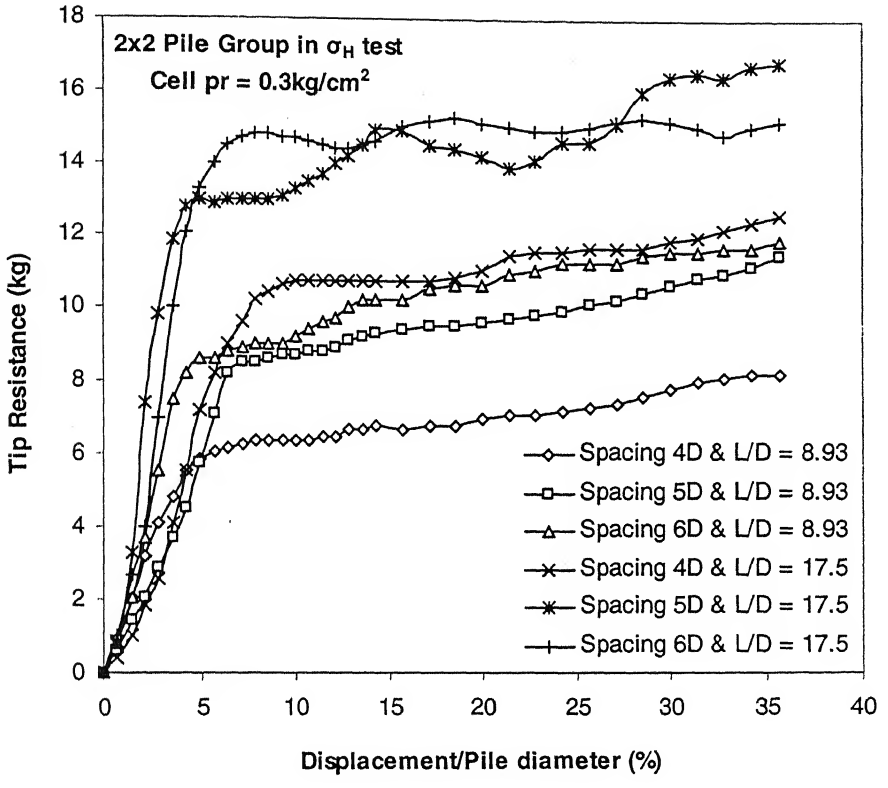

Fig. 4.17. Load displacement behaviour of 2x2 pile group for tip resistance (σ_H test, Cell pr = 0.3kg/cm^2)

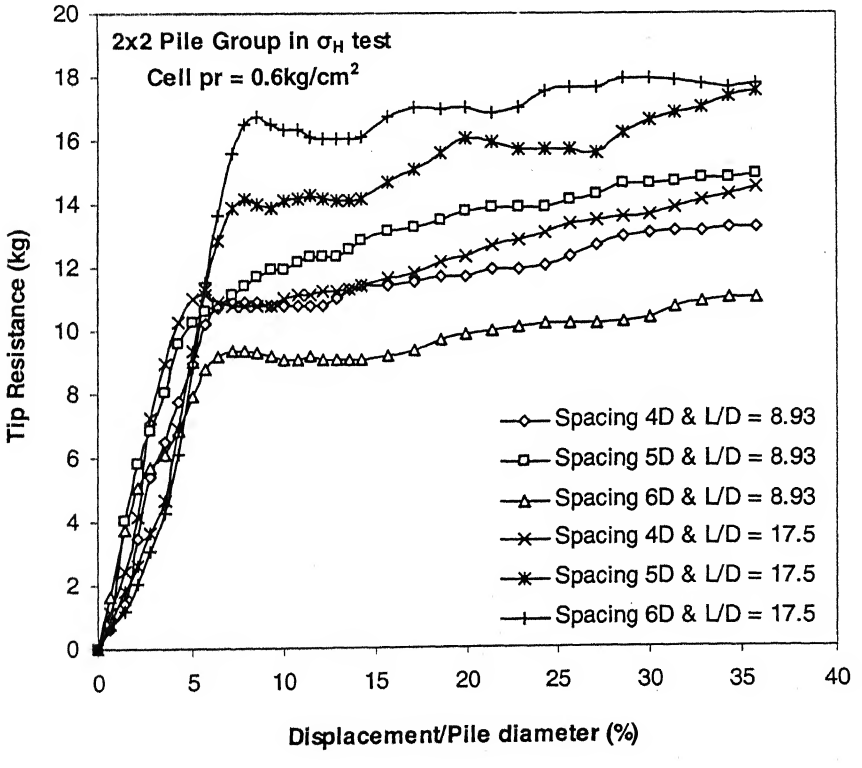

Fig. 4.18. Load displacement behaviour of 2x2 pile group for tip resistance (σ_H test, Cell pr = 0.6kg/cm^2)

The rate of increase of tip resistance of 2x2 pile groups for various cell pressures for different spacing in σ_H test is shown in Table 4.13. It is observed that the tip resistance of 2x2 pile group increases with increase in cell pressure for all spacing and L/D ratios. The percentage increase in tip resistance is about 4% to 58 %. The rate of increase is more for L/D = 8.93 than L/D =17.5.

Table 4.13. Rate of increase of tip resistance with cell pressure (σ_H test, 2x2 Pile Group)

Spacing	L/D	Tip Resistance (kg)		% of Increment
		Cell pr = 0.3 (kg/cm^2)	Cell pr = 0.6 (kg/cm^2)	
4D	8.93	6	9.5	58.33333
	17.5	10.8	11.2	3.703704
5D	8.93	8.5	11	29.41176
	17.5	13.2	14.2	7.575758
6D	8.93	8.8	9.5	7.954545
	17.5	14.5	16.6	14.48276

4.3.2.2. Shaft Resistance from σ_H Tests

4.3.2.2.1. Single Pile

Load displacement behaviour of single pile is shown for shaft resistance in σ_H tests in Fig. 4.19. The ultimate value of shaft resistance is observed at a pile head displacement of 4 to 6% of pile diameter.

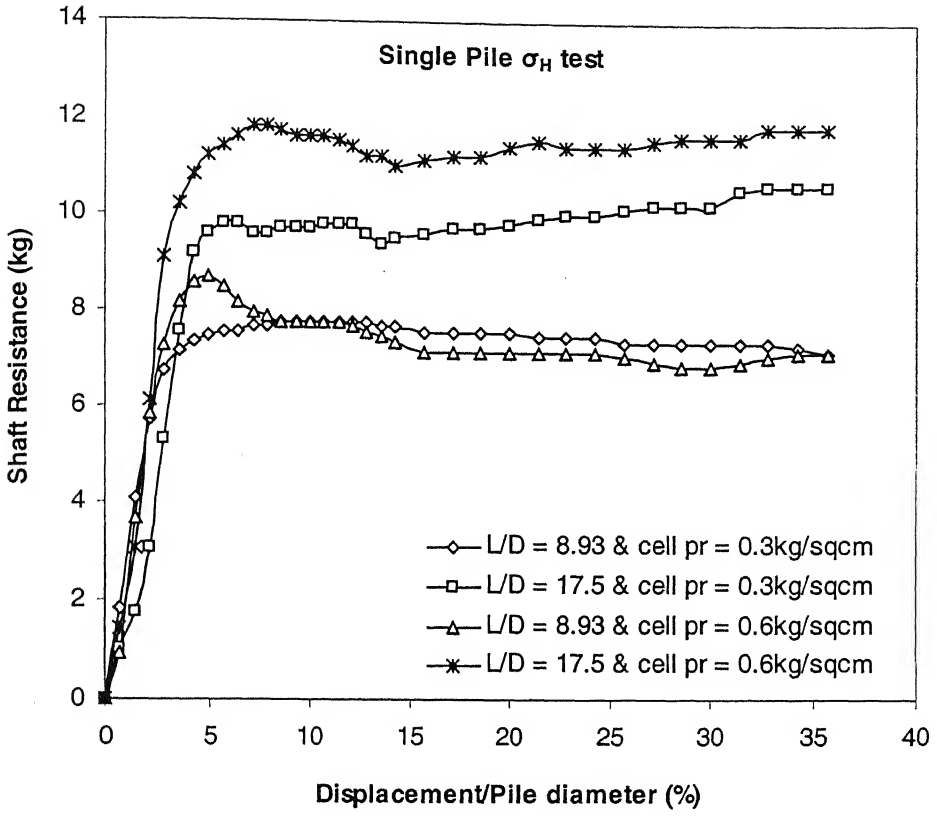

Fig. 4.19. Load displacement behaviour of single pile (σ_H test)

4.3.2.2.2. Line Pile Group (2x1)

For 2x1 pile group in σ_H tests load displacement curves were plotted to determine the shaft resistance for pile spacing of 4D, 5D and 6D for different vertical cell pressures and L/D ratios. The load displacement curves for cell pressure 0.3kg/cm^2 and 0.6kg/cm^2 for two different L/D ratios are shown in Fig. 4.20 and Fig. 4.21. The load displacement characteristics of all the curves for shaft resistances in σ_H test are almost same as reported earlier for σ_V tests. Shaft resistance reaches its maximum value at a displacement of 3 to 6% of pile diameter at cell pressure of 0.3kg/cm^2 and 4 to 9% of pile diameter at cell pressure of 0.6kg/cm^2.

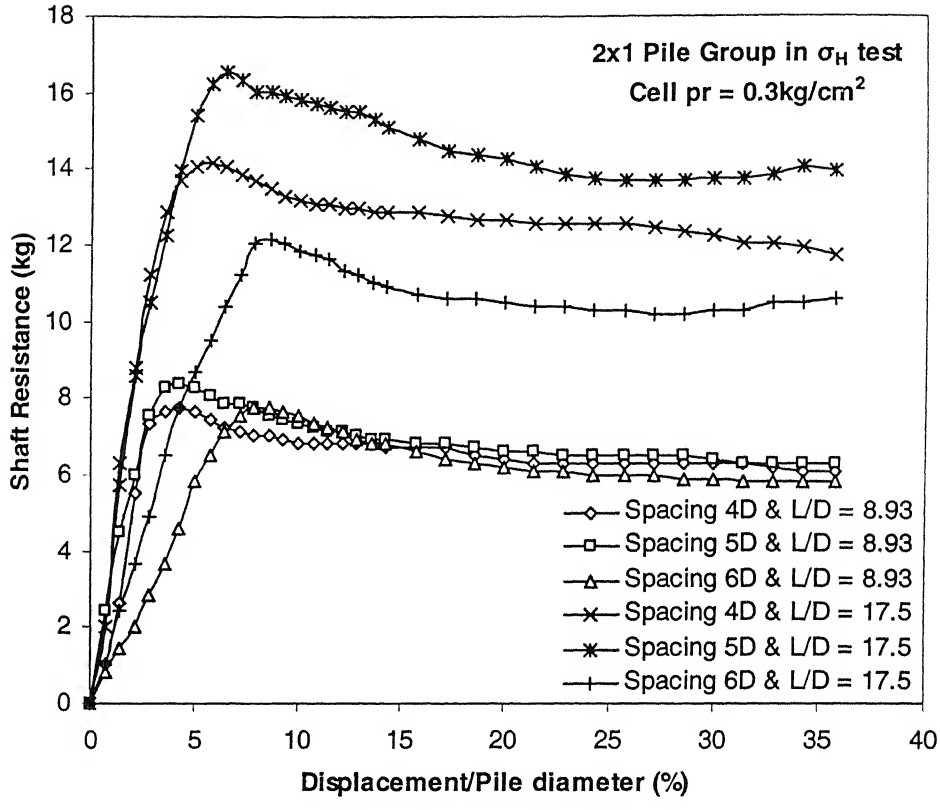

Fig. 4.20. Load displacement behaviour of 2x1 pile group for shaft resistance (σ_H test, Cell pr = 0.3kg/cm^2)

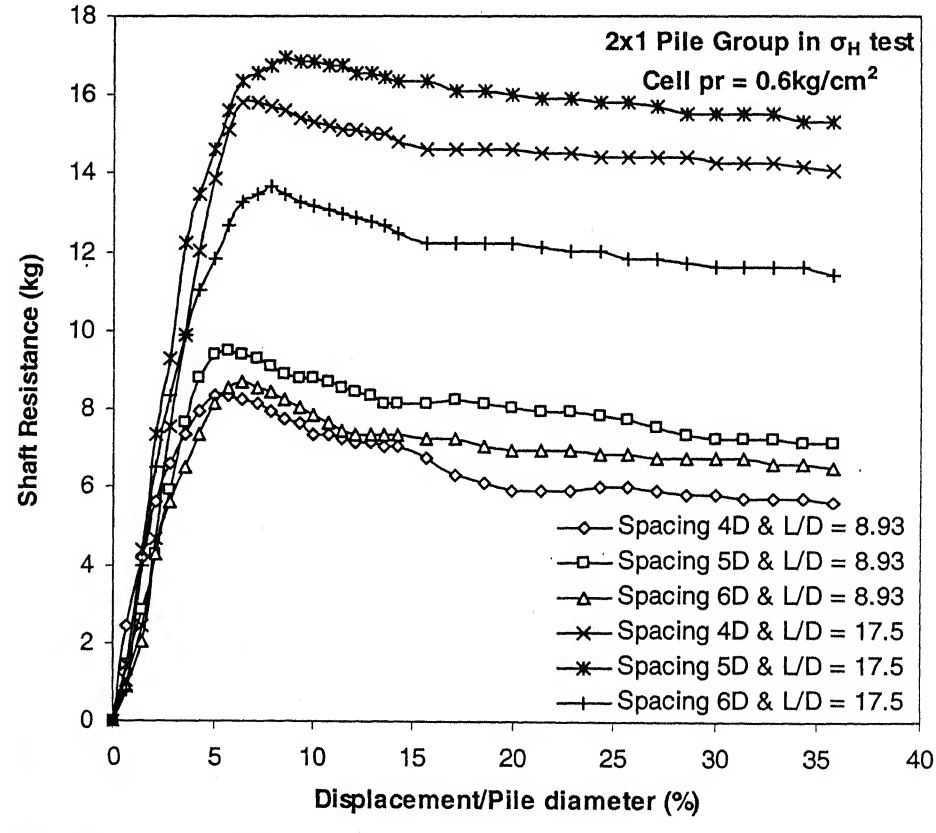

Fig. 4.21. Load displacement behaviour of 2x1 pile group for shaft resistance (σ_H test, Cell pr = 0.6kg/cm^2)

It is observed that the shaft resistance increases with increase in cell pressure for all spacing and L/D ratios. The rate of increment for various cell pressures for different spacing for 2x1 pile group in σ_H test is shown in Table 4.14. It is about 3% to 14%.

Table 4.14. Rate of increase of shaft resistance with cell pressure (σ_H test, 2x1 Pile Group)

Spacing	L/D	Shaft Resistance (kg)		% of Increase
		Cell pr = 0.3 (kg/cm^2)	Cell pr = 0.6 (kg/cm^2)	
4D	8.93	8.3	8.4	1.204819
	17.5	14.2	15.9	11.97183
5D	8.93	8.4	9.6	14.28571
	17.5	16.8	17.2	2.380952
6D	8.93	7.8	8.7	11.53846
	17.5	12.3	13.7	11.38211

4.3.2.2.3. Square Pile Group (2x2)

The load displacement curves for shaft resistance at cell pressures 0.3kg/cm^2 and 0.6kg/cm^2 for two different L/D ratios are shown in Fig. 4.22 and Fig. 4.23. From the figure it is observed that the ultimate value of shaft resistance is reached at a pile displacement of 5 to 12% of pile diameter at cell pressure of 0.3kg/cm^2 and 4 to 10% of pile diameter at cell pressure of 0.6kg/cm^2.

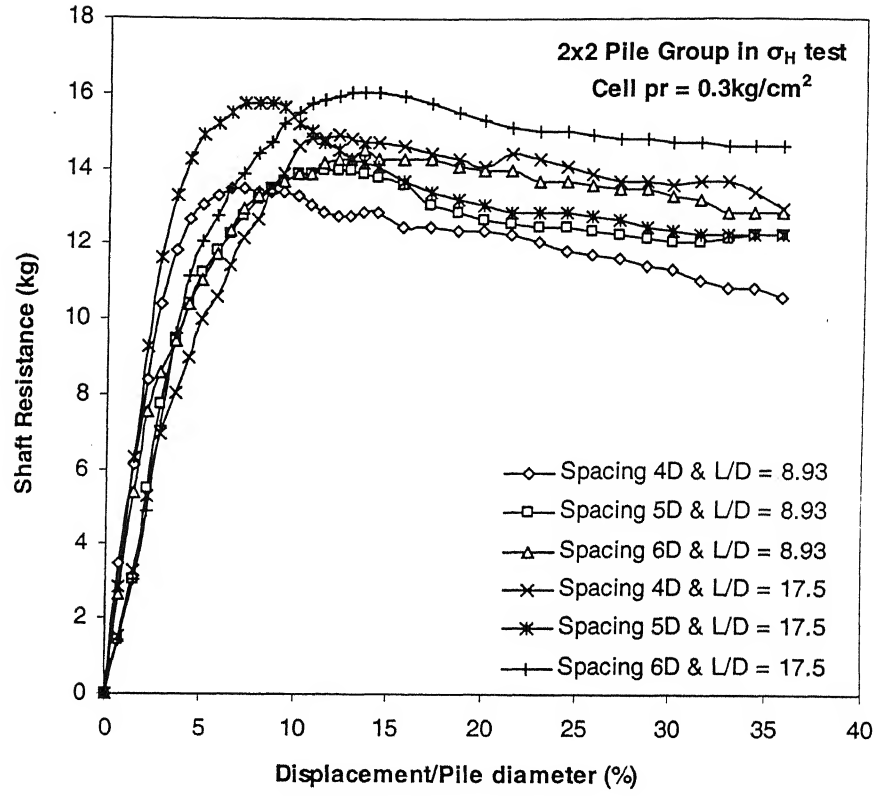

Fig. 4.22. Load displacement behaviour of 2x2 pile group for shaft resistance (σ_H test, Cell pr = 0.3kg/cm^2)

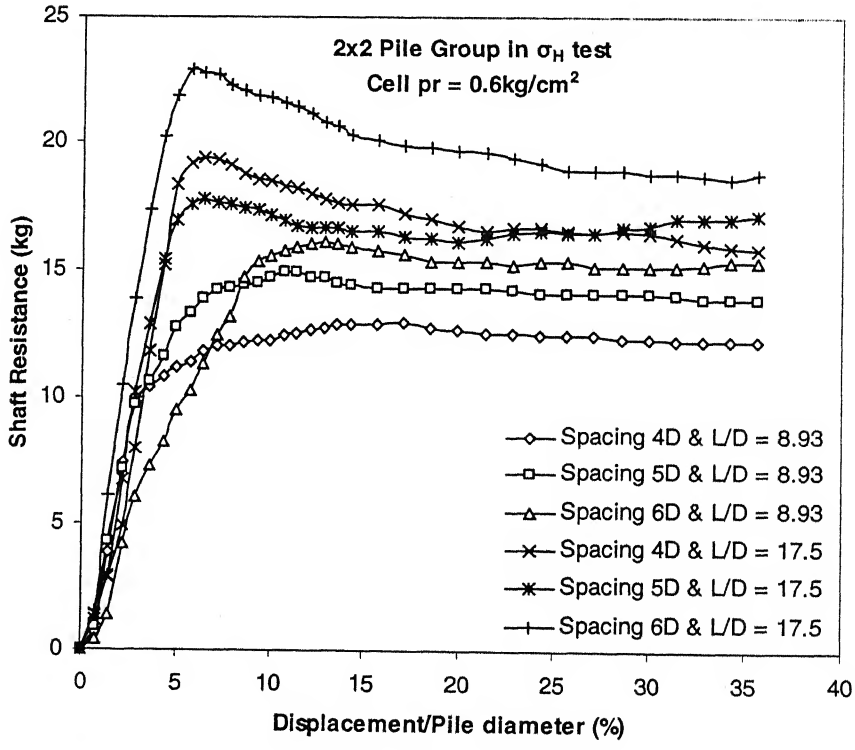

Fig. 4.23. Load displacement behaviour of 2x2 pile group for shaft resistance (σ_H test, Cell pr = 0.6kg/cm^2)

The rate of increase of shaft resistance of 2x2 pile groups for various cell pressures is shown in Table 4.15. It is observed that the shaft resistance increases with increase in cell pressure for all spacing and L/D ratios. Maximum rate of increase is observed in case of spacing 6D and L/D = 17.5 and minimum is for spacing 5D and L/D = 8.93.

Table 4.15. Rate of increase of shaft resistance with cell pressure (σ_H test, 2x2 Pile Group)

Spacing	L/D	Shaft Resistance (kg)		% of Increase
		Cell pr = 0.3 (kg/cm^2)	Cell pr = 0.6 (kg/cm^2)	
4D	8.93	12.5	13.5	8
	17.5	14.8	19.5	31.75676
5D	8.93	13.5	14.5	7.407407
	17.5	15.8	17.8	12.65823
6D	8.93	14.5	16	10.34483
	17.5	16.3	23.5	44.17178

4.3.2.3. Total Resistance in σ_H Tests

Total resistance in σ_H test is determined for piles under axially compressive load by the following relation:

Total Resistance = Tip Resistance + Shaft Resistance

In σ_V test the tip and shaft resistance are determined by experiments.

4.3.2.3.1. Single Pile

Total resistance increases with increase in cell pressure for both L/D. The percentage increase of total resistance for two different cell pressures is 14.28% for L/D = 8.93 and 23.31% for L/D = 17.5 is shown in Table 16. The rate of increase for L/D = 17.5 is more than the L/D = 8.93 which has a similar trend for total resistance of single pile in σ_V test.

Table 4.16. Rate of increase of total resistance with cell pressure (σ_H test, Single Pile)

Pile	L/D	Shaft Resistance (kg)		% of Increment
		Cell pr = 0.3 (kg/cm^2)	Cell pr = 0.6 (kg/cm^2)	
Single	8.93	11.9	13.6	14.28
	17.5	16.3	20.1	23.31

4.3.2.3.2. Line Pile Group (2x1)

The total resistance increases with increase in horizontal cell pressure for all spacing and L/D ratios. The rate of increase of total resistance is more for L/D of 8.93 than L/D of 17.5 which contradicts with results for total resistance in σ_V condition. It is shown in Table 4.17.

Table 4.17. Rate of increment of total resistance with cell pressure (σ_H test, 2x1 Pile Group)

Spacing	L/D	Total Resistance (kg)		% of Increment
		Cell pr = 0.3 (kg/cm^2)	Cell pr = 0.6 (kg/cm^2)	
4D	8.93	13.7	16.4	19.708029
	17.5	21.6	25.5	18.055556
5D	8.93	13.9	18.8	35.251799
	17.5	24.3	26.7	9.8765432
6D	8.93	13.4	17.5	30.597015
	17.5	20.2	24.5	21.287129

The variation of total resistance for different L/D ratios and pile spacing at cell pressure of 0.3kg/cm^2 and 0.6kg/cm^2 are shown in Table 4.18. and Table 4.19.

Table 4.18. Rate of change of total resistance with spacing

(σ_H test, 2x1 Pile Group, Cell pr = 0.3kg/cm^2)

Cell pr = 0.3kg/cm^2					
L/D = 8.93					
s/D		% of Increase	s/D		% of Decrease
4	5		5	6	
13.7	13.9	1.46	13.9	13.4	3.59
L/D = 17.5					
s/D		% of Increase	s/D		% of Decrease
4	5		5	6	
21.6	24.3	12.5	24.3	20.2	16.87

Table 4.19. Rate of change of total resistance with spacing

(σ_H test, 2x1 Pile Group, Cell pr = 0.6kg/cm^2)

Cell pr = 0.6kg/cm^2					
L/D = 8.93					
s/D		% of Increase	s/D		% of Decrease
4	5		5	6	
16.4	18.8	14.63	18.8	17.5	6.91
L/D = 17.5					
s/D		% of Increase	s/D		% of Decrease
4	5		5	6	
25.5	26.7	4.7	26.7	24.5	8.24

4.3.2.3.3. Square Pile Group (2x2)

For 2x2 pile group the total resistance increases with increase in cell pressure but the rate of increase is different for different L/D ratios and cell pressures. The rate of increase of total resistance of 2 x 2 pile group for various cell pressures is shown in Table 4.20. The maximum percentage of increase of total resistance for 2x2 pile group at σ_H condition is about 9 % to 25 % and 19 % to 30 % for L/D= 8.93 and L/D = 17.5.

Table 4.20. Rate of increase of total resistance with cell pressure (σ_H test, 2x2 Pile Group)

Spacing	L/D	Total Resistance (kg)		% of Increment
		Cell pr = 0.3 (kg/cm^2)	Cell pr = 0.6 (kg/cm^2)	
4D	8.93	18.5	23	24.324324
	17.5	25.6	30.7	19.921875
5D	8.93	22	25.5	15.909091
	17.5	29	32	10.344828
6D	8.93	23.3	25.5	9.4420601
	17.5	30.8	40.1	30.194805

The variation of total resistance for different L/D ratios and pile spacing at cell pressure of 0.3kg/cm^2 and 0.6kg/cm^2 are shown in Table 4.21. and Table 4.22.

Table 4.21. Rate of change of total resistance with spacing (σ_H test, 2x2 Pile Group, Cell pr = 0.3kg/cm^2)

Cell pr = 0.3kg/cm^2					
L/D = 8.93					
s/D		% of Increase	s/D		% of Increase
4	5		5	6	
18.5	22	18.92	22	23.3	5.9
L/D = 17.5					
s/D		% of Increase	s/D		% of Increase
4	5		5	6	
25.6	29	13.28	29	30.8	6.2

Table 4.22. Rate of change of total resistance with spacing (σ_H test, 2x2 Pile Group, Cell pr = 0.6kg/cm^2)

Cell pr = 0.6kg/cm^2					
L/D = 8.93					
s/D		% of Increase	s/D		% of Increase
4	5		5	6	
23	25.5	10.87	25.5	25.5	0
L/D = 17.5					
s/D		% of Increase	s/D		% of Increase
4	5		5	6	
30.7	32	4.23	32	40.1	25.31

4.4. Variation of Capacity of Piles with Pile Spacing

In the present study the tip, shaft and total resistance are determined for 2x1 pile group and 2x2 pile group with three pile spacing i.e. 4D, 5D and 6D with two L/D ratio at different stress condition. There is a variation of resistance with pile spacing for two different pile groups.

4.4.1. Line Pile Group (2x1)

4.4.1.1. Tip Resistance in 2x1 Pile Group

The variation of tip resistance with pile spacing for σ_V test and σ_H test are shown in Fig. 4.24 and Fig. 4.25.

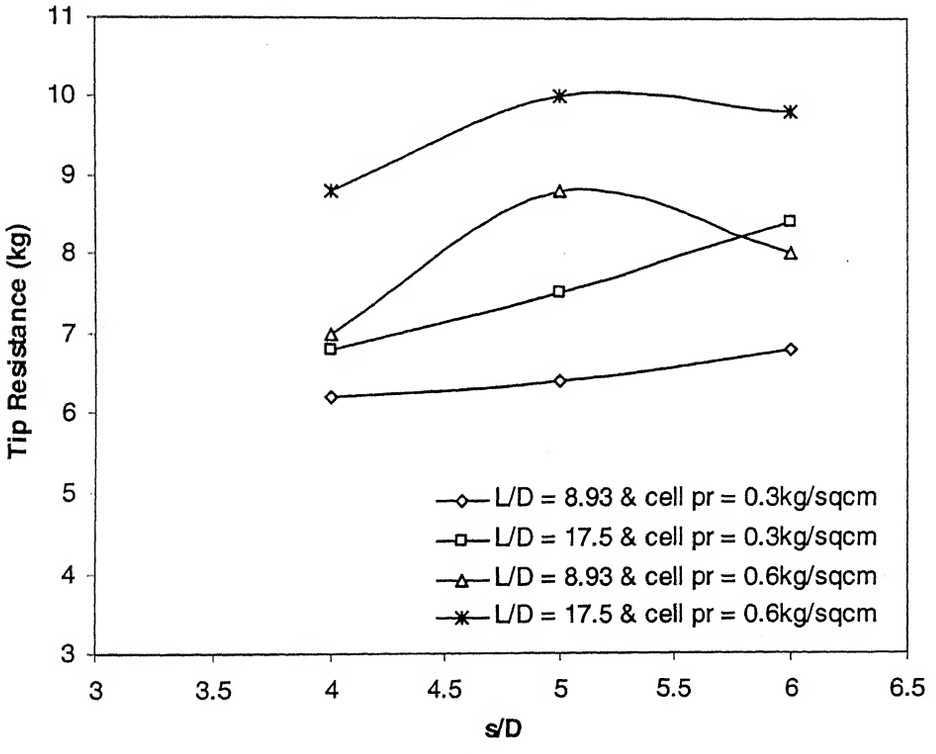

Fig. 4.24. Tip resistance vs. pile spacing (σ_V test, 2x1 Pile Group)

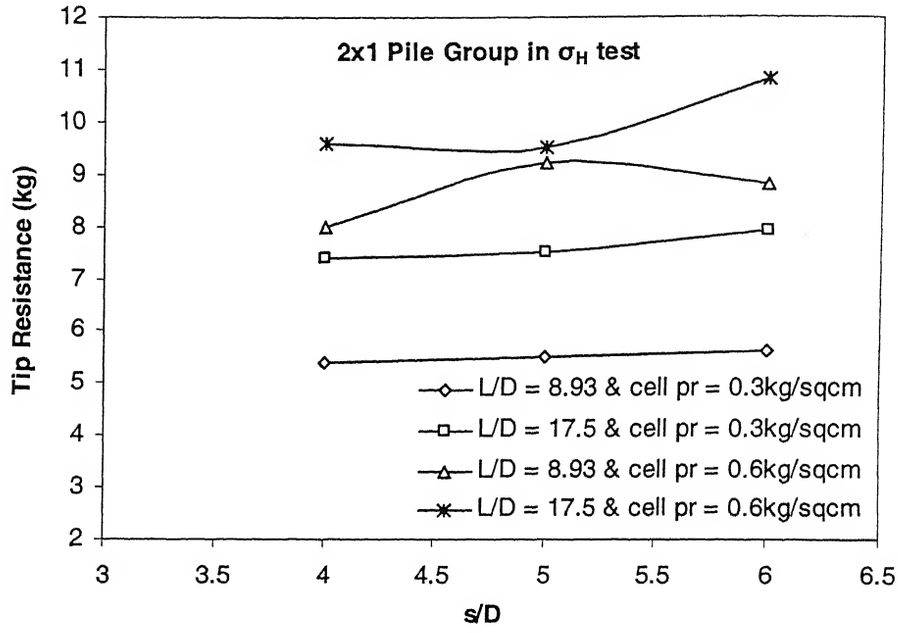

Fig. 4.25. Tip resistance vs. pile spacing (σ_H test, 2x1 Pile Group)

In σ_V test at cell pressure of 0.6kg/cm^2, the tip resistance increases with increase in spacing from 4D to 5D and then decreases from 5D to 6D. However, for cell pressure of 0.3kg/cm^2, the tip resistance increases with increase in spacing.

In σ_H test generally the tip resistance increases with increase in spacing for both cell pressures and L/D ratio.

4.4.1.2. Shaft Resistance in 2x1 Pile Group

The variation of shaft resistance for 2x1 pile group in σ_V test and σ_H test with pile spacing are shown in Fig. 4.26 and Fig. 4.27.

In σ_V test the shaft resistance increases with spacing from 4D to 5D and then it decreases from 5D to 6D for all L/D ratios.

In σ_H test for L/D = 8.93 the shaft resistance increases with increase in spacing from 4D to 5D and remains almost constant from spacing 5D to 6D. However, for

L/D = 17.5 the shaft resistance of line pile group increases from spacing 4D to 5D and decreases sharply from 5D to 6D.

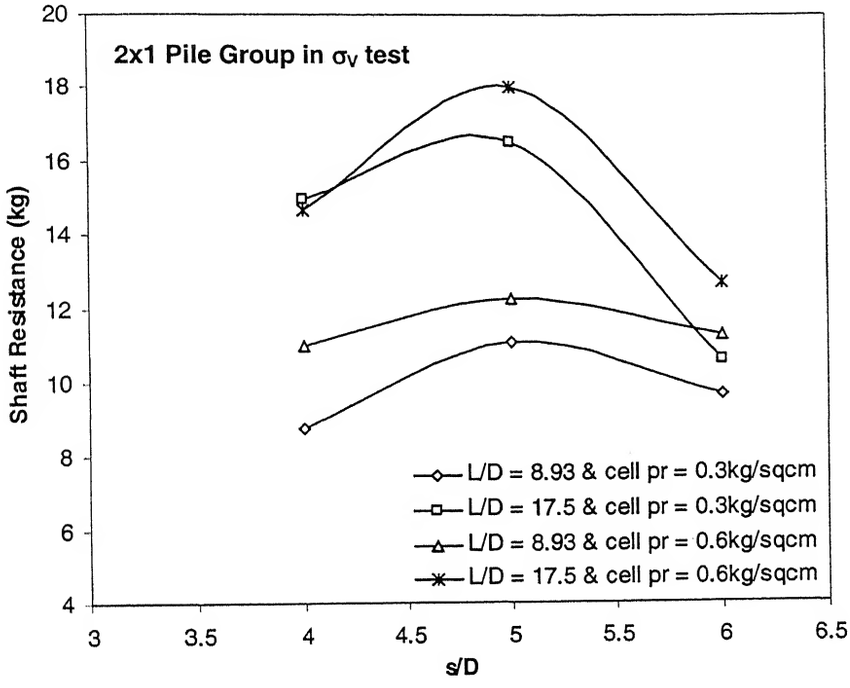

Fig. 4.26. Shaft resistance vs. pile spacing (σ_V test, 2x1 Pile Group)

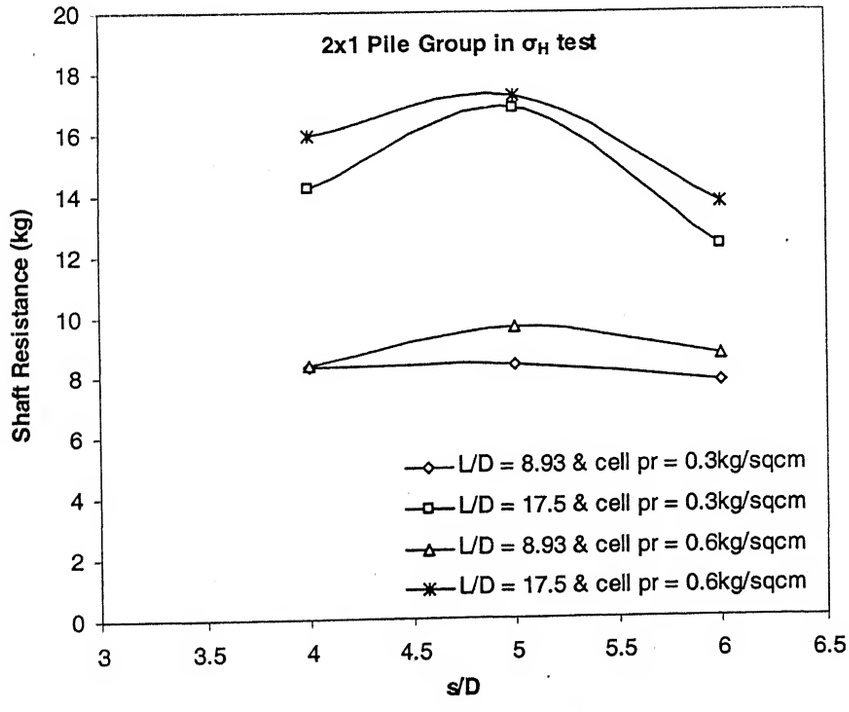

Fig. 4.27. Shaft resistance vs. pile spacing (σ_H test, 2x1 Pile Group)

It may be concluded that for a given length and number of piles in a 2x1 pile group, there was a critical value of spacing at which pile and soil inside the piles acts as a one unit; i.e. group action occurs. Hence 5D is the critical spacing up to which group action occurs.

4.4.1.3. Total Resistance in 2x1 Pile Group

The total resistance versus pile spacing in σ_V test and σ_H test for different cell pressure and L/D ratio are shown in Fig. 4.28 and Fig. 4.29.

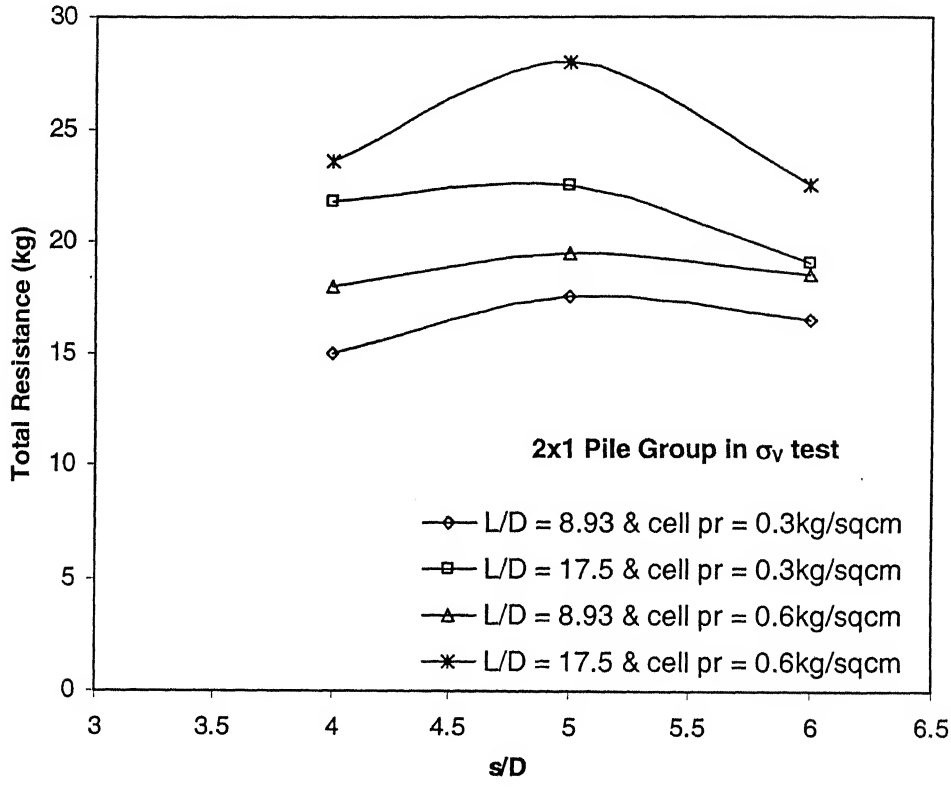

Fig. 4.28. Total resistance vs. pile spacing (σ_V test, 2x1 Pile Group)

In σ_V test the total resistance increases with increase in pile spacing from 4D to 5D for all L/D ratio and cell pressures and it remains almost constant from spacing 5D to 6D for L/D = 8.93 and decreases sharply from 5D to 6D for L/D = 17.5.

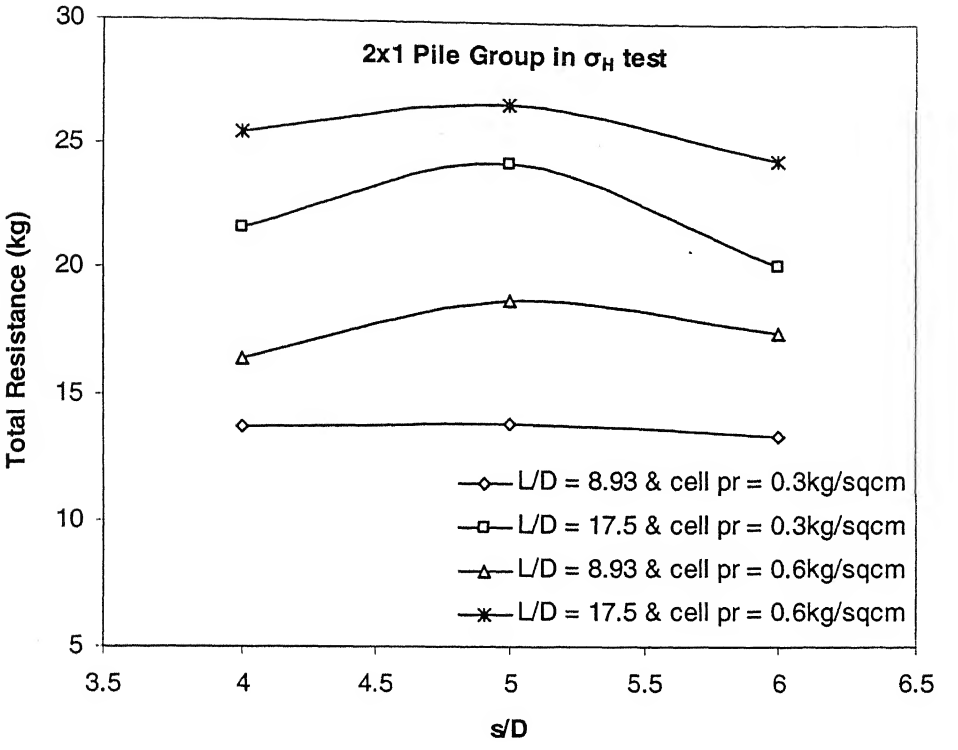

Fig. 4.29. Total resistance vs. pile spacing (σ_H test, 2x1 Pile Group)

In case of 2x1 piles group in σ_H test the total capacity increases with pile spacing upto 5D and decreases from 5D to 6D for all L/D ratio and cell pressure which gives the similar trend for total resistance in σ_V test.

4.4.2. Square Pile Group (2x2)

4.4.2.1. Tip Resistance in 2x2 Pile Group

The variation of tip resistance with pile spacing for σ_V test and σ_H test are shown in Fig. 4.30 and Fig. 4.31.

In σ_V test for cell pressure 0.6kg/cm^2, the tip resistance increases with increase in spacing from 4D to 5D and then decreases from 5D to 6D. However, for cell pressure of 0.3kg/cm^2, the tip resistance increases with increase in spacing. Similar trend has been observed for line pile groups. In σ_H test, tip resistance increases with increase in pile spacing for 2x2 groups.

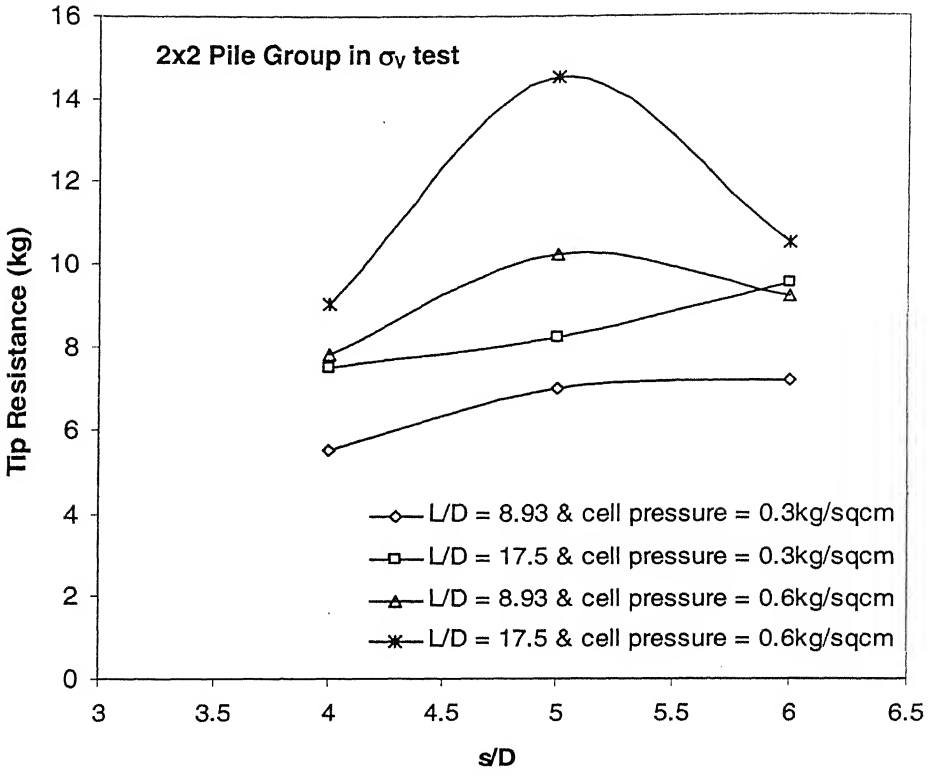

Fig. 4.30. Tip resistance vs. pile spacing (σ_V test, 2x2 Pile Group)

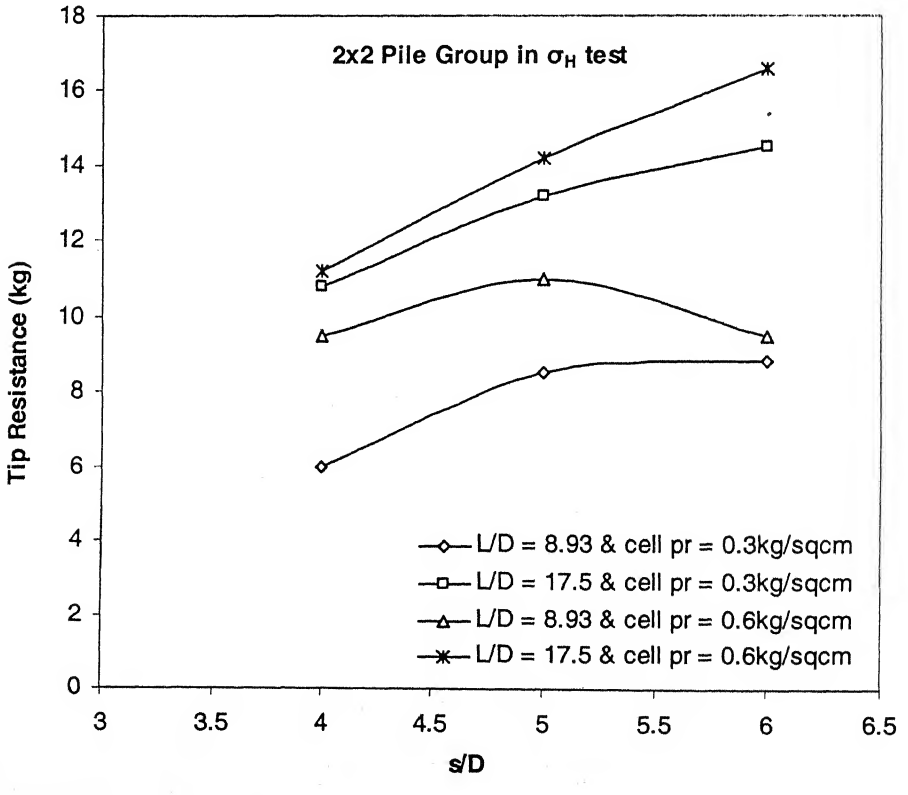

Fig. 4.31. Tip resistance vs. pile spacing (σ_H test, 2x2 Pile Group)

4.4.2.2. Shaft Resistance in 2x2 Pile Group

The variation of shaft resistance for 2x2 pile group in σ_V test and σ_H test with pile spacing are shown in Fig. 4.32 and Fig. 4.33.

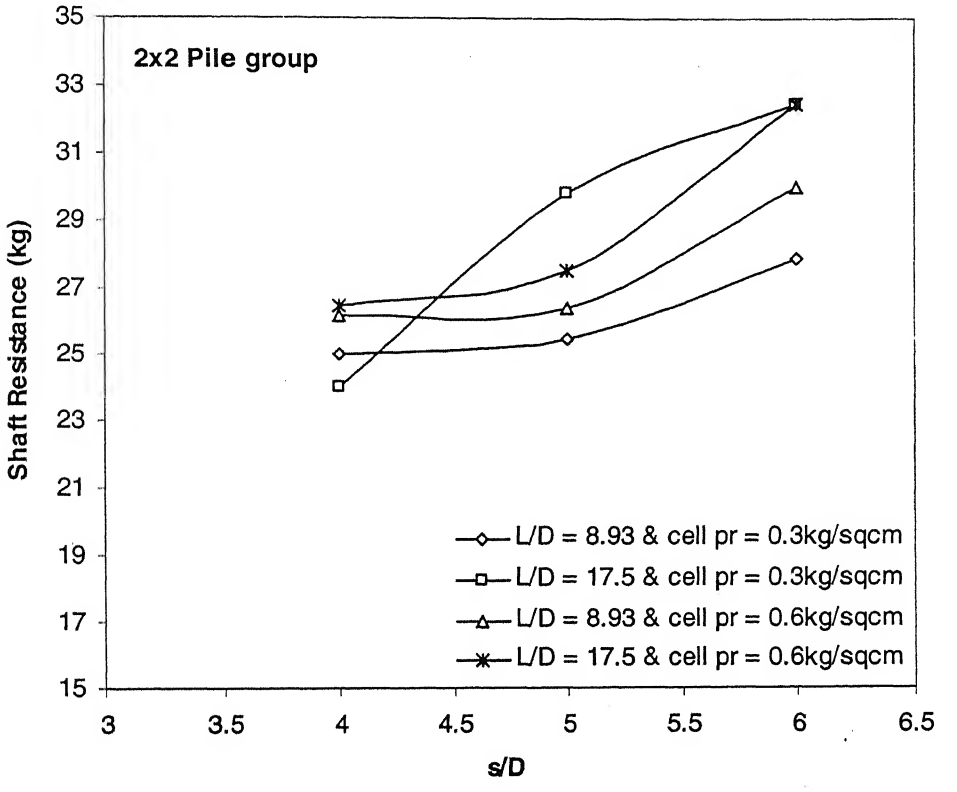

Fig. 4.32. Shaft resistance vs. pile spacing (σ_V test, 2x2 Pile Group)

In general, the shaft resistance increases with increase in pile spacing for σ_V test in 2x2 pile group. It may be concluded that for 2x2 pile group, group action occurs up to 6D spacing.

In σ_H condition it is observed that shaft resistance increases with increase in spacing from 4D to 6D for 2x2 pile group in for all cases.

It may be concluded that group action may occur from spacing 4D to 6D for 2x2 pile groups in both stress conditions.

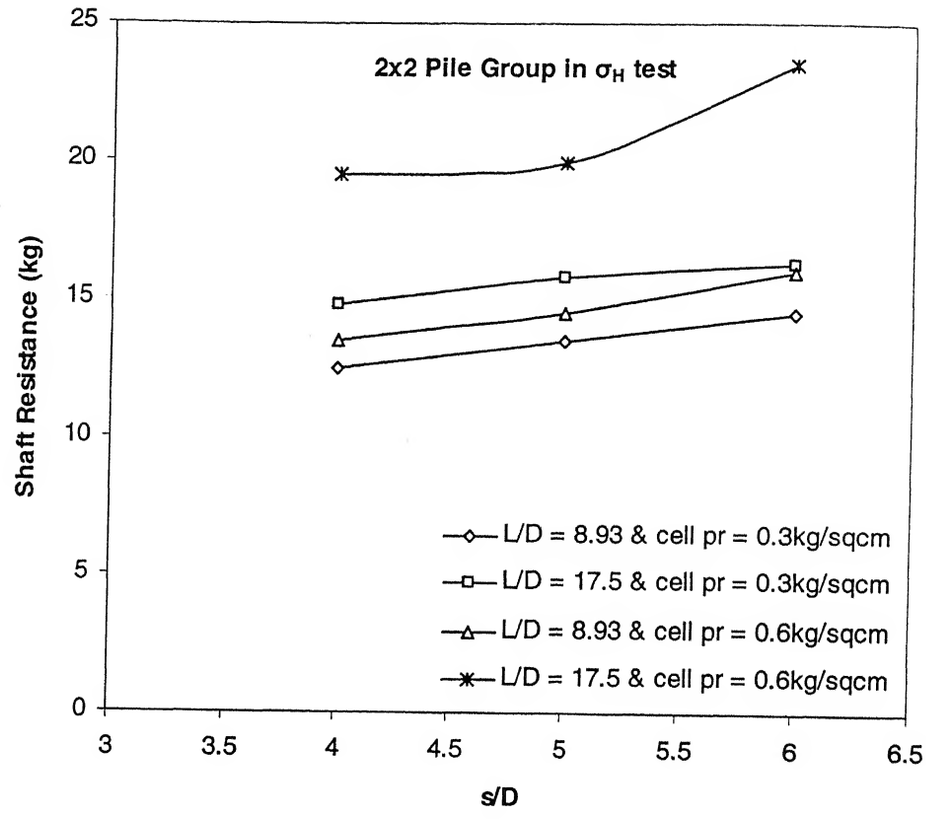

Fig. 4.33. Shaft resistance vs. pile spacing (σ_H test, 2x2 Pile Group)

4.4.2.3. Total Resistance in 2x2 Pile Group

The total resistance versus pile spacing in σ_V test and σ_H test for different cell pressure and L/D ratio are shown in Fig. 4.34 and Fig. 4.35.

In σ_V test the total resistance increases linearly with increase in pile spacing from 4D to 6D.

In case of 2x2 piles group, the total capacity in σ_H test increases with pile spacing ranges from 4D to 6D for all L/D ratio and cell pressure which is similar trend for σ_V test for total resistance.

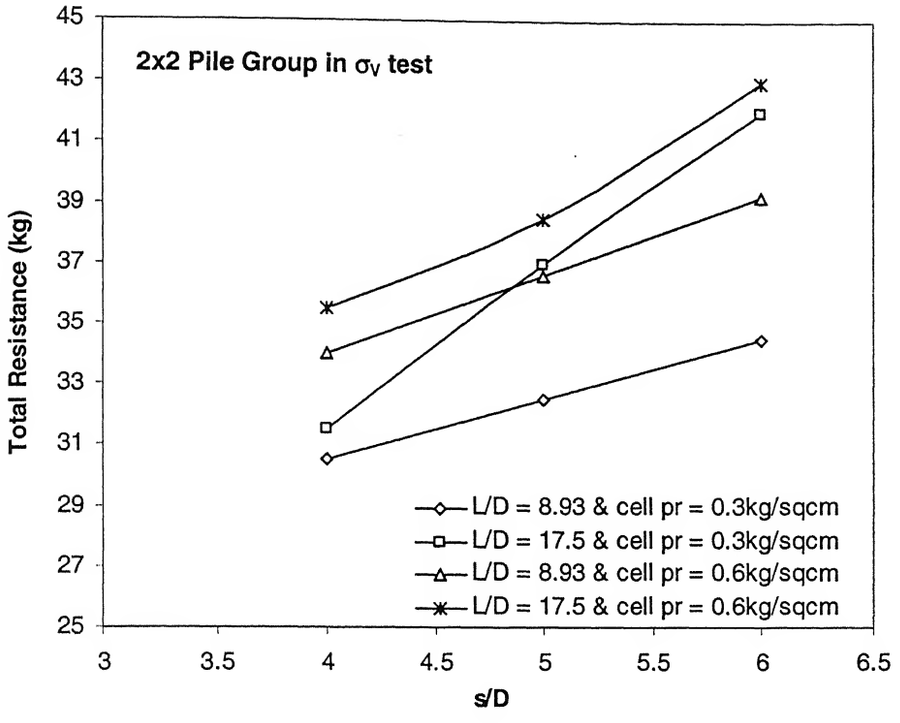

Fig. 4.34. Total resistance vs. pile spacing (σ_V test, 2x2 Pile Group)

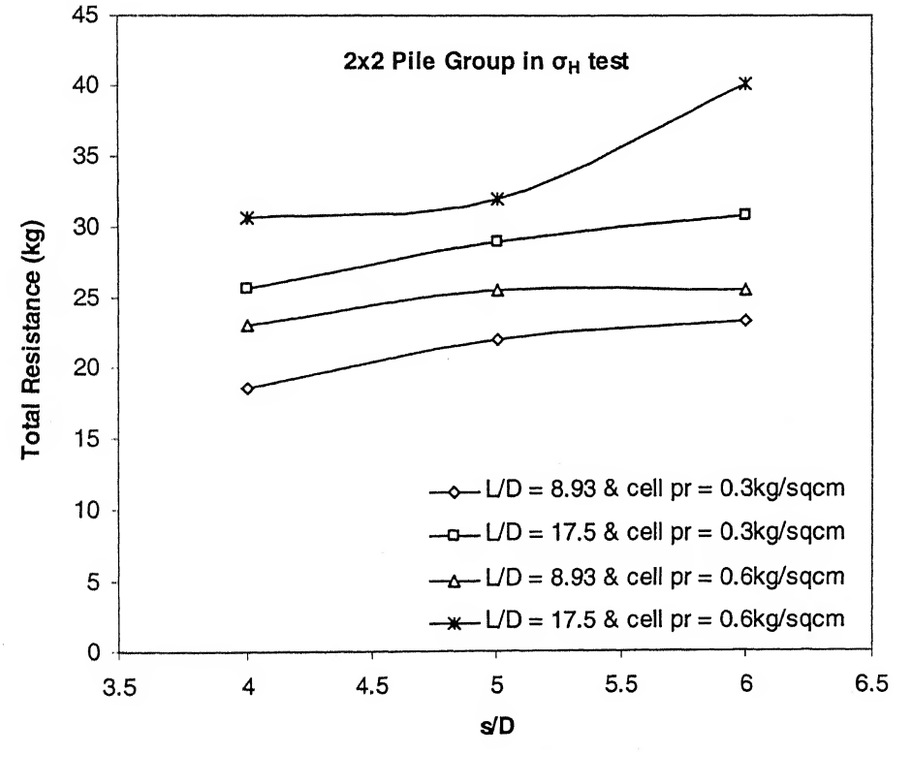

Fig. 4.35. Total resistance vs. pile spacing (σ_H test, 2x2 Pile Group)

4.5. Determination of Bearing Capacity Factor (N_c) and Adhesion Factor (β)

By conducting independent test for point resistance and shaft resistance the bearing capacity factor N_c and adhesion factor α can be determined in case of single pile from the following expressions.

$$q_p = c_u N_c + \sigma_V \quad \text{.....(4.1)}$$

$$f_S = \beta c_u \quad \text{.....(4.2)}$$

Bearing capacity factor (N_c) is determined from tip resistance in σ_V test data by using Eq. 4.1.The N_c values computed from the measured tip load are presented in Table 4.23. The value of N_c is dependent on the values of c_u and vertical stress level.

Table 4.23. Variation of bearing capacity factor, N_c with stress level

L/D	Cell pressure (σ_V) kg/cm^2	Shear Strength of soil (c_u) kg/cm^2	Unit Tip Resistance (q_p) kg/cm^2	Bearing Capacity Factor (Nc)
8.93	0.3	0.25	2.72727273	9.709091
8.93	0.6	0.25	2.85714286	9.028571
17.5	0.3	0.25	2.92207792	10.48831
17.5	0.6	0.25	3.24675325	10.58701

From the above table it is observed that the values of N_c increases with increase in pile length. The values of N_c ranges from as low as 9 to as high as 10.5 in contrast with the generally accepted value of 9. Such high values of N_c have also been obtained by other investigators (Butterfield and Ghosh, 1977).

Adhesion factor (β) computed from Eq. 4.2. obtained from σ_H test for shaft resistance data for different cases have been shown in Table 4.24. This adhesion factor is dependent on horizontal stress level and cohesion of soil.

Table 4.24. Variation of adhesion factor, β with stress level

L/D	Cell pressure (σ_V) kg/cm^2	Shear Strength of soil (c_u) kg/cm^2	Unit Shaft Resistance fs (kg/cm^2)	Adhesion Factor (β)
8.93	0.3	0.25	0.2130682	0.852273
8.93	0.6	0.25	0.2443182	0.977273
17.5	0.3	0.25	0.1484848	0.593939
17.5	0.6	0.25	0.1787879	0.715152

The adhesion factor increases as the stress level increases. The values of adhesion factor obtained in the present study almost fall within the range as reported Kerisel (1965).

4.6. Comparison of σ_V test and σ_H test Results

The values of total resistance of pile and pile groups for cell pressures of 0.3kg/cm^2 and 0.6kg/cm^2 are shown in Table 4.25 and 4.26.

Table 4.25. Values of total capacity of piles in both σ_V and σ_H test condition at cell pressure of 0.3kg/cm^2

Cell pr = 0.3kg/cm^2				
Type of Pile and Pile Group			Vertical Test (σ_V Test)	Vertical Test (σ_H Test)
L/D	Spacing (s)	Type	Total Resistance q_{tV} (kg)	Total Resistance q_{tH} (kg)
8.93		Single	9.4	11.9
	4D	2x1	15	13.7
		2x2	30.5	18.5
	5D	2x1	17.5	13.9
		2x2	32.5	22
	6D	2x1	16.5	13.4
		2x2	34.5	23.3
17.5		Single	12	20.1
	4D	2x1	21.75	25.5
		2x2	31.5	30.7
	5D	2x1	22.5	26.7
		2x2	37	32
	6D	2x1	19	24.5
		2x2	42	40.1

Table 4.26. Values of total capacity of piles in both σ_V and σ_H test condition at cell pressure of 0.6kg/cm^2

Cell pr = 0.6kg/cm^2				
Type of Pile and Pile Group			Vertical Test (σ_V Test)	Vertical Test (σ_H Test)
L/D	Spacing (s)	Type	Total Resistance q_{tV} (kg)	Total Resistance q_{tH} (kg)
8.93		Single	11.9	13.6
	4D	2x1	13.7	16.4
		2x2	18.5	23
	5D	2x1	13.9	18.8
		2x2	22	25.5
	6D	2x1	13.4	17.5
		2x2	23.3	25.5
17.5		Single	16.3	20.1
	4D	2x1	21.6	25.5
		2x2	25.6	30.7
	5D	2x1	24.3	26.7
		2x2	29	32
	6D	2x1	20.2	24.5
		2x2	30.8	40.1

From the above two tables the following conclusions have been drawn:

1. For single pile, the total resistances from σ_H test are always greater than the values from σ_V test.
2. At cell pressure of 0.3kg/cm^2 and L/D= 8.93, the total resistances from σ_V tests are always greater than the values from σ_H tests for all group piles.
3. At cell pressure of 0.3kg/cm^2 and for L/D = 17.5, the total resistance from σ_H tests is greater than values from σ_V tests for 2x1 pile groups. However reverse trend is observed for 2x2 pile groups
4. At cell pressure of 0.6 kg/ cm^2, the total resistances from σ_H tests are always greater than that obtained from σ_V tests for all pile groups and L/D ratios.

It is observed that the effect of horizontal pressure is to increase the total capacity by enhancing the adhesion factor and skin friction of piles. This is responsible for the σ_H values being higher than all values under σ_V condition in the case of the higher cell pressure viz. 0.6 kg/cm^2. This trend, however, is not present in the case of the lower cell pressure.

Chapter - V

Analysis by using Discrete Element Method

5.1. General

The Discrete Element Method (DEM) is a family of related techniques designed to solve problems in applied mechanics especially problems which exhibit gross motion or deformation that may be of a discontinuous nature. This method is used as a numerical model to simulate the behaviour of any system which consisting of discrete particles. The DEM is a direct simulation tool that falls in the realm of Scientific Computing. The problems that are amenable to DEM analysis are often very large and time intensive involving thousands of particles modeled over hundreds of thousands of time steps. These simulations can take from hours to days to run even on fast workstations. This investigation will focus on soil-structure interaction problem such as pile foundation in both cohesionless and cohesive soil. The effect on pile resistance in terms of both tip and shaft resistance at the time of installation and settlement due to compressive loading at various stress condition are separately analyzed here by DEM.

5.2. The Algorithm

The algorithm of the computer code employed in this thesis work was conceptually very simple to understand. Every particle was identified separately, with its own mass, radius, moment of inertia and contact properties. For every particle, lists were kept of the particles in immediate contact and also in close proximity. Each element was considered to be geometrically inviolate, with deformable contacts. The amount and rate of overlap between neighboring elements were used to determine the normal and shear force contacts. The total unbalanced force acting on each particle

was computed by summing the contact forces arising from direct neighbors. The unbalanced force was then used to estimate each particle's current acceleration, which was integrated in turn for the velocity and displacement at the next instant of time. This cycle was repeated till the simulation was stopped.

Before the start of simulation, the soil sample geometry was set and the particles were randomly created and allowed to settle. So the initial position of all particles and walls were known. At the start of the simulation, the pile was given a fixed translation velocity in y-direction. So the initial velocity of the pile was known. Also the time duration for which the simulation was required was fixed. The following steps were followed in the simulation:

1. First, the wall of pile moved according to the set velocity in y-direction. This movement disturbed the particles adjacent to the wall, which in turn sets in motion other soil particles.
2. This caused the formation of new contacts and breakage of existing contacts with other particles and walls. Here "contact" referred to the point of collision between a pair of particles, or between a particle and a wall of pile. All these collisions gave rise to forces at the point of contacts and the trajectories of particles follow the magnitude and directions of these forces. The unbalanced force on a particle was then calculated by adding up these individual contact forces on the particle. Contact information for each particle was stored in a list, which was referred to as the contact list.
3. The net unbalanced force was used to compute the particle acceleration, which was then integrated to yield the velocity and displacement of the particle. The new location of the particle was stored, in order to update the contact with the

other particles in the vicinity. Also, particle locations were stored in a file for graphical animation.

A flow chart (Mishra, 1991) of the sequence of calculations involved in DEM is given in Fig. 5.1.

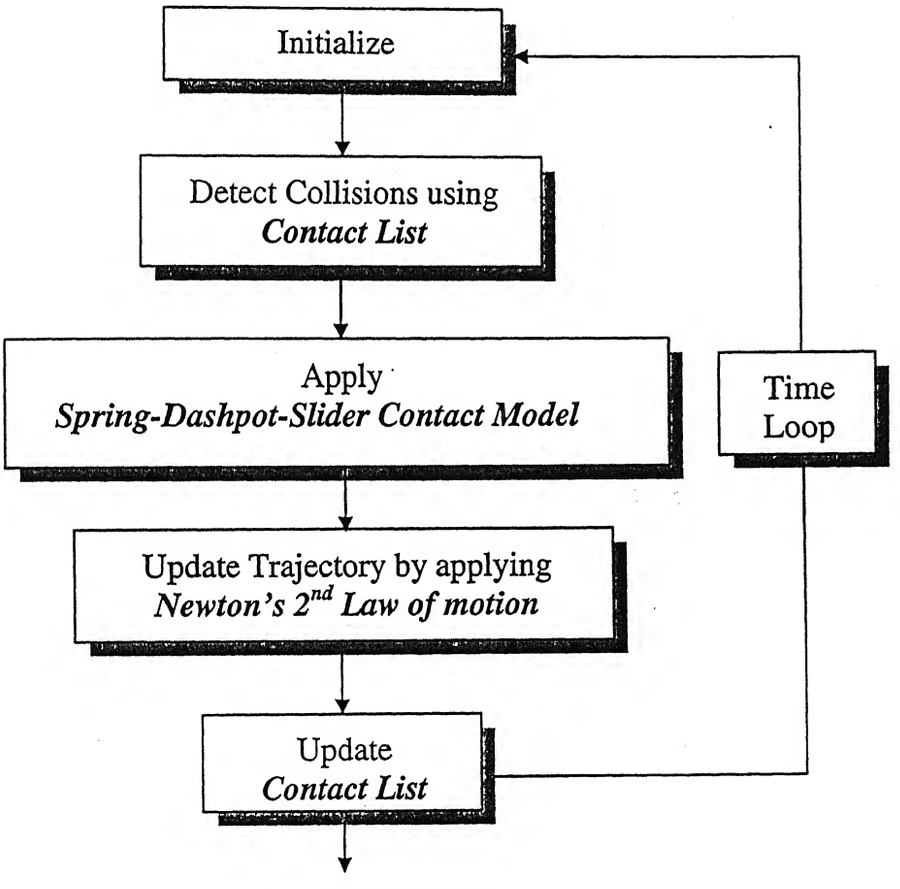

Fig. 5.1. DEM Algorithm

5.3. Numerical Model

The numerical scheme adopted in the DEM formulation applies Newton's second law to the particles and a force displacement law at the contacts. Newton's second law gives the motion of the particles resulting from the forces acting on them.

The forces developing at the contacts were modeled by a pair of normal and tangential spring-dashpots at every contact point.

The implementation of the particle-particle and particle-wall contact was the basis of the simulation. Walls were assumed to be smooth and rigid. Likewise, particles were assumed to be smooth and rigid. Thus, each particle made a single-point contact with each of the other particles or walls. The main objective of DEM was to calculate these contact forces. The linear contact law used the combination of a spring and a dashpot in the normal and shear directions to calculate the incremental contact forces. This spring and dashpot model was shown in Fig. 5.2. The spring stands for the force component that was stored in the particle, and the dashpot stood for the force dissipated during the collision. The provision of viscous contact damping models, for the system realistically because the coefficients for restitution for different contacts were used to compute the damping constants. Also, friction damping occurs during sliding when the absolute value of shear force at any contact exceeded a maximum value found by the product of the normal force at the contact and the coefficient of friction.

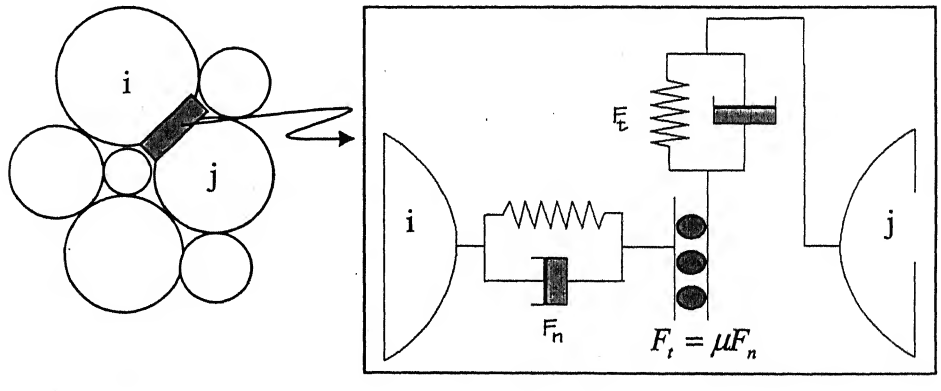

Fig. 5.2. Normal and shear spring-dashpot representation at the point of collision

The forces were developed when two or more bodies in the simulation were in contact. All such information regarding different bodies in contact was kept in a list, which was typically referred to as "contact list". This was a list of bodies that were currently in contact with a particle. This list was maintained for all the particles in the charge. The positions of all the bodies in the simulations were tracked during each time step to maintain this contact list. The calculations were kept utterly simple, so that all one needs to do was repeat these calculations individually for each and every particle.

The dynamic equilibrium equation can be written for a particle was characterized by displacement x, mass m and moment of inertia I as follows;

$$m\ddot{x}_i + C_{ij}\dot{x}_i + K_i x_i = F_i \qquad \text{i} = 1, 2 \qquad \text{..... (5.1)}$$

$$I\ddot{\theta} + \sum_{i=1}^{2}(K_i x_i + C_i \dot{x}_i)s_i = M \qquad \text{..... (5.2)}$$

where F_i is the force acting in the direction i, M is the moment about centroid of the sample and s_i is the perpendicular distance from the line of action of the force $(K_i x_i + C_i \dot{x}_i)$ to the centroid of the particle. The parameters K and C are the spring and dashpot constants respectively. The direction i = 1 and 2 refer to the coordinate axis.

The above two equations were special cases of the second order nonlinear differential equation of the following form:

$$\ddot{x} + a\dot{x} = \frac{1}{mF(x, \dot{x})} \qquad \text{..... (5.3)}$$

The quantity $[F(x,\dot{x})]$ is the force generated from contact and other applied forces. During a small time step t to $t+\partial t$, this equation can be integrated by finite difference approximations of the derivatives:

$$\ddot{x} = \frac{\dot{x}(t+\partial t) - \dot{x}(t)}{\partial t} \qquad \text{..... (5.4)}$$

$$\dot{x} = \frac{\dot{x}(t+\partial t) + \dot{x}(t)}{2} \qquad \text{..... (5.5)}$$

Thus by repeating this calculation for each particle, the new position of all the particles was determined. By repeating the entire set of calculation at successive time steps, gave the movement of the change in the x-y coordinate space.

In the spring-dashpot model, for the calculation of the normal and shear forces, a linear elastic behaviour of the springs was assumed (F_s = K.x), whereas the force in the dashpot was proportional to the relative velocity of the colliding bodies (F_d = C.v). The proportionality constants, that was the stiffness and the damping constant, determine the time step with which calculation would proceed. The integration scheme outlined above was a central difference scheme; the stability of this numerical scheme depends on the time step chosen. The time step that used to assure numerical stability was given in terms of the mass and the stiffness of the smallest particle as:

$$\partial t \leq 2\sqrt{\frac{m}{K}} \qquad \text{..... (5.6)}$$

However, since the geometry and stiffness of the system changed from time step to time step, there was no unique "critical" time step size which was valid at all times. While it might be convenient to choose an arbitrarily small time step to guarantee accuracy, such a choice may be computationally impractical. Consequently, it was crucial to estimate this critical time step as accurately as possible for all likely

system geometries. Based on this stability criterion the critical time step was evaluated.

5.4. The Computer Program

The computer program Millsoft (Rajamani et al, 1999) used here calculates the particle-charge trajectory by small time steps and tracked the position of each particles and energy spend in all the collisions during the entire period of simulation. The program had been implemented using the FORTRAN programming language. It was compiled using a Microsoft FORTRAN PowerStation Compiler, version 4.0.
The graphical user interface simplifies all the design and operating parameters used in the program. These included the dimension of soil sample, size distribution of soil particles, diameter and length of pile, installation speed of pile and settlement rate of pile. This user interface had written with Microsoft Visual Basic software. The graphical visualization program enabled the animation of the pile motion in soil sample on the computer screen. The graphical visualization code had been written using Microsoft Visual C++ and utilizes the Open GL graphical libraries.

The computer program was modified to generate particles at any level of particle filling and also modified to produce ordered arrangement of particles within a specified volume. All the simulation invariably started with specifying the dimension of soil sample and also pile. The length and height of sample and pile and parameter for the soil particle were given as input parameter. In addition, certain operating parameters such as the speed and duration of simulation were specified. The numerical method was also parameter dependent. Therefore, parameters pertaining to the contact model such as material stiffness, coefficient of friction and restitution were also needed to be specified. Once this phase of simulation was over the

computer code performs calculation that enables to determine to forces generated at pile and also visualization of the motion of particles.

5.5. DEM Implementation on Testing Program

The DEM implementation in my testing program can be divided in five parts. It was done step by step to simulate with the testing condition and it is described below:

5.5.1. Generation of particles or Soil Particles

First a rectangular sample was made with specified dimensions (0.195mx0.5m). Then 9000 particles with known dimensions were randomly created in space within the rectangular sample. Here two type particles were taken of radius 0.001m (60%) and 0.0015m (40%) respectively. The particles were arranged in layers. It was necessary to introduce some randomness into this type of simulation or it would remain artificially ordered. The particles were allowed to fall down and came to rest due to contact damping. The program started by reading all input variables either interactively or from a file; it generated a gradual input method, and performed the calculations at each time step. The code stored the position, velocity and force information for all particles. All forces were accounted for in these runs (i.e. normal elastic, normal damping, tangential damping, cohesion, friction, gravitational). The current scenario modeled with various time steps is shown in Fig. 5.3.

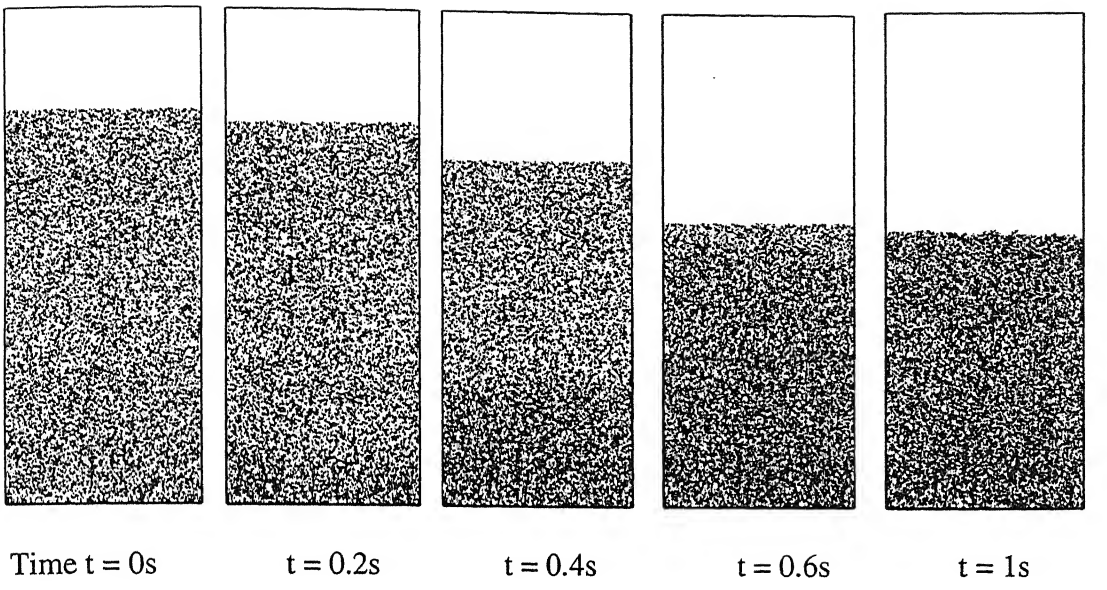

Fig. 5.3. Scenario modeled, showing falling of 9000 particles into sample

5.5.2. Dimensioning the Pile and Soil Sample and Installation of Pile into the sample

After settling down all the particles and get a desired density it was found that the maximum y-coordinate of particle is 0.281187m. But the height of sample used in testing was 0.28m. To give the exact dimension of sample some particles this was above the height of 0.28m were cut out. After doing this the total number of particle became 8979. Now the pile of length 0.175m and diameter 0.014m was created in such a position that its bottom just in touch with the upper layer of soil sample. Now pile velocity of 0.075m/s in the y direction was introduced for a certain simulation time so that it could achieve its desired embedded length (L/D = 8.93). Forces generated at side face and bottom of pile were also determined at the time of installation. In this simulation all gradation information are given in Table 5.1.

Table 5.1. Gradation information and properties for simulation

Gradation Information			Properties	Particle-particle	Particle-wall	Type of soil
Size	1	2	Coefficient of restitution (e)	0.45	0.45	
Radius (m)	0.001	0.0015	Cohesion (c_u) (KN/m^2)	0.25	0.25	Clay
Number (%)	60.32	39.68	Angle of internal friction (φ_u) (deg)	3	3	
Mass (kg)	3.35×10^{-5}	4.24×10^{-5}	Cohesion (c_u) (KN/m^2)	0	0	Sand
MOI (Io)	1.68×10^{-7}	4.77×10^{-4}	Angle of internal friction (φ_u) (deg)	30.96	30.96	

The installation of pile with various time steps is shown in Fig. 5.4.

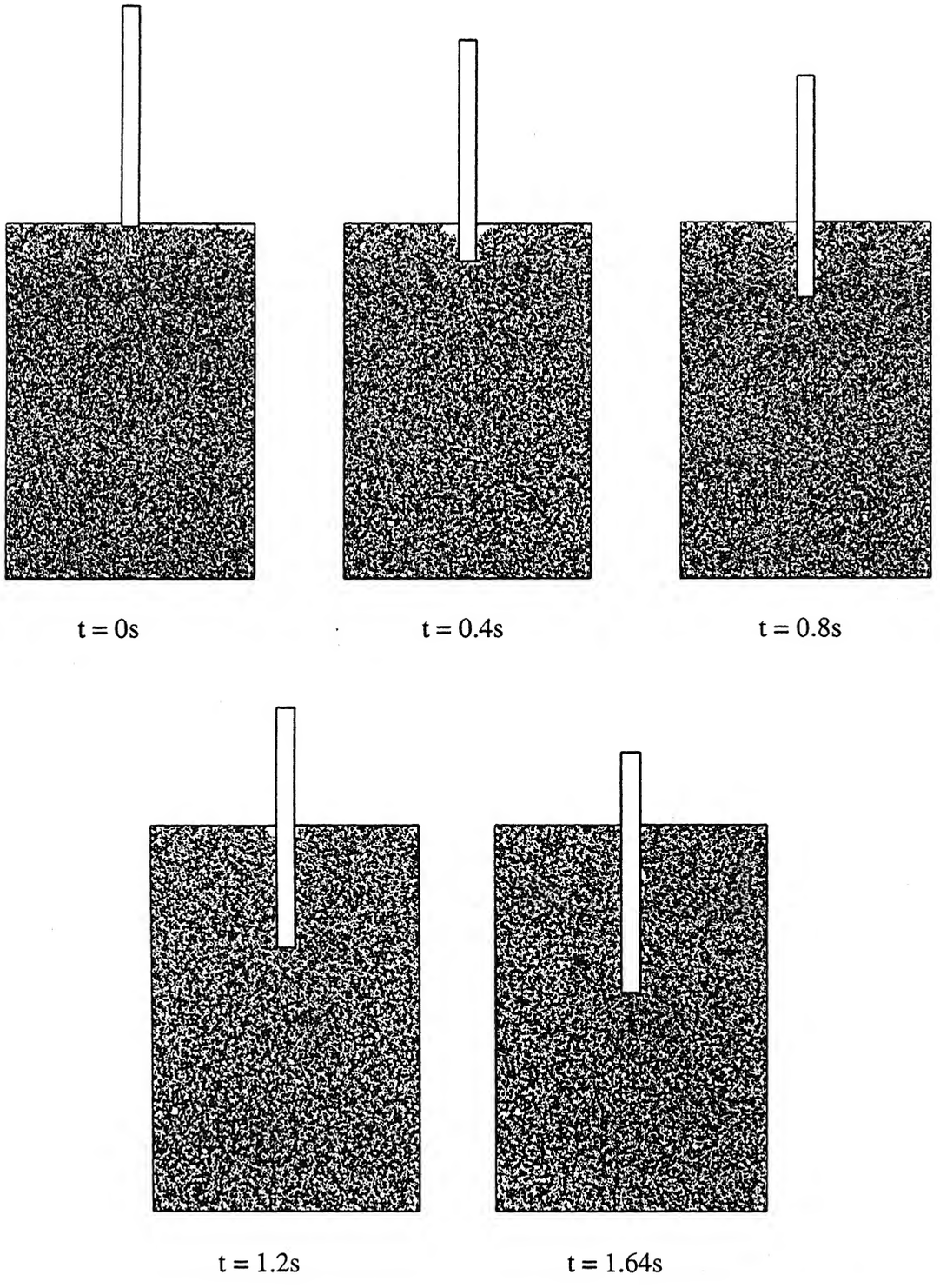

Fig. 5.4. Different position of pile at various time step at the time of installation

5.5.3. Relaxation of Pile and Releasing the Stress

In this part the program was run for a relaxation time of 0.5sec and made the pile velocity zero here in y direction. There was no movement of pile here but soil particles were changed their position due to releasing the stress from the pile and side walls of the sample. In this step forces releasing from wall and pile were calculated with different time steps. After the pile had become stationary soil particles continued to move due to stress release, which can be shown clearly with the help of DEM. The changes of orientation of soil particles can be clearly shown by 2D animation. Different positions of particles at different time steps are shown in Fig. 5.5.

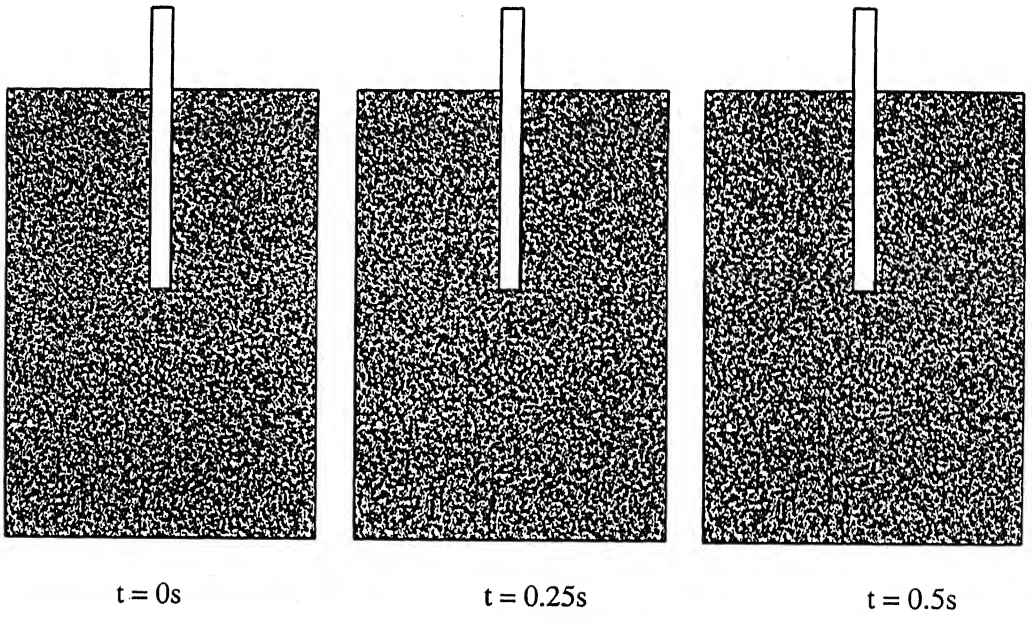

Fig. 5.5. Changing the orientation of soil particles due to releasing of stresses

5.5.4. Application of Cell Pressure at Top and Bottom wall of Soil Sample

This was the most important part of DEM to simulate exactly with the experimental program. In the experiment the values of applied cell pressure in both horizontal and vertical direction were 0.3kg/cm^2 and 0.6kg/cm^2 respectively. In the

previous step the values of pressure in the walls of the soil sample were known at the end of relaxation period. When the cell pressure was applied to the soil sample, the pressure at the walls of the soil sample was reduced by an amount equal to the applied cell pressure. By knowing the reduced pressure the simulation was again started for a particular time period to get that exact reduced pressure at both horizontal and vertical walls. The orientation of soil particles at that condition was also determined after the simulation.

5.5.5. Determination of Bearing Capacity due to Settlement of Pile

After getting all the soil particle data at particular specified wall pressure both in horizontal and vertical direction separately due to cell pressure the pile was allowed to settle at the velocity of 0.01m/sec into the soil sample for a simulation time of 1.5sec. The model parameters were remaining same as Table1 and 2 except the total simulation time and value of pile velocity. At the end of simulation force at the side and bottom walls of pile with each time step were generated as an output file. From the force data load-settlement can be plotted to get the failure load of pile. The settlement of pile at different time steps is shown in Fig. 5.6.

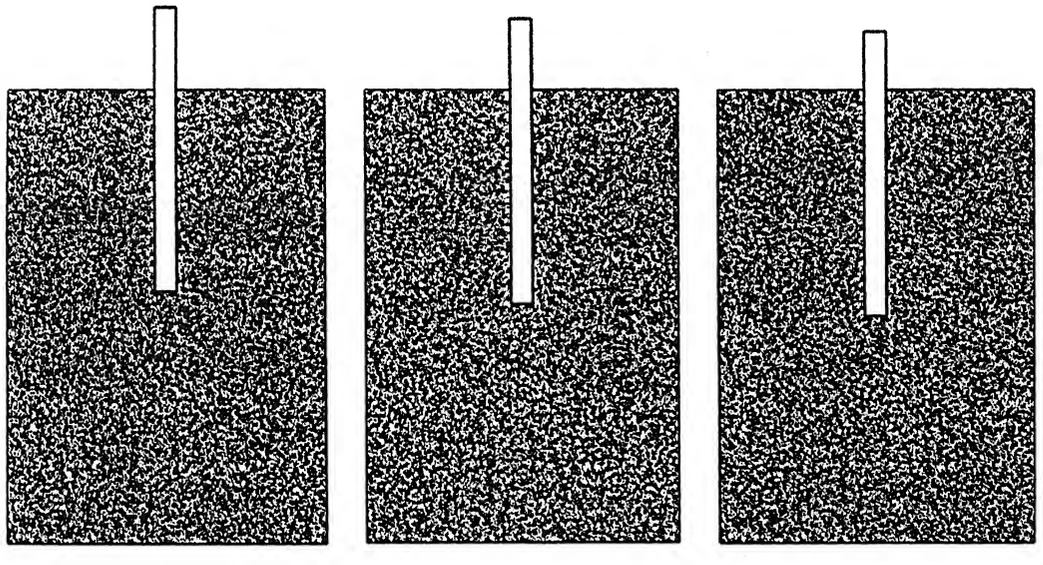

Fig. 5.6. Settlement of pile at different time step

5.6. Results by DEM

Results obtained from DEM are discussed separately for sandy and clayey soil for various stress condition.

5.6.1. For Sand

At the time of installation force were generated with time at pile wall and the magnitude of forces increase with time. The forces in both y and x direction obtained by DEM at the time of installation of pile are shown in Fig. 5.7. and Fig. 5.8.

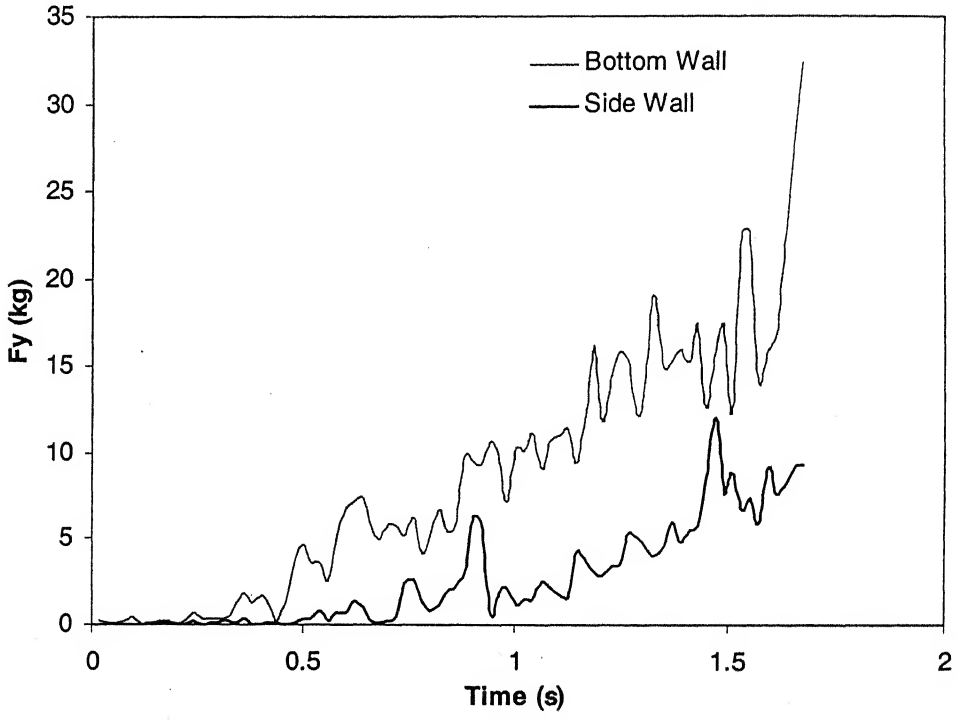

Fig. 5.7. Time vs. Fy at pile walls at installation of pile in sand

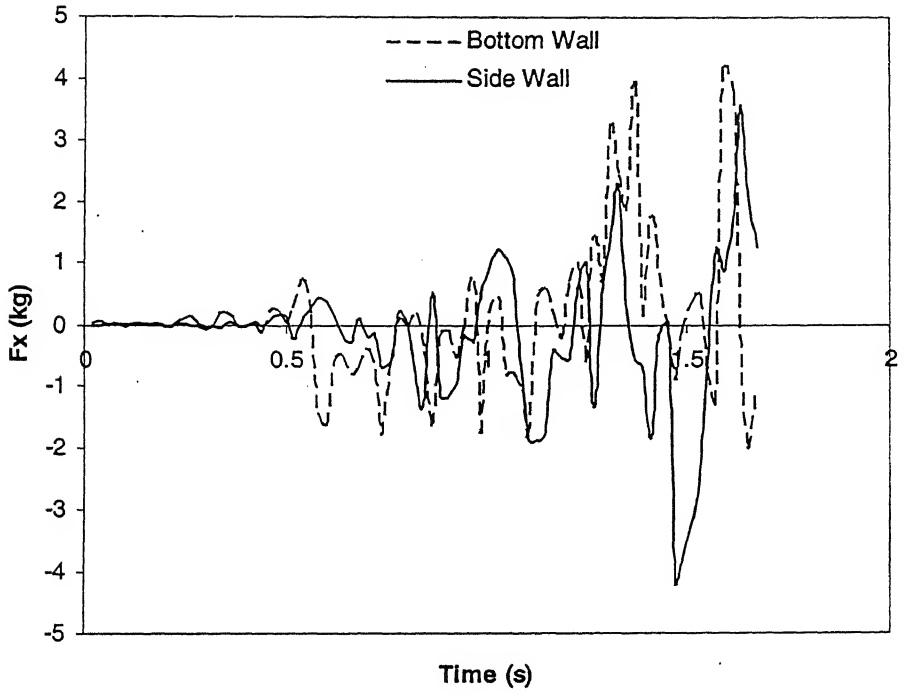

Fig. 5.8. Time vs. Fx at pile walls at installation of pile in sand

It is observed from the above plot that the value of force in y direction at bottom wall is increasing more than side wall with time but in x direction it is very less. The sum of all forces at pile walls in x direction at any time was almost zero as there was no external force applied in x direction.

In the relaxation part the pile and walls of the sample released its stress with time. The total period for relaxation was 0.5sec in this case. The force both y and x direction at pile walls with time at relaxation period is shown in Fig. 5.9. and Fig. 5.10.

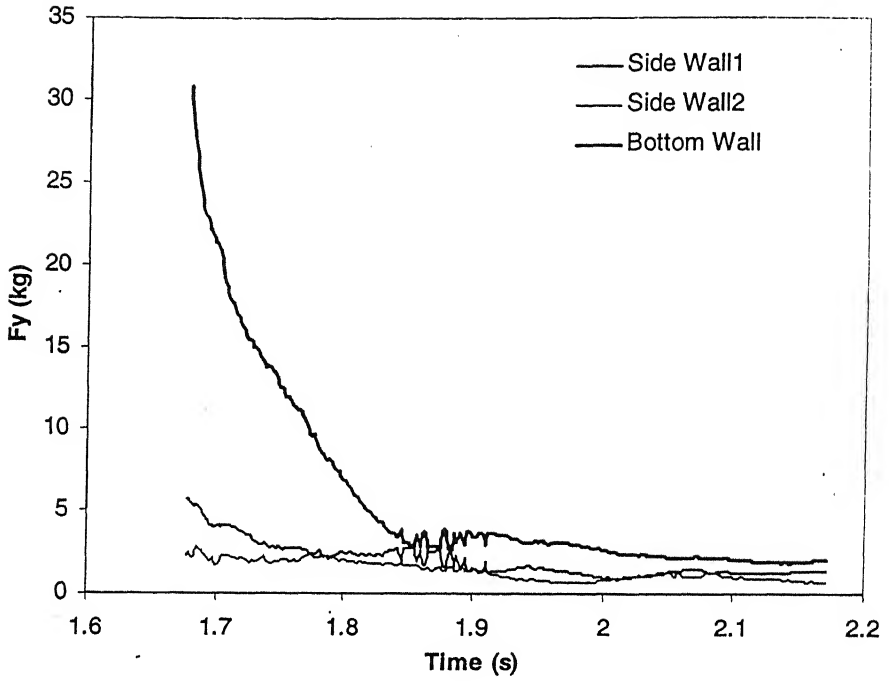

Fig. 5.9. Time vs. Fy at pile walls at relaxation time step in sand

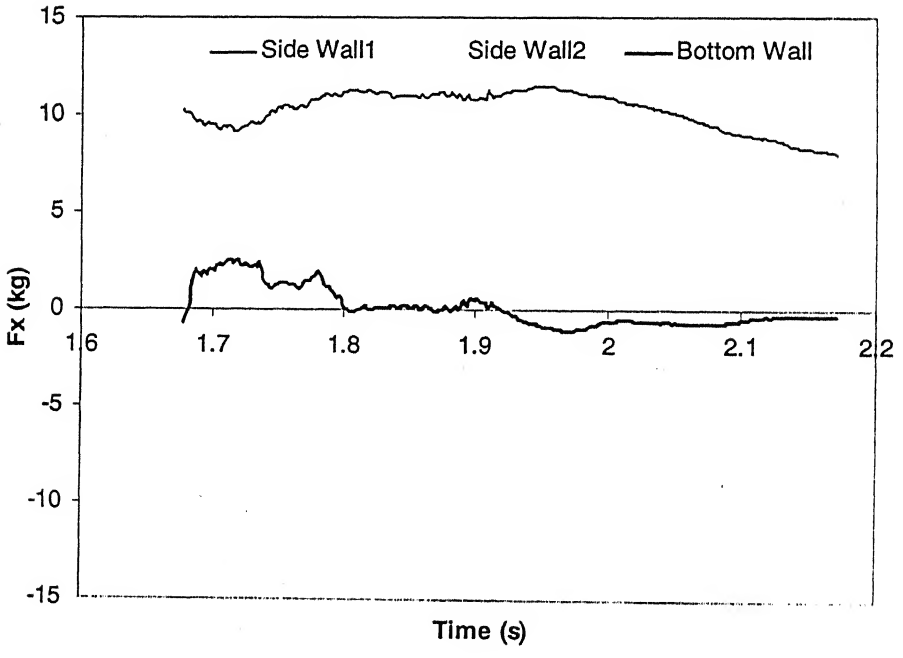

Fig. 5.10. Time vs. Fx at pile walls at relaxation time step in sand

From the above two plots it can be concluded that forces at x and y direction decreases with time as it released stresses. As there was no external force applied in x direction the sum of all force at pile walls was about to zero. At the end of relaxation time of 0.5sec, the loads in y direction at two side walls and bottom wall were 1.362kg, 0.7kg and 2.087kg respectively and in x direction 7.985kg, 9.08kg and 0.259kg respectively.

The pressures at the walls of the sand sample were also calculated to find out the wall pressure of sample at the end of relaxation period. The variation of pressure of walls of soil sample with time interval is shown in Fig. 5.11. and Fig. 5.12.

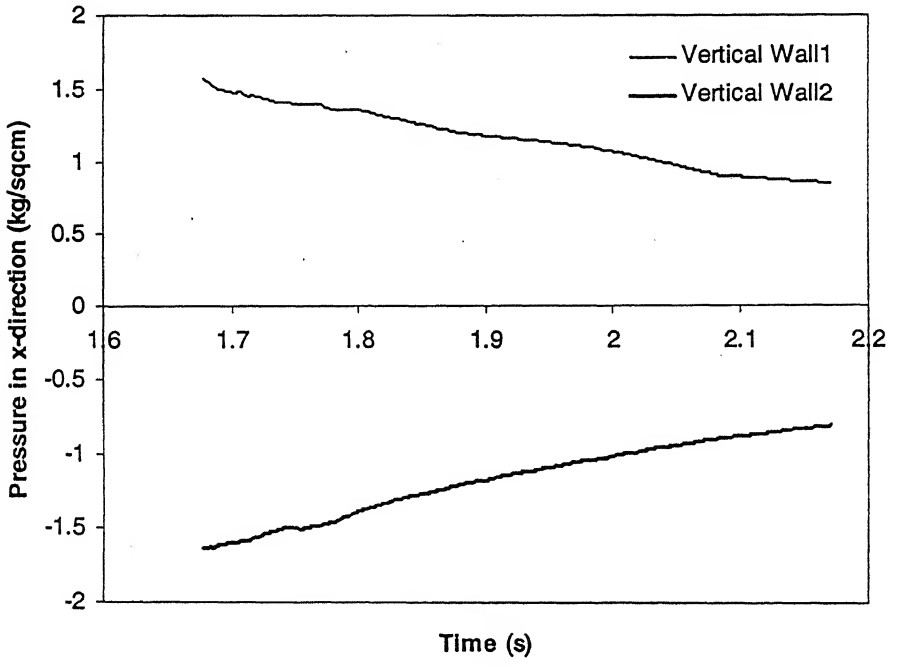

Fig. 5.11. Variation of pressure in x direction with time at vertical walls of sand sample

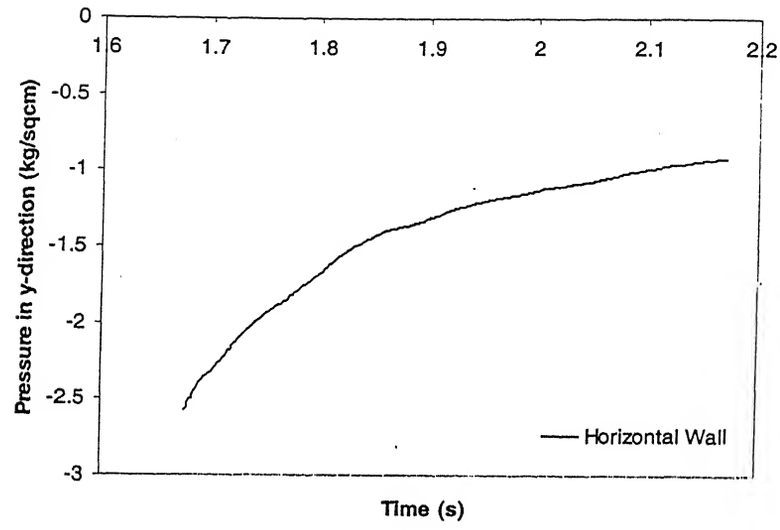

Fig. 5.12. Variation of pressure in y direction with time at horizontal walls of sand sample

It is seen from the above two plots that pressure in x and y direction decreases with relaxation time. At the end of relaxation time the pressures in x direction at vertical walls of the sample were 0.842kg/cm^2 and 0.811 kg/cm^2 and pressure in y direction at horizontal wall was 0.918kg/cm^2.

In the next step i.e. application of cell pressure in both horizontal and vertical direction, the cell pressure (0.3 and 0.6kg/cm^2) value would be deducted from the present pressure in soil sample as they were acting in the opposite direction. After getting the particular pressure at the walls of soil sample after deducting the cell pressure of different direction separately the bearing capacity was determined due to settlement under axial compressive load. The bearing capacity was determined for single pile in terms of shaft resistance and tip resistance separately for every stress condition. The typical load-displacement curves were obtained by DEM and from this curve failure load for pile was determined in terms of shaft and tip resistance separately. Various load-displacement curves by using DEM for different stress conditions are shown in Fig. 5.13, 5.14, 5.15 and 5.16.

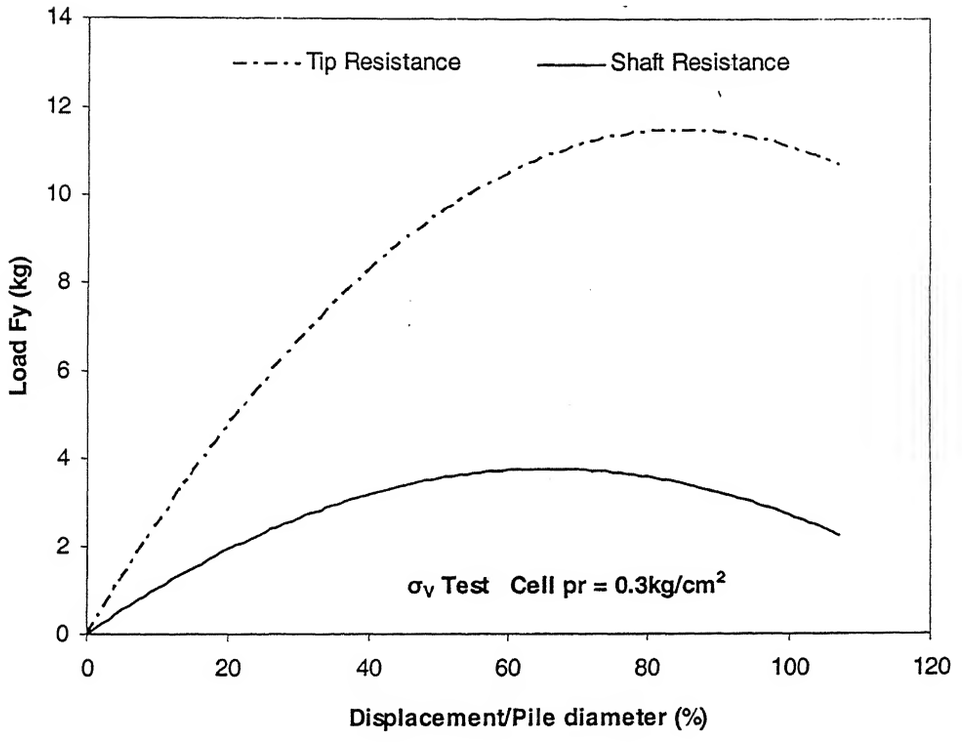

Fig. 5.13. Load-displacement curve for sand (σ_V test, cell pr = of 0.3kg/cm^2)

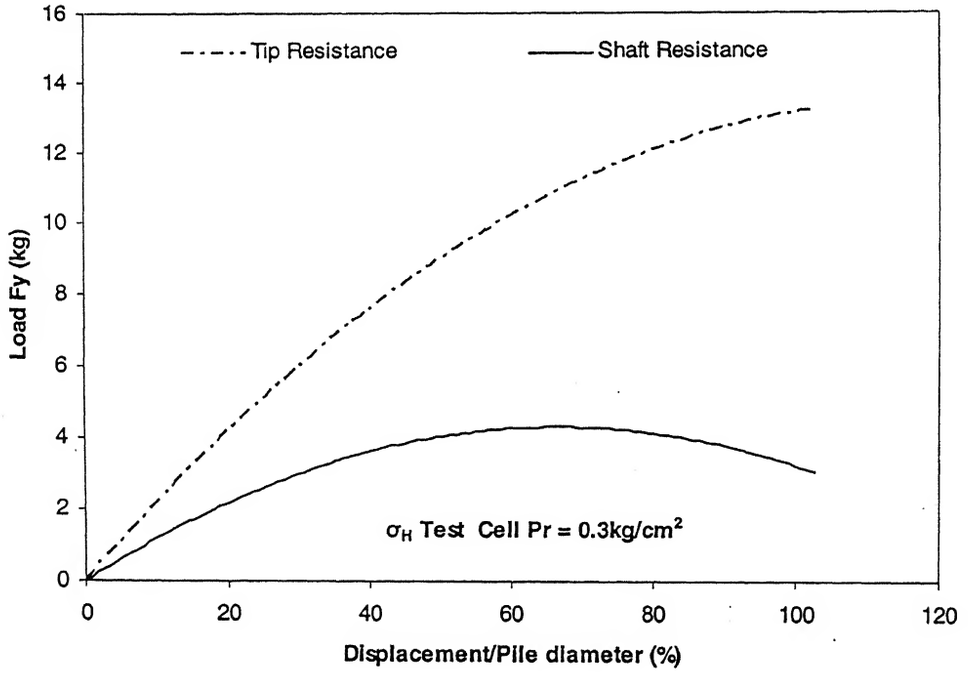

Fig. 5.14. Load-displacement curve for sand (σ_H test, cell pr = 0.3kg/cm^2)

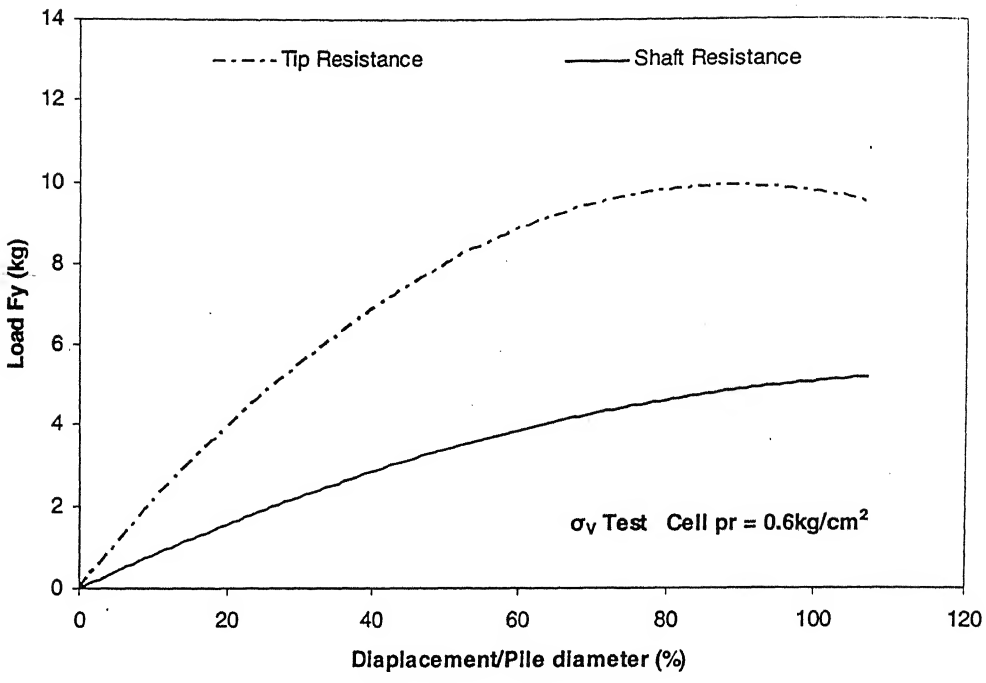

Fig. 5.15. Load-displacement curve for sand (σ_V test, cell pr = 0.6kg/cm^2)

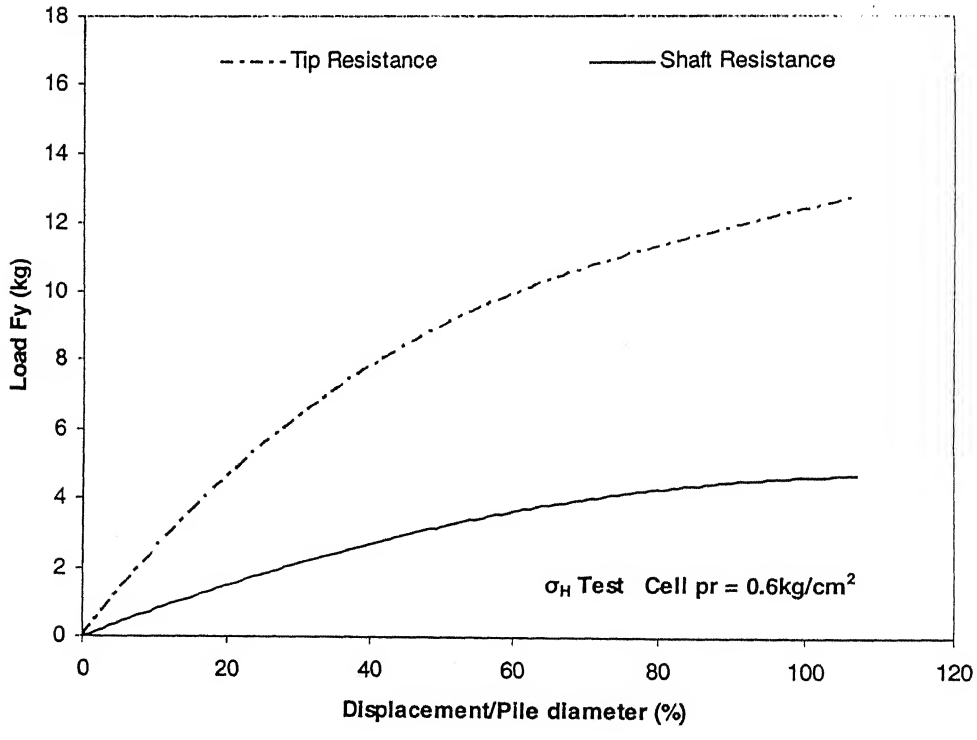

Fig. 5.16. Load-displacement curve for sand (σ_H test, cell pr = 0.6kg/cm^2)

Typical load-displacement curve is shown for load in x direction of wall of pile in Fig. 5.17. As the pile was settled only for compressive load and there was no lateral load, the sum of load at pile walls approximately equal to zero at every stress condition.

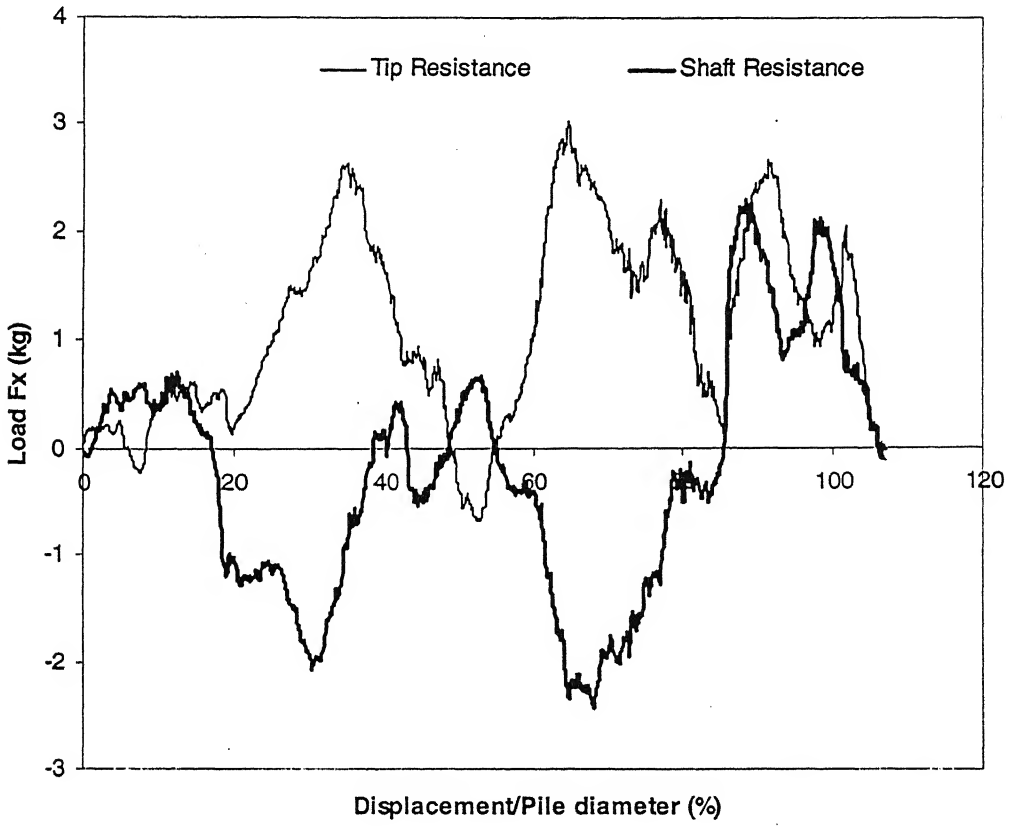

Fig. 5.17. Load-displacement curve for sand in σ_V test condition at cell pressure of 0.3kg/cm^2 in the x direction

The value of total capacity of single pile in sand at different stress condition by DEM is shown in Table 5.2.

Table 5.2. Values of total capacity of single pile (L/D = 8.93) in sand by DEM

Cell Pressure (kg/cm^2)	Vertical Test (σ_V Test)			Horizontal Test (σ_H Test)		
	Tip Resistance q_{pV} (kg)	Shaft Resistance fs_V (kg)	Total Resistance q_{tV}(kg)	Tip Resistance q_{pH} (kg)	Shaft Resistance f_{sH} (kg)	Total Resistance q_{tH}(kg)
0.3	9.3	3.5	12.8	10.4	3.8	14.2
0.6	10.2	4.3	14.5	11.2	4.0	15.2

5.6.2. For Clay

Similarly for clay the load in both x and y direction generated at the time of installation were plotted to show the variation of increasing load with time. The variation of load with time at installation in y and x direction is shown in Fig. 5.18 and Fig 5.19.

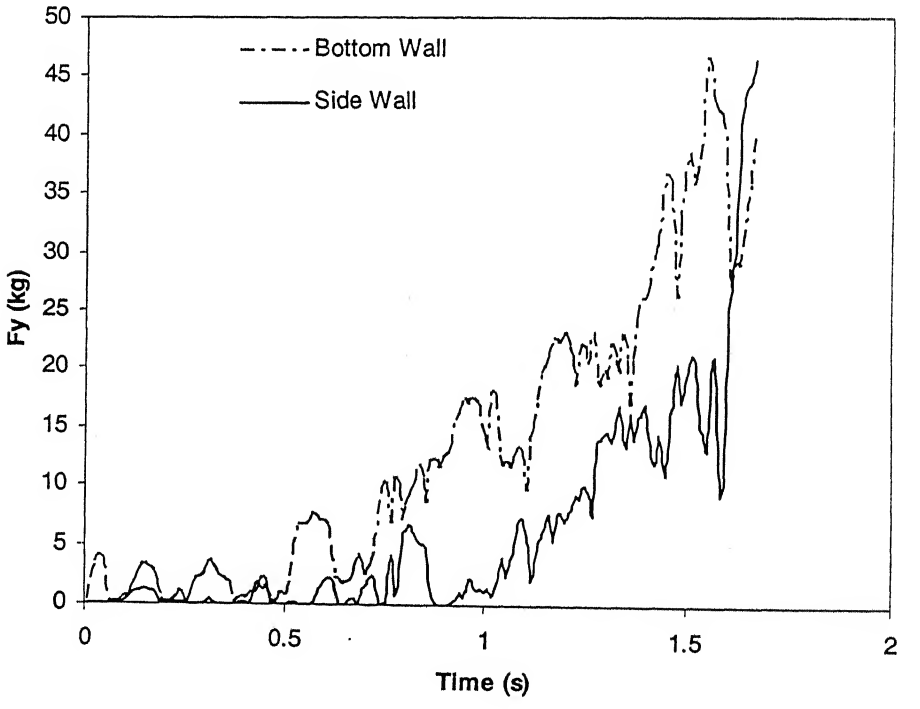

Fig. 5.18. Time vs. Fy at pile walls at installation of pile

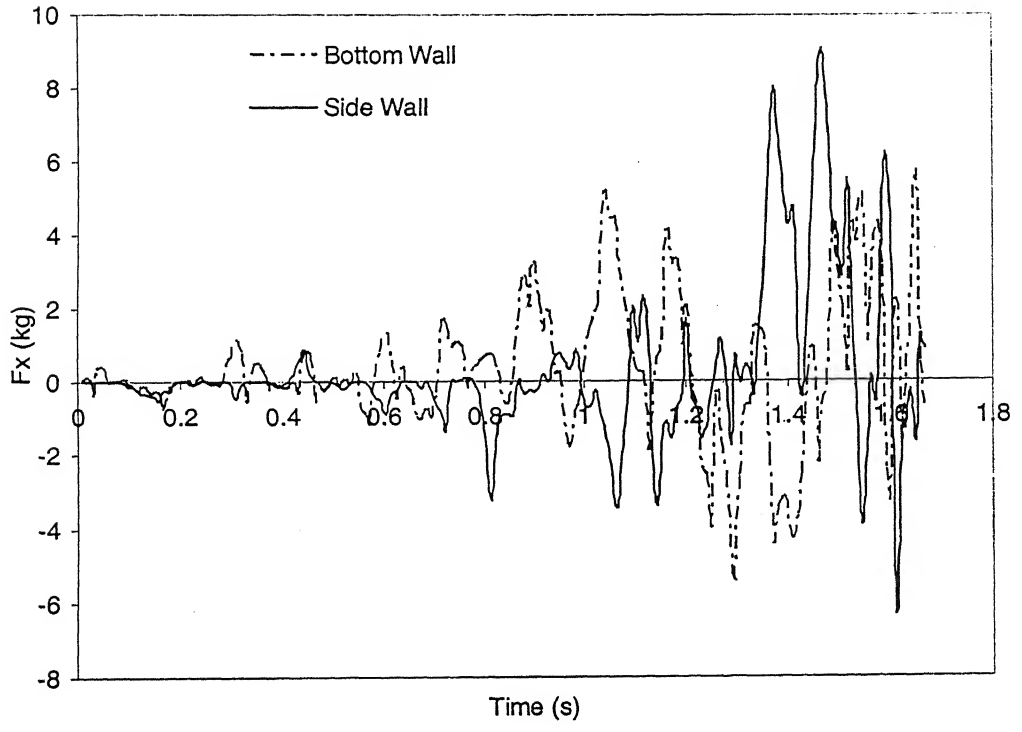

Fig. 5.19. Time vs. Fx at pile walls at installation of pile

Here it is also seen that the sum of all forces at pile walls in x direction at any time was almost zero as there was no external force applied in x direction.

In the relaxation part for clay it also released stress with time both in x and y direction in the pile walls. Here also period of relaxation time was chosen 0.5sec. Load was also decreasing with time here in both directions in pile walls as there were no loads on pile in relaxation period. The force both y and x direction at pile walls in clay with time at relaxation period is shown in Fig. 5.20. and Fig. 5.21.

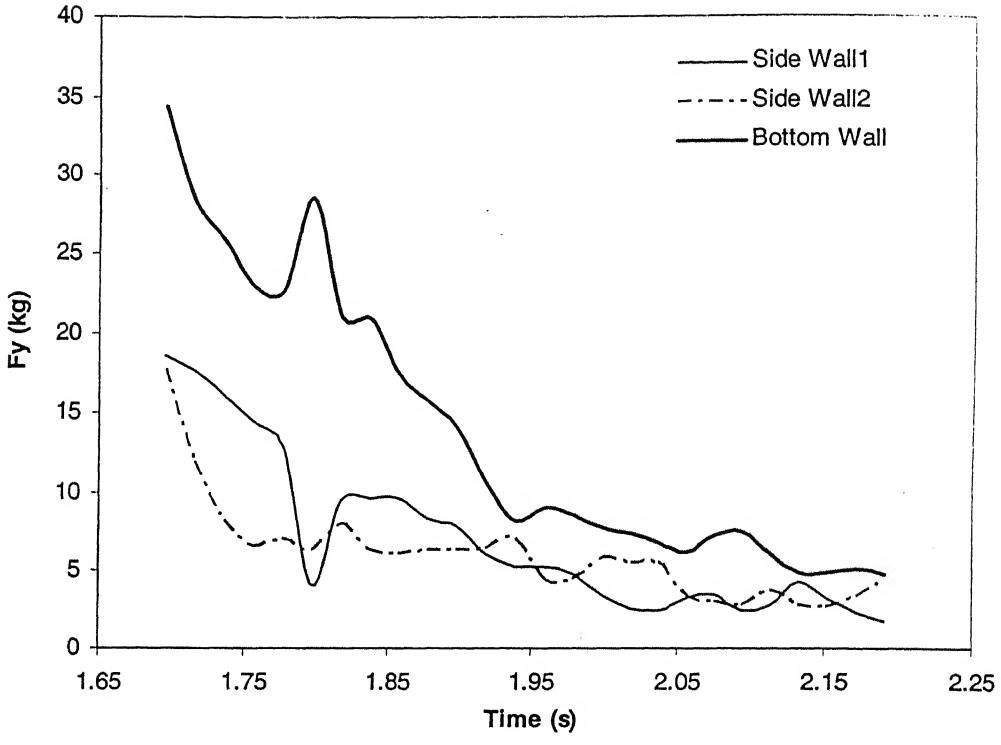

Fig. 5.20. Time vs. Fy at pile walls at relaxation time step in clay

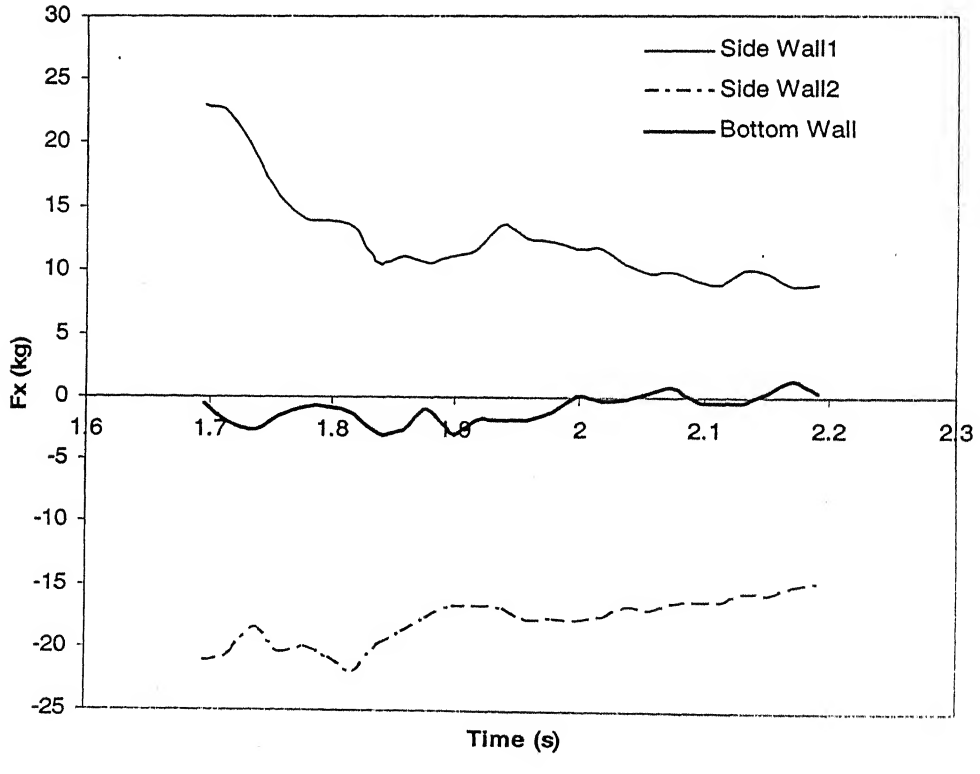

Fig. 5.21. Time vs. Fx at pile walls at relaxation time step in clay

The variations of pressure on clay sample wall in both directions were also determined. Stresses were also released from clay sample wall at the relaxation period. The variation of pressure with time in x and y direction is shown in Fig. 5.22. and 5.23. to estimate the pressure on the wall of clay before applying axial load and cell pressure. Variation of pressure in x direction was determined in vertical walls and pressure in y direction in horizontal walls of clay sample.

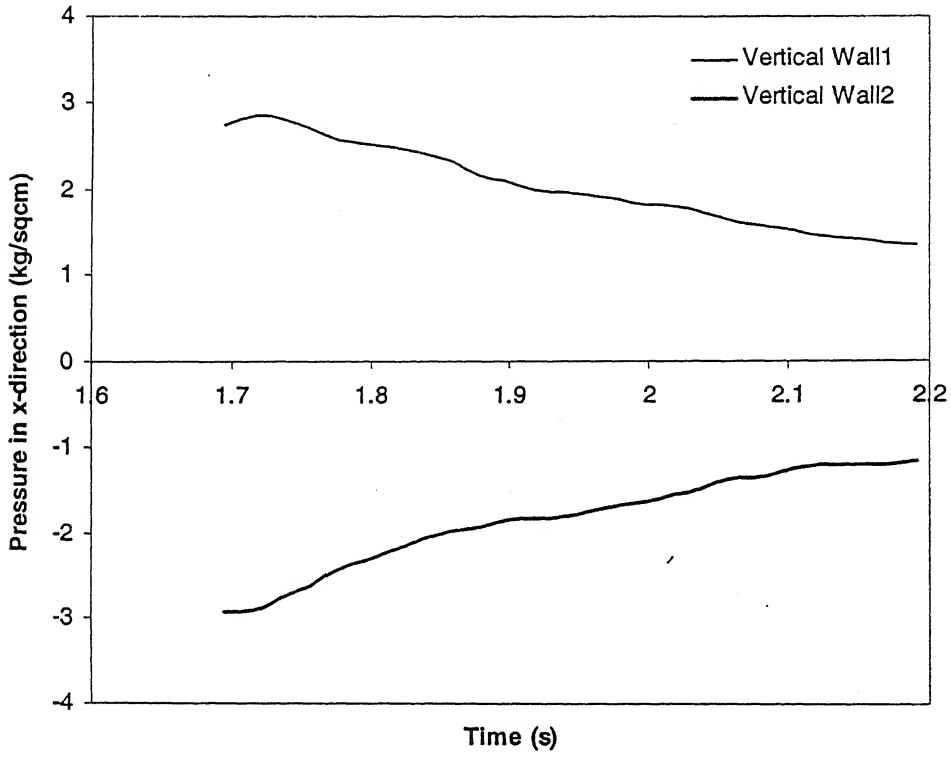

Fig. 5.22. Variation of pressure in x direction with time at vertical walls of clay sample

From the above figure it is seen that at the end of relaxation period the pressure in x direction in vertical walls were 1.353kg/cm^2 and 1.167kg/cm^2. As at the time of σ_H tests the cell pressure was applied from the horizontal direction only the resultant pressure would be the difference between the present pressure at the vertical walls of clay and cell pressure in horizontal direction.

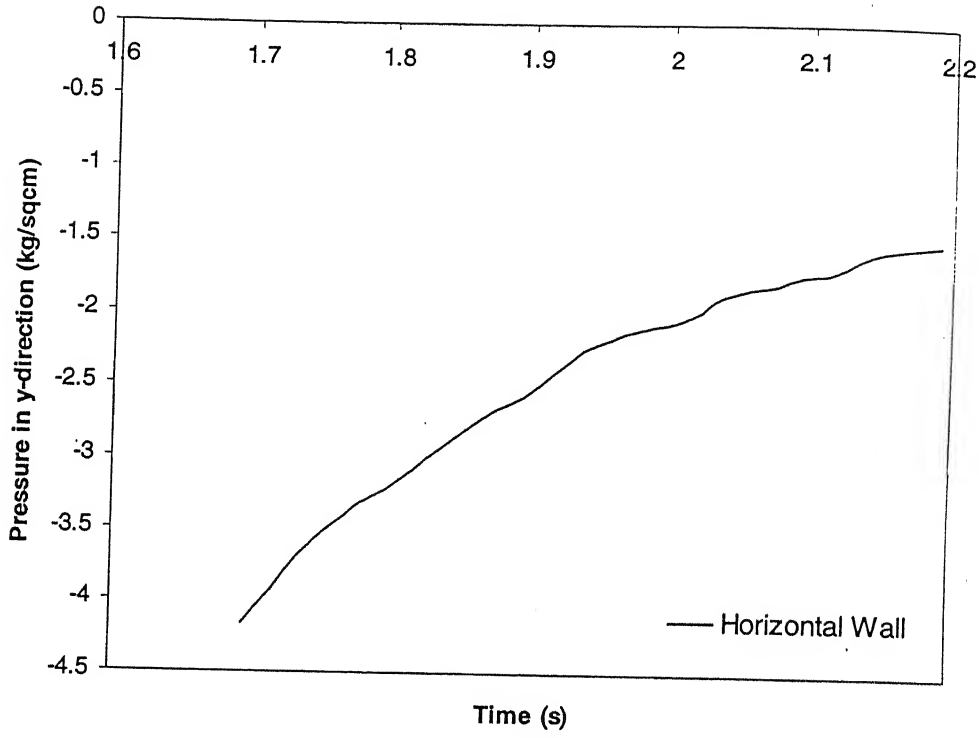

Fig. 5.23. Variation of pressure in y direction with time at horizontal walls of clay sample

Similarly in case of σ_H test cell pressure was coming from the vertical direction of clay sample. Here from the above plot it is measured that at the end of relaxation period the pressure in horizontal wall was 1.516kg/cm^2. So after the application of vertical cell pressure the resultant pressure acting on the clay was the difference between the value obtained from the graph and the cell pressure.

In next step the cell pressure was applied different stress condition and allowed to settle due to compressive load and load deflection curves were plotted and ultimately from that curves the total capacity of pile were determined in terms of tip resistance and shaft resistance due to compressive load only. Various load-displacement curves by using DEM for different stress conditions in clay are shown in Fig. 5.24, 5.25, 5.26 and 5.27.

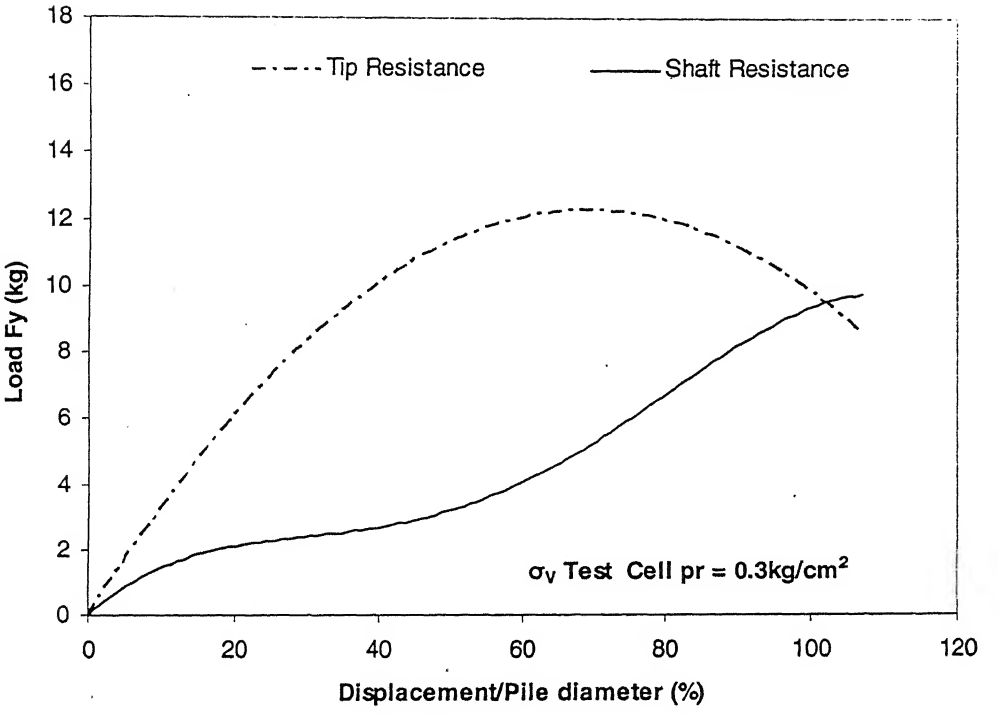

Fig. 5.24. Load-displacement curve for clay (σ_V test, cell pr = 0.3kg/cm^2)

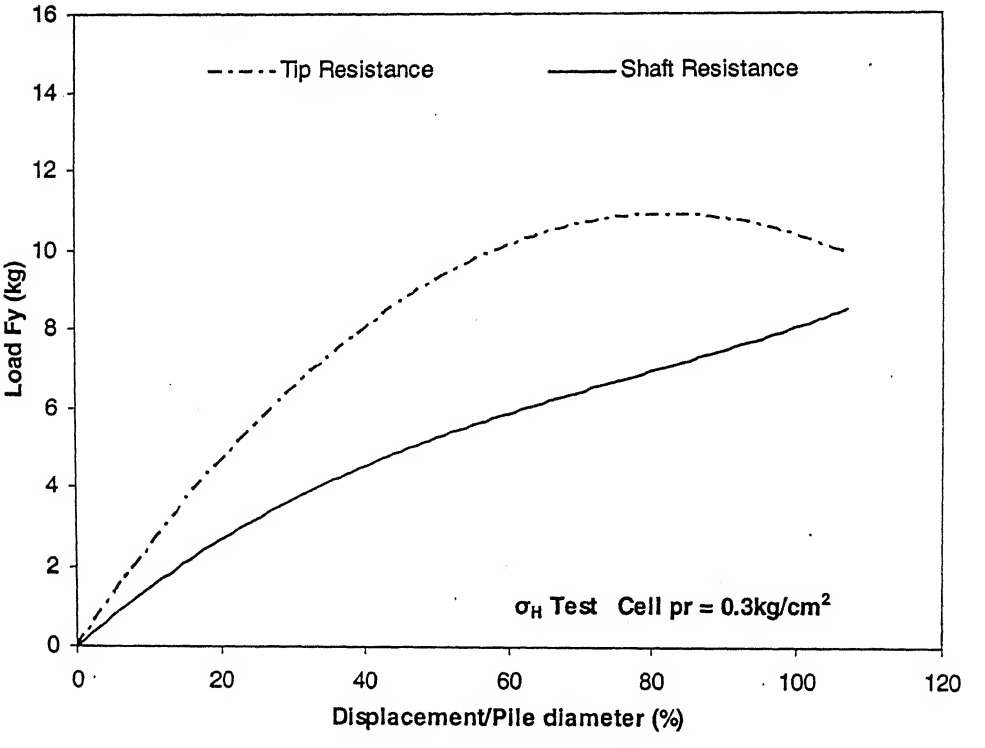

Fig. 5.25. Load-displacement curve for clay (σ_H test, cell pr = 0.3kg/cm^2)

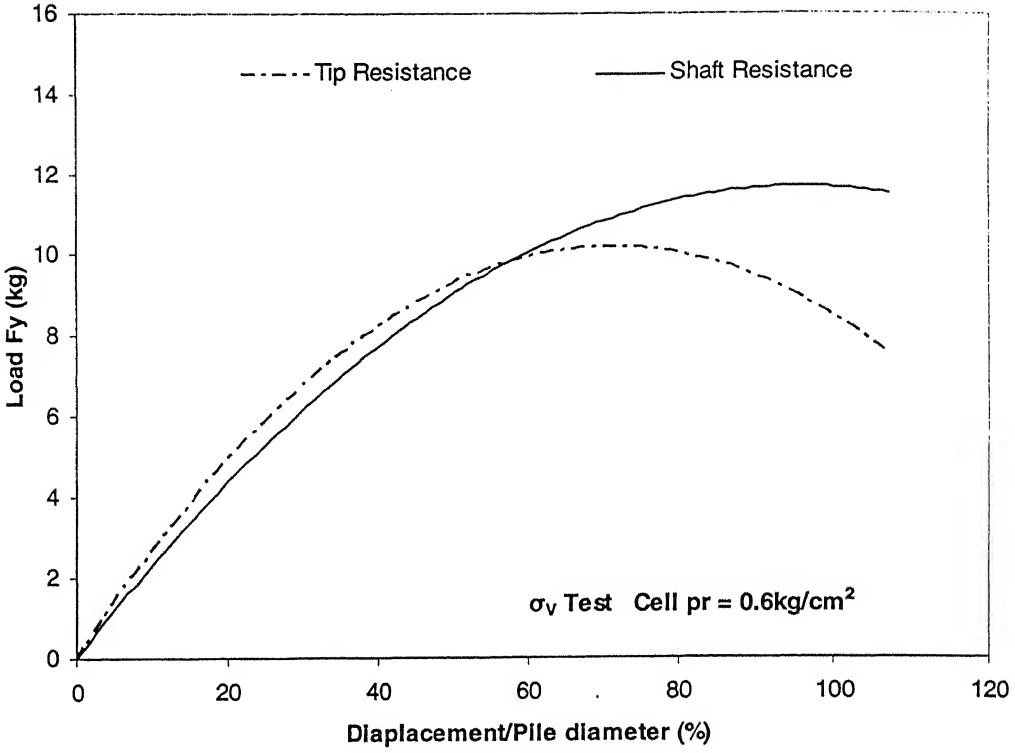

Fig. 5.26. Load-displacement curve for clay (σ_V test, cell pr = 0.6kg/cm^2)

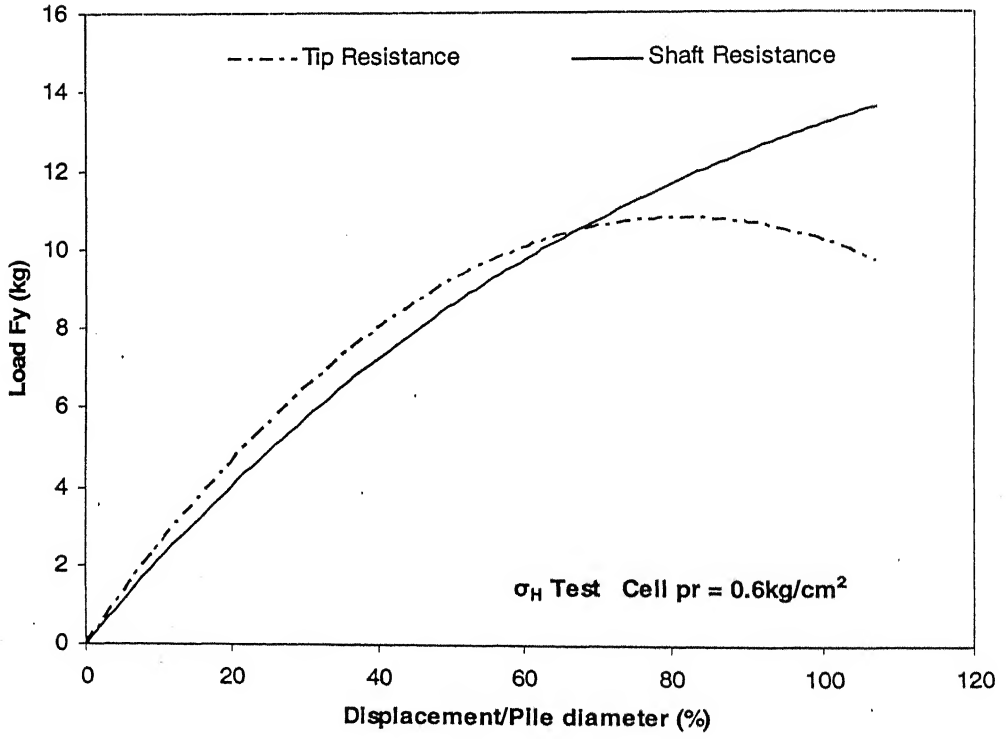

Fig. 5.27. Load-displacement curve for sand (σ_H test, cell pr = 0.6kg/cm^2)

Load in the x direction also produced in the walls of the pile at the time of settlement due to axial compressive loads in clay. Typical load settlement curve is shown to determine the load in x direction in Fig. 5.28.

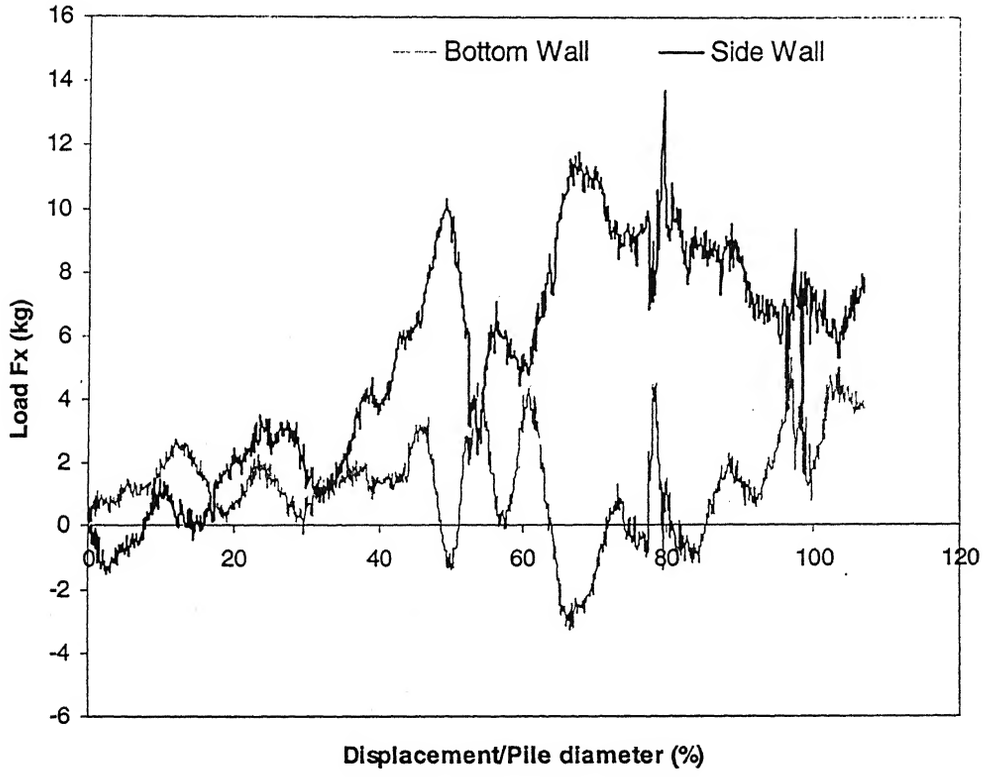

Fig. 5.28. Load-displacement curve for clay in σ_H test condition at cell pressure of 0.3kg/cm^2 in the x direction.

From the above plot it is seen that the summation of loads induced in the walls of piles give a positive value at every point though there was no force applied externally. But its magnitude of force neglected at the time of calculation of total capacity of pile. As the soil particles in the sample about the pile was not symmetrically settled i.e. the total soil particle density in the left side of pile was not equal to the right side of the pile, the summation of forces in the pile walls in x axis was not about to zero. But this value would not be considered to maintain the equilibrium condition in x direction of the axisymmetric problem.

The value of total capacity of single pile in clay at different stress condition by DEM is shown in Table 5.3.

Table 5.3. Values of total capacity of single pile (L/D = 8.93) in clay by DEM

Cell Pressure (kg/cm^2)	Vertical Test (σ_V Test)			Horizontal Test (σ_H Test)		
	Tip Resistance q_{pV} (kg)	Shaft Resistance f_{sV} (kg)	Total Resistance q_{tV}(kg)	Tip Resistance q_{pH} (kg)	Shaft Resistance f_{sH} (kg)	Total Resistance q_{tH}(kg)
0.3	9.0	6.2	15.2	10.2	5.8	16.0
0.6	10.0	10.5	20.5	11.0	11.2	22.2

5.7. Comparison of Results by DEM for Sand and Clay

At the time of installation the magnitude of force induced in y direction at pile walls in clay was greater than sand. In sand, the force induced at the end of installation in bottom wall was 32.36kg whereas for clay it was 39.95kg. Similarly for side walls this forces were in sand and clay 9.29kg and 46.29kg respectively. The magnitude of side wall force in clay was very large as compared to sand due to the adhesion property of clay. But the force induced in the x direction at pile walls in clay was smaller than in sand. In case of sand the forces in x direction at the end of installation in bottom and side walls were 1.05kg and 1.25kg whereas for clay it was 0.8kg and 0.9kg respectively.

In the relaxation period the load released for bottom and side walls at different rate for sand and clay. It was observed that the rate of load released in y direction at bottom wall for sand was more than clay. For example at time period of 1.67sec the value of force in y direction of bottom wall for sand was 30.85kg and in time period

1.85sec it was 2.96kg i.e. the rate of releasing load was 154.94kg/sec. But for the clay this rate was for bottom wall 94.61kg/sec. But for side walls of pile it showed totally opposite results. The load releasing in y direction at side walls was more in clay than sand. The average rate of load released at side walls in clay was 30kg/sec whereas in case of sand it was 5.9kg/sec.

From the load settlement curve at various stress condition the ultimate capacity of single piles were determined in terms of tip and shaft resistance. It was shown that the tip resistance for sand was more than clay for all cases but the difference between those values was very small. For example the tip resistances for sand in σH test for cell pressure 0.3kg/cm^2 and 0.6 kg/cm^2 were 10.4kg and 11.2kg respectively but in case of clay these values were 10.2kg and 11.0kg respectively. But in case of shaft resistance the values were greater for clay than sand. For example the shaft resistances in sand in σ_V test for cell pressure 0.3kg/cm2 and 0.6 kg/cm2 were 3.5kg and 4.3kg but in case of clay these values were 6.2kg and 10.5kg respectively. As there was cohesion between pile and soil particle the shaft resistance was more in case of clay. It was also seen that the total resistance for pile in controlled horizontal stress condition (σ_H test) was more than controlled vertical stress condition (σ_V test) in both sand and clay.

Chapter - VI

Determination of Interaction Factor and Efficiency of Pile Groups by Regression Analysis

6.1. General

The aim of this investigation was to develop a simplified method of arriving at the efficiency of the group pile in clay under different stress conditions. An experimental cum empirical procedure was suggested here by, to determine the efficiency of pile groups under compressive loads. The procedure is based on the concept of interaction factor (Poulos and Mattes, 1971). The underlying principle of the present approach is that the total group capacity of a pile under axial compressive load in clay is influenced by the presence of adjacent pile, and effect of the same can be incorporated using the concept of interaction factor.

6.2. Formulation of the analysis

6.2.1. Two-Pile Interaction under Compressive Load

A group of two identical equally loaded piles is shown in Fig. 5.1. Now suppose for the case of pure compressive load on pile group, following characteristics can be specified as under:

L = Length of pile

D = Diameter of pile

s = Spacing of pile group

E_s = Modulus of elasticity of soil medium

E_p = Modulus of elasticity of pile material

P_{ul} = Ultimate load carrying capacity in compression of the single pile

P_2 = Axial compressive load carried by each pile of two pile group

PU_2 = Ultimate compressive load carried by each pile of two pile group

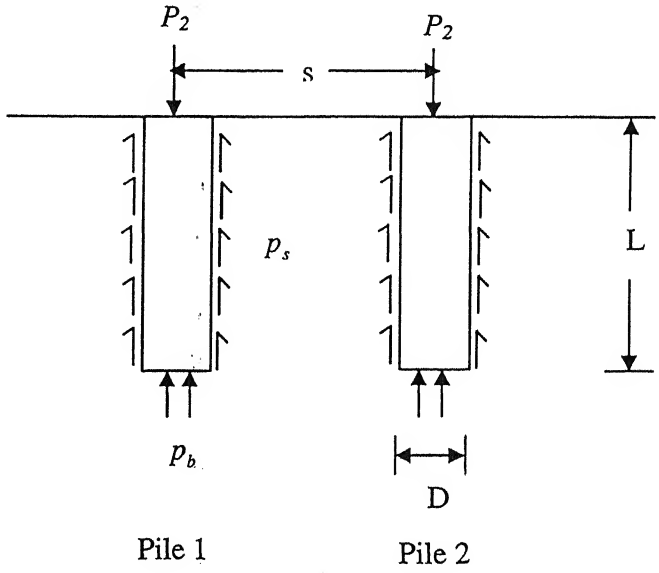

Fig. 6.1. Two pile group under compressive load

Now,

$$R_A = \frac{A_p}{\frac{\pi D^2}{4}}$$

= Ratio of area of pile section A_p to area bounded by outer circumference of pile

R_A = 1 for solid pile (as also in the present case)

$K = \frac{E_p R_A}{E_s}$ = Relative compressibility of pile (or relative stiffness)

$= \frac{E_p}{E_s}$ (for present case, $R_A = 1$)

H = Depth of bearing stratum

ν_s = Poisson's ratio of soil media

The settlement of pile 1 is given by

$$\rho = \frac{P_2 I}{E_s D} + \Delta\rho \qquad \text{..... (6.1)}$$

Where, I = settlement influence factor

$$I = f(L/D, K, L/H)$$

And $\Delta\rho$ is the additional settlement experienced by each pile due to influence of other pile.

Equation (5.1) may be modified as (for the influence of other pile)

$$\rho = \frac{P_2 I}{E_s D} + \alpha\frac{P_2 I}{E_s D} \qquad \text{..... (6.2)}$$

Where α is a pile-pile interaction factor and is defined as

$$\alpha = \frac{\text{Additional settlement caused by adjacent pile}}{\text{Settlement of pile under its own load}}$$

α is a function of ratios of the length of the pile (L) to pile size (D), spacing of the piles (S) to pile size(D), length of the pile(L) to depth of bearing stratum(H), relative pile-soil stiffness(K) and Poisson's ratio (ν) and thus the same can be written as follows,

$$\alpha = f(L/D, S/D, K, L/H, \nu_s)$$

Equation (6.2) may be rewritten as

$$\rho = \frac{P_2 I(1+\alpha)}{E_s D}$$

When P_2 tends to PU_2, the settlement of the pile tends towards the infinity and the term $PU_2(1+\alpha)$ tends to P_{ul}, the maximum load the single pile can take i.e.

$$PU_2 + \alpha PU_2 = P_{ul} \qquad \text{..... (6.3)}$$

Equation (6.3) yields,

$$\frac{PU_2}{P_{ul}} = \frac{1}{1+\alpha} \qquad \text{..... (6.4)}$$

Efficiency in compression of two pile group is defined as

$$\eta_2 = \frac{\text{2 x ultimate compressive load carried by each pile of pile group}}{\text{2 x ultimate compressive load carrying capacity of single pile}}$$

Or $\eta_2 = \dfrac{1}{1+\alpha}$

Hence efficiency of two pile group and interaction factor is interrelated by;

$$\eta_2 = \frac{1}{1+\alpha} \qquad \text{..... (6.5)}$$

6.2.2. Four-Pile Interaction under Compressive Load

Applying the principle of superposition, as suggested by Madhav and Pooroshab (1985), the efficiency in compression of four pile group of similar spacing (shown in Fig. 6.2.) can be derived from the efficiency of two pile group given by Eq. 6.6.

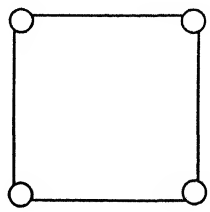

Fig. 6.2. Four pile groups with equal pile spacing

Similarly in four pile group, two piles at spacing of s and one pile at spacing of $\sqrt{2}s$ is available to interact with other pile. Hence one addition in interaction factor at spacing s and one additive interaction factor at spacing $\sqrt{2}s$ are needed i.e.

$$\eta_4 = \frac{1}{1+2\alpha(s)+\alpha(\sqrt{2}s)} \qquad \text{..... (6.6)}$$

6.3. Regression Model

In the present study the efficiency (η) of pile group is a function of s/D, stress (σ) and L/D. So a model is fitted for the efficiency for 2x1 pile group and 2x2 pile group separately to get the relation of s/D, σ and L/D with efficiency in different stress condition. In the present case Quadratic Response Surface Regression designs are adopted to get the relation. Quadratic Response Surface Regression designs are a hybrid type of design with characteristics of both polynomial regression designs and fractional factorial regression designs. Quadratic response surface regression designs contain all the same effects of polynomial regression designs to degree 2 and additionally the interaction effects of the predictor variables. The regression equation for a quadratic response surface regression design for 3 continuous predictor variables *P*, *Q*, and *R* would be

$$y = b_0 + b_1P + b_2P^2 + b_3Q + b_4Q^2 + b_5R + b_6R^2 + b_7P*Q \qquad \text{..... (6.7)}$$

6.3.1. Model for 2x1 Pile Group

For 2x1 pile group for both σ_V test and σ_H test the following linear model for efficiency is proposed:

$$\eta = a_1(s/D)^2 + a_2(s/D) + a_3 + a_4(\sigma)^2 + a_5(L/D)^2 + a_6(L/D)(\sigma) \qquad \text{..... (6.8)}$$

The relation of s/D, σ and L/D with efficiency (η) determined from the experimental results is shown below:

η = Quadratic relation with s/D when σ and L/D are fixed

η = Quadratic relation with L/D when σ and s/D are fixed

η = Quadratic relation with σ when s/D and L/D are fixed

(L/D)(σ) = Interaction effect

On the basis of the above relation of s/D, σ and L/D with efficiency (η) the model (Eq. 6.8) is determined.

6.3.2. Model for 2x2 Pile Group

For 2x2 pile group for both σ_V test and σ_H test the following linear model for efficiency is proposed:

$$\eta = a_1(s/D)^2 + a_2(s/D) + a_3 + a_4(\sigma) + a_5(L/D)^2 + a_6(L/D)(\sigma) \quad \ldots\ldots\ldots\ldots (6.9)$$

The relation of s/D, σ and L/D with efficiency (η) determined from the experimental results is shown below:

η = Quadratic relation with s/D when σ and L/D are fixed

η = Quadratic relation with L/D when σ and s/D are fixed

η = Linear relation with σ when s/D and L/D are fixed

(L/D)(σ) = Interaction effect

On the basis of the above relation of s/D, σ and L/D with efficiency (η) the model (Eq. 6.9) is determined.

6.4. Parameter Estimation by Least Square Method

The Curve Fitting Toolbox uses the method of least squares when fitting data. The fitting process requires a model that relates the response data to the predictor data with one or more coefficients. The result of the fitting process is an estimate of the "true" but unknown coefficients of the model.

To obtain the coefficient estimates, the least squares method minimizes the summed square of residuals. The residual for the *i*th data point r_i is defined as the difference between the observed response value y_i and the fitted response value $\bar{y}_i$, and is identified as the error associated with the data.

Now, Residual = Data – Fit

$$r_i = y_i - \bar{y}_i \qquad \text{..... (6.10)}$$

The summed square of residuals is given by

$$S = \sum_{i=1}^{n} r_i^2 = \sum_{i=1}^{n} (y_i - \bar{y}_i)^2 \qquad \text{..... (6.11)}$$

where n is the number of data points included in the fit and S is the sum of squares error estimate.

The Curve Fitting Toolbox uses the linear least squares method to fit a linear model to data. A linear model is defined as an equation that is linear in the coefficients. To illustrate the linear least squares fitting process, the n data points can be modeled by a polynomial: $y = b_0 + b_1P + b_2P^2 + b_3Q + b_4Q^2 + b_5R + b_6R^2 + b_7P*Q$

To solve this equation for the unknown coefficients b_0 to b_7, S can be written as a system of n simultaneous linear equations in 7 unknowns. If n is greater than the number of unknowns, then the system of equations is overdetermined.

$$S = \sum_{i=1}^{n} (y_i - (b_0 + b_1P + b_2P^2 + b_3Q + b_4Q^2 + b_5R + b_6R^2 + b_7P*Q))^2 \quad \ldots\ldots\ldots (6.12)$$

Because the least squares fitting process minimizes the summed square of the residuals, the coefficients are determined by differentiating S with respect to each parameter, and setting the result equal to zero.

$$\frac{\partial S}{\partial b_0} = 0 \; ; \quad \frac{\partial S}{\partial b_1} = 0 ; \quad \frac{\partial S}{\partial b_2} = 0 ; \quad \ldots\ldots\ldots\ldots\ldots ; \quad \frac{\partial S}{\partial b_7} = 0 \qquad \ldots\ldots\ldots\ldots (6.13)$$

Solve the 7 number of equations (6.13) to find b_1, b_2, b_3, ..., b_7. The Least Square Method to solve the present problem manually is very tedious.

6.5. Matlab Program

In the present study to find out the unknown coefficient is very difficult. So it is better to find this solution by iterative method. For that reason to get a optimal solution a code was developed in Matlab. In this code a function 'fminsearch' (Multidimensional unconstrained nonlinear minimization) were used to determine the optimal solution for unknown coefficient for all cases.

6.6. Results by Regression Analysis

6.6.1. Line Pile Group (2x1) in σ_V test

From the regression analysis the unknown coefficients were determined and new efficiency formula was proposed for 2x1 pile group in σ_V test condition which is shown by the Eq. 6.14.

$$\eta = -9.965\ (s/D)^2 + 99.1275\ (s/D) - 149.6163 + 69.8243\ (\sigma)^2 + 0.0683\ (L/D)^2 - 5.6411(L/D).(\sigma) \quad \ldots\ldots\ldots\ldots\ldots\ldots (6.14)$$

Fitted observation and experimental observation data with data point were plotted for the efficiency of 2x1 pile group in σ_V test condition and it is shown in Fig. 6.3.

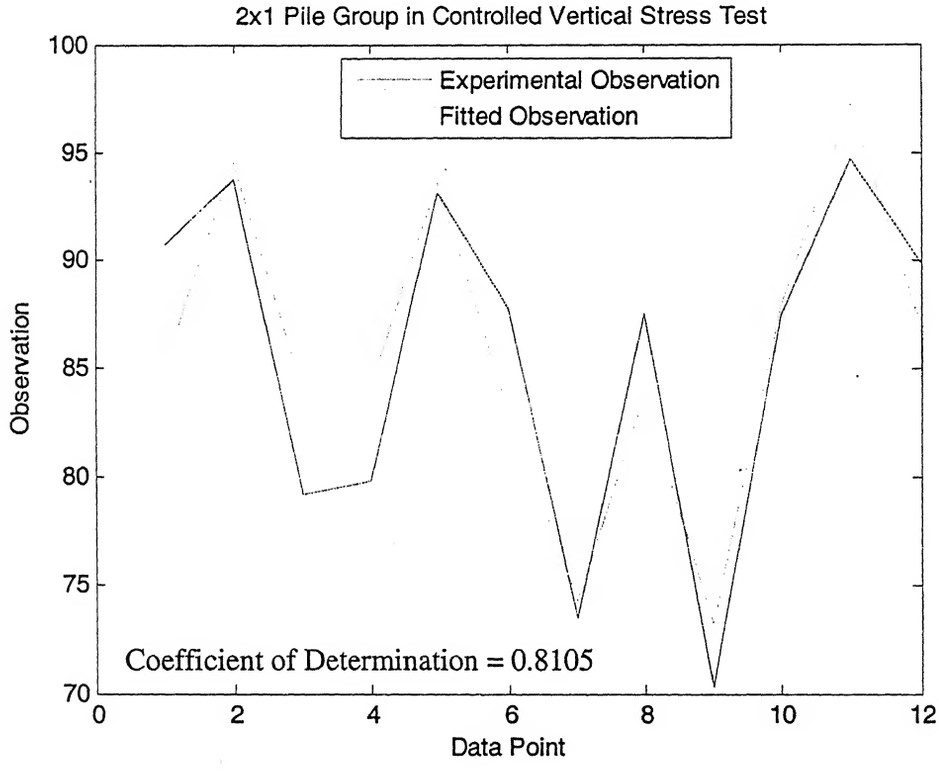

Fig. 6.3. Variation of fitted and experimental observation (σ_V test , 2x1 pile group)

6.6.2. Line Pile Group (2x1) in σ_H test

A different efficiency formula was proposed for 2x1 pile group on the basis of the experimental results in σ_H test condition by regression analysis which is shown by Eq. 6.15.

$$\eta = -5.7338\ (s/D)^2 + 56.8388\ (s/D) - 81.7545 + 69.5742\ (\sigma)^2 + 0.0941\ (L/D)^2 - 4.3368(L/D).(\sigma) \quad \ldots\ldots\ldots\ldots\ldots\ldots (6.15)$$

The variation of efficiency for 2x1 pile group in σ_H condition in fitted observation and experimental observation data is shown in Fig. 6.4.

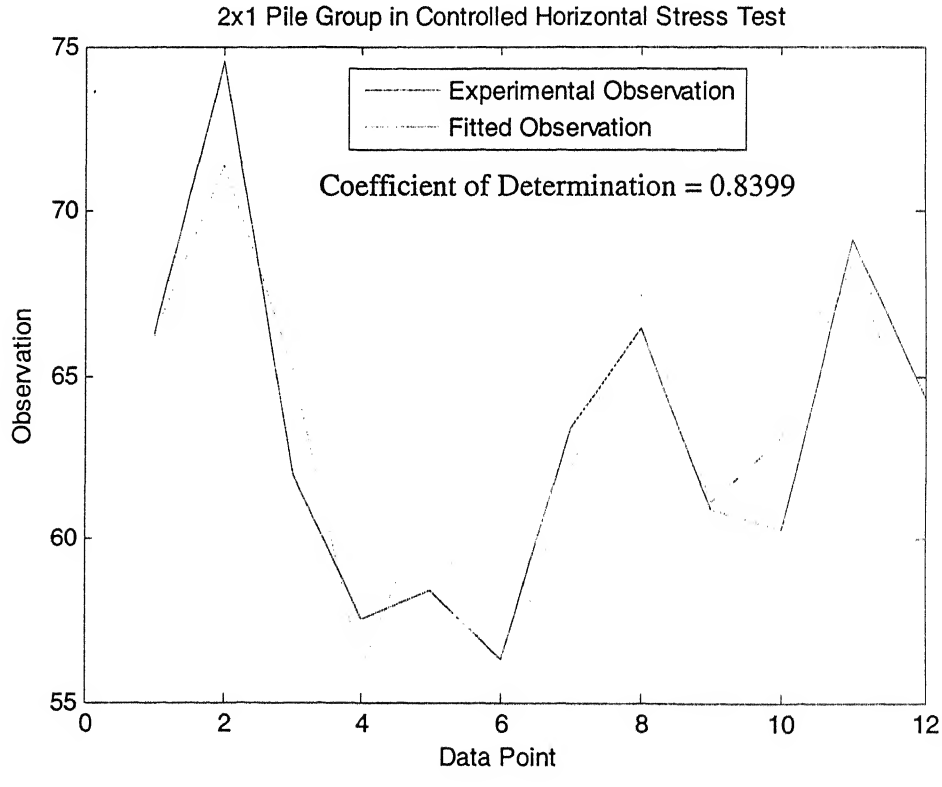

Fig. 6.4. Variation of fitted and experimental observation (σ_H test , 2x1 pile group)

6.6.3. Square Pile Group (2x2) in σ_V test

For 2x2 pile group in σ_V test condition a new formula was proposed on the basis of the experimental results to predict the efficiency for any s/D, L/D and stress condition which is shown by Eq. 6.16. It gives the best results than the other fitting observation.

$$\eta = -2.2513\ (s/D)^2 + 29.6838\ (s/D) - 10.3848 + 77.8149\ (\sigma) + 0.0475\ (L/D)^2 - 7.8193(L/D).(\sigma) \quad \ldots\ldots\ldots\ldots\ldots\ldots\ (6.16)$$

Fitted observation and experimental observation data with data point were plotted for the efficiency of 2x2 pile groups in σ_V test condition and variation of fitted and experimental observation data is shown in Fig. 6.4.

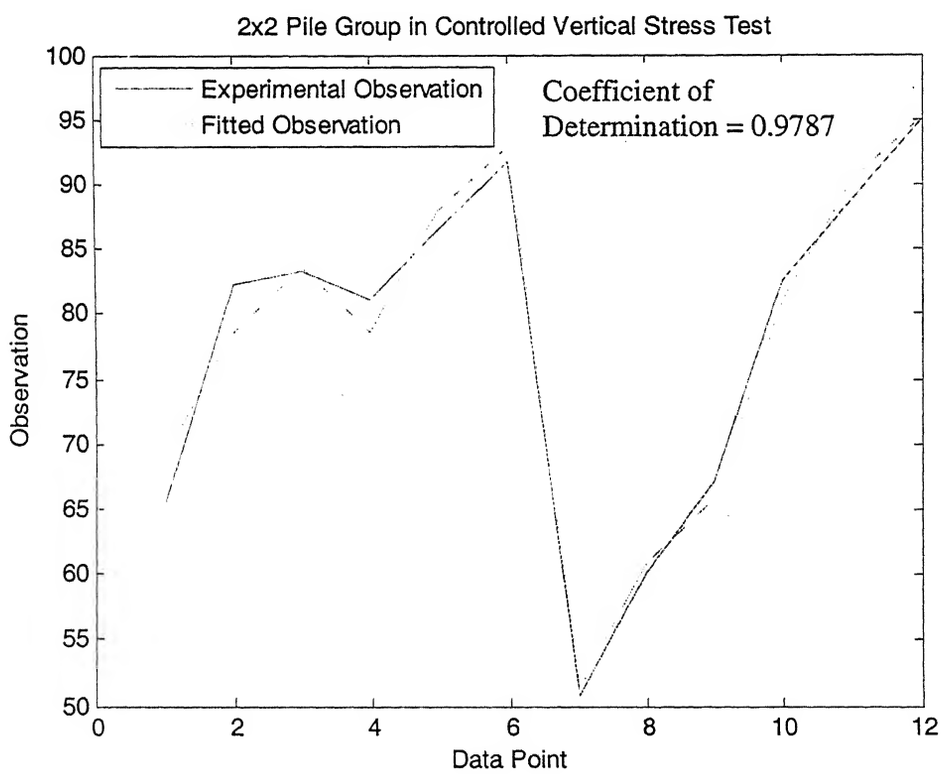

Fig. 6.5. Variation of fitted and experimental observation (σ_V test, 2x2 pile group)

6.6.4. Square Pile Group (2x2) in σ_H test

A similar new efficiency formula was proposed on the basis of the experimental results for 2x2 pile group in σ_H test condition for various s/D, L/D and horizontal stress condition which is shown by Eq. 6.17.

$$\eta = 0.8925\ (s/D)^2 - 3.5975\ (s/D) + 41.3461 + 2.5183\ (\sigma) + 0.0135\ (L/D)^2 - 0.8842(L/D).(\sigma) \quad \ldots\ldots\ldots\ldots\ldots\ldots\ (6.17)$$

The variation of efficiency for 2x2 pile group in σ_H condition in fitted observation and experimental observation data is shown in Fig. 6.6.

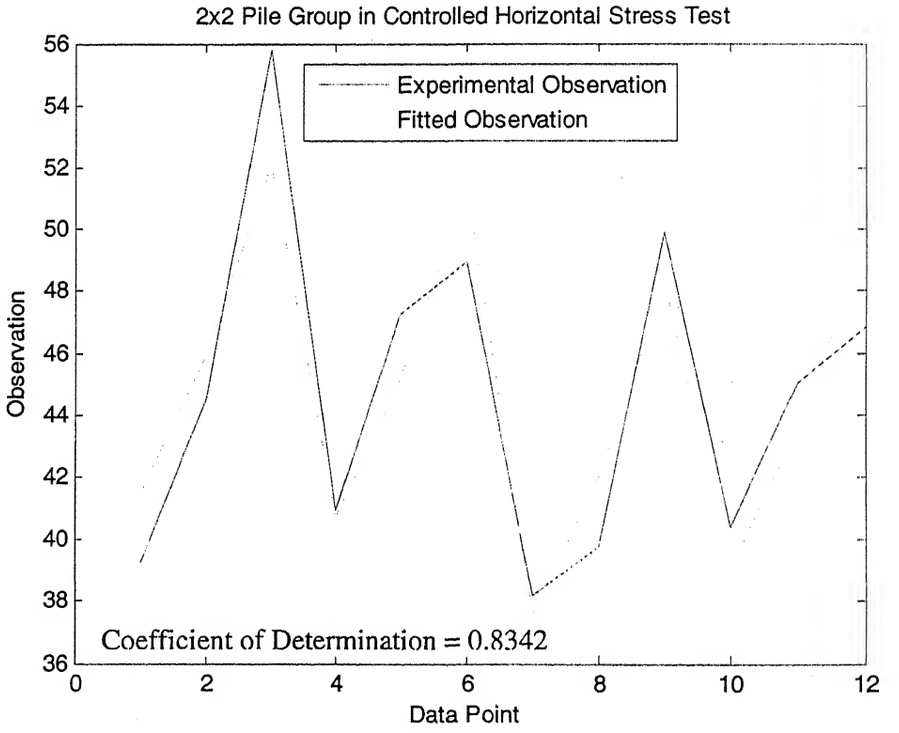

Fig. 6.6. Variation of fitted and experimental observation (σ_H test, 2x2 pile group)

6.7. Efficiency Analysis on basis of Regression Results

6.7.1. Line Pile Group (2x1)

6.7.1.1. Line Pile Group (2x1) in σ_V test

Efficiency of 2x1 pile group is calculated for different s/D, L/D and cell pressure on the basis of Eq. 6.14. The variation of group efficiency with spacing for different L/D and stress is shown Fig. 6.5.

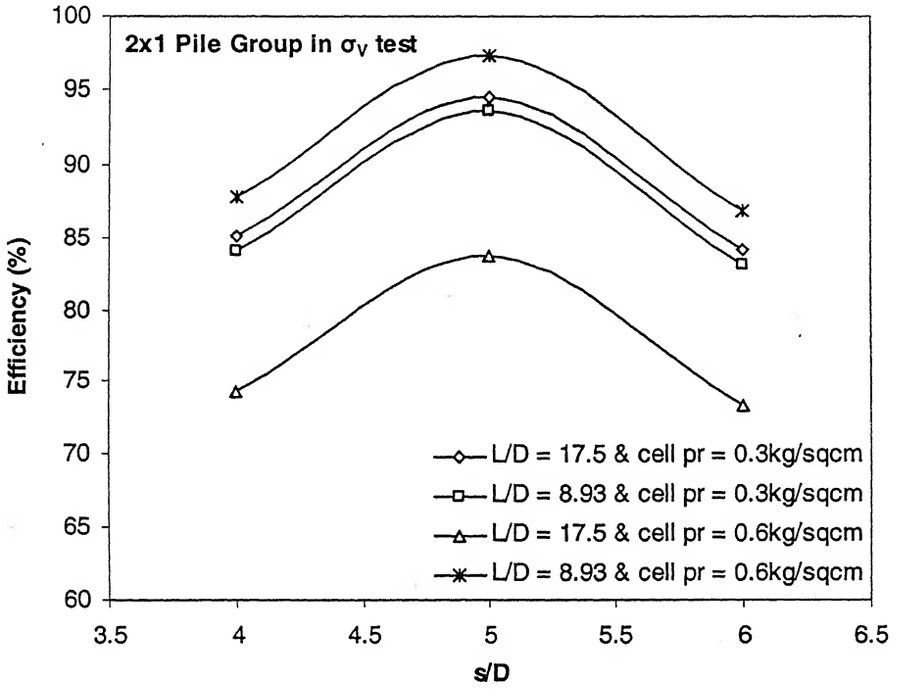

Fig. 6.7. Spacing vs. efficiency for 2x1 pile group in σ_V test

It is observed that group efficiency increases with increase in spacing from spacing 4D to 5D but it decreases from spacing 5D to 6D. For L/D of 8.93, the efficiency increases with increase in cell pressure. However for L/D of 17.5 it decreases with increase in cell pressure.

6.7.1.12. Line Pile Group (2x1) in σ_H test

The trend of efficiency was similar for 2x1 pile group in σ_H test as it was in σ_V test. The values are shown in Table 6.1.

Table 6.1. Values of efficiency for 2x1 pile group

2x1 Pile Group in σ_V test				2x1 Pile Group in σ_H test			
s/D	L/D	σ	η	s/D	L/D	σ	η
4	17.5	0.3	85.0475	4	17.5	0.3	66.1708
5	17.5	0.3	94.49	5	17.5	0.3	71.4058
6	17.5	0.3	84.0025	6	17.5	0.3	65.1733
4	8.93	0.3	84.0742	4	8.93	0.3	56.0075
5	8.93	0.3	93.5167	5	8.93	0.3	61.2425
6	8.93	0.3	83.0292	6	8.93	0.3	55.01
4	17.5	0.6	74.2842	4	17.5	0.6	62.1875
5	17.5	0.6	83.7267	5	17.5	0.6	67.4225
6	17.5	0.6	73.2392	6	17.5	0.6	61.19
4	8.93	0.6	87.8142	4	8.93	0.6	63.1742
5	8.93	0.6	97.2567	5	8.93	0.6	68.4092
6	8.93	0.6	86.7692	6	8.93	0.6	62.1767

6.7.2. Square Pile Group (2x2)

6.7.2.1. Square Pile Group (2x2) in σ_V test

The efficiency of 2x2 pile group was evaluated for σ_V test condition for various pile spacing, L/D and cell pressure. The variation of efficiency with pile spacing for 2x2 pile group is shown in Fig. 6.6.

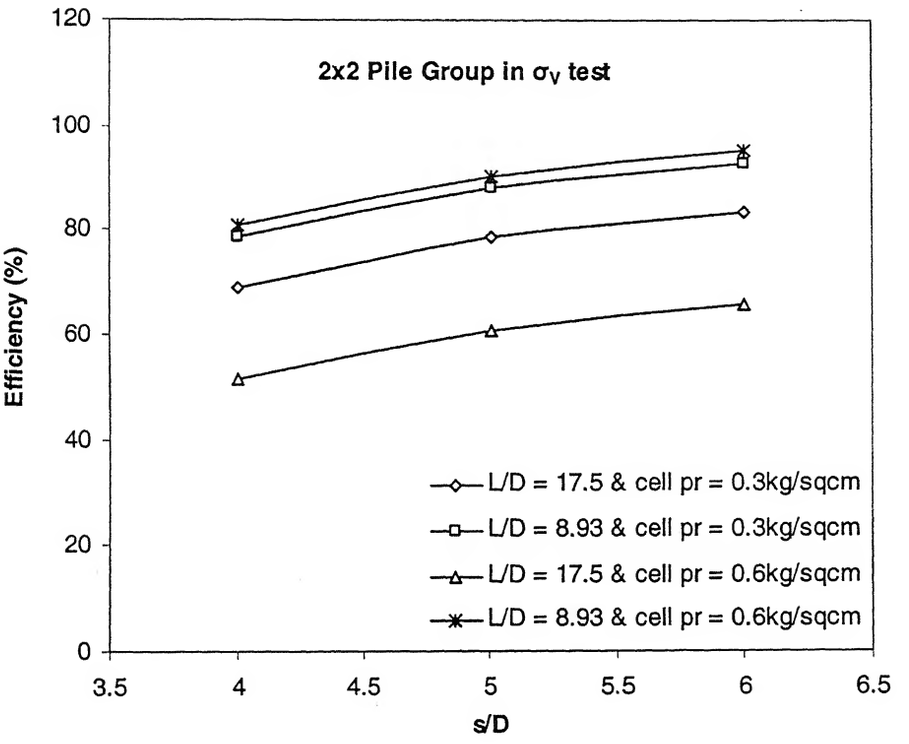

Fig. 6.8. Spacing vs. efficiency for 2x2 pile group in σ_V test

It is observed from the plot that for 2x2 pile group in σ_V test the efficiency increases with increase in pile spacing. For L/D of 8.93, the efficiency increases with increase in cell pressure but for L/D of 17.5 it decreases with increase in cell pressure which shows the similar trend as for efficiency for 2x1 pile group in σ_V test.

6.7.2.2. Square Pile Group (2x2) in σ_H test

Here also for 2x2 pile group in σ_H test the group efficiency increases with increase in pile spacing. The values of 2x2 pile group efficiency for both test conditions is shown in Table 6.2.

Table 6.2. Values of efficiency for 2x2 pile group

2x2 Pile Group in σ_V test				2x2 Pile Group in σ_H test			
s/D	L/D	σ	η	s/D	L/D	σ	η
4	17.5	0.3	69.1583	4	17.5	0.3	41.4733
5	17.5	0.3	78.5808	5	17.5	0.3	45.9083
6	17.5	0.3	83.5008	6	17.5	0.3	52.1283
4	8.93	0.3	78.5117	4	8.93	0.3	40.6967
5	8.93	0.3	87.9342	5	8.93	0.3	45.1317
6	8.93	0.3	92.8542	6	8.93	0.3	51.3517
4	17.5	0.6	51.4517	4	17.5	0.6	37.5867
5	17.5	0.6	60.8742	5	17.5	0.6	42.0217
6	17.5	0.6	65.7942	6	17.5	0.6	48.2417
4	8.93	0.6	80.9083	4	8.93	0.6	39.0833
5	8.93	0.6	90.3308	5	8.93	0.6	43.5183
6	8.93	0.6	95.2508	6	8.93	0.6	49.7383

6.8. Prediction of New Interaction Factor (α)

A new interaction factor was proposed with s/D for various L/D and stress level at both horizontal and vertical stress conditions. The interaction factor was calculated on the basis of Eq. 6.5. By the proposed interaction factor it is possible to find out the interaction factor of pile group for any L/D and stress level. Pile stiffness factor (K) for all the cases is 20000 and Poisson's ratio is 0.5.

6.8.1. Interaction Factor for Vertical (σ_V) Stress Condition

The interaction factor vs. pile spacing at L/D of 8.93 with different vertical stress level is shown in Fig. 6.7. The interaction factor decreases with pile spacing from 4D to 5D but its value increases from spacing 5D to 6D.

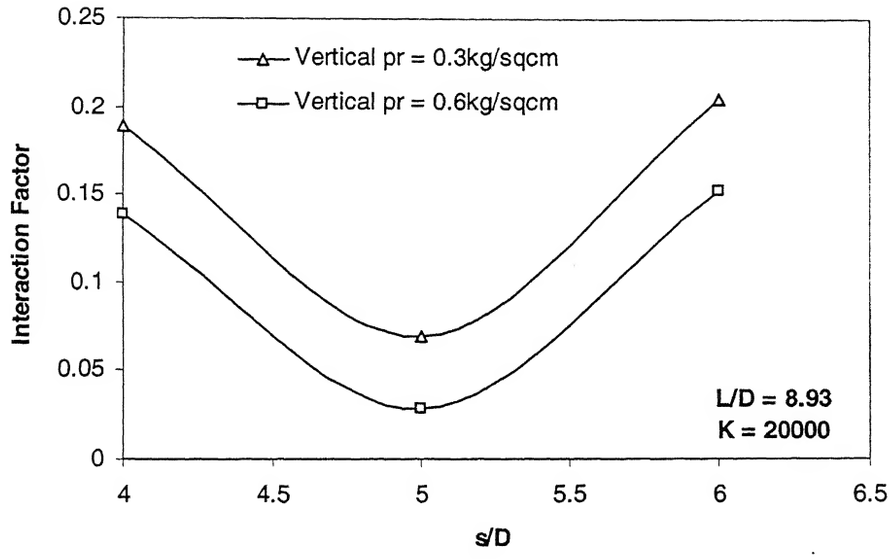

Fig. 6.9. Interaction factor for vertical stress condition, L/D = 8.93

The interaction factor for L/D of 17.5 for different vertical stress condition is shown in Fig. 6.8.

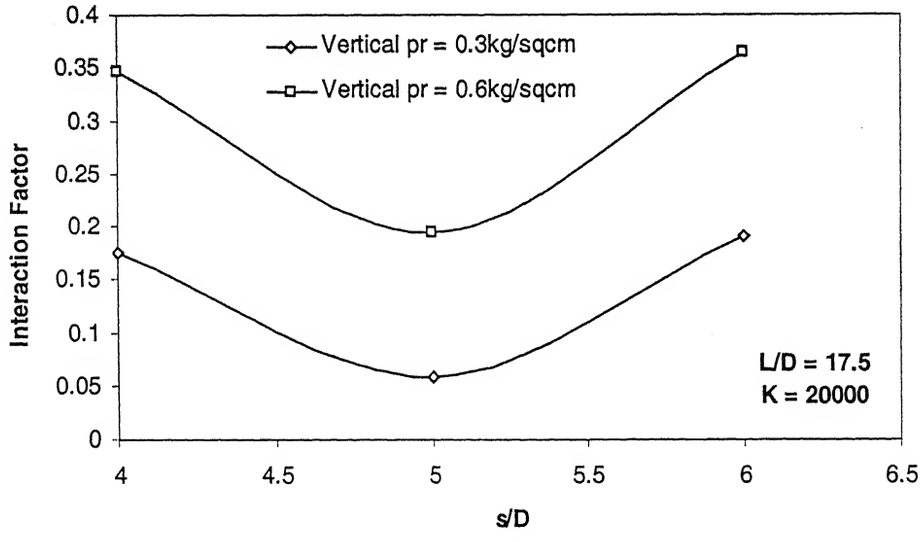

Fig. 6.10. Interaction factor for vertical stress condition, L/D = 17.5

The trend of the α in the present condition contradicts with the proposed interaction factor by Poulos and Mattes (9171). This is because in the present case vertical stress of different level is applied on a soil mass.

6.8.2. Interaction Factor for Horizontal (σ_H) Stress Condition

Interaction factor vs. spacing with different L/D and horizontal stress is also proposed to get the behaviour of pile due to adjacent pile in a group under various horizontal stresses. Here also the interaction factor decreases with pile spacing from 4D to 5D and increases from spacing 5D to 6D. Interaction factor for vertical stress condition for L/D of 8.93 and 17.5 are shown in Fig. 6.9. and Fig. 6.10.

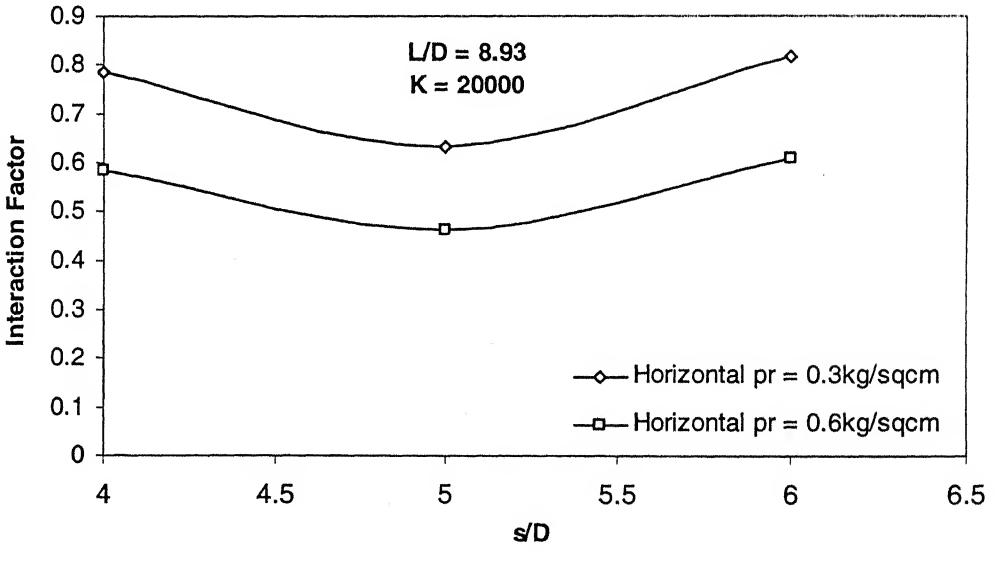

Fig. 6.11. Interaction factor for Horizontal stress condition, L/D = 8.93

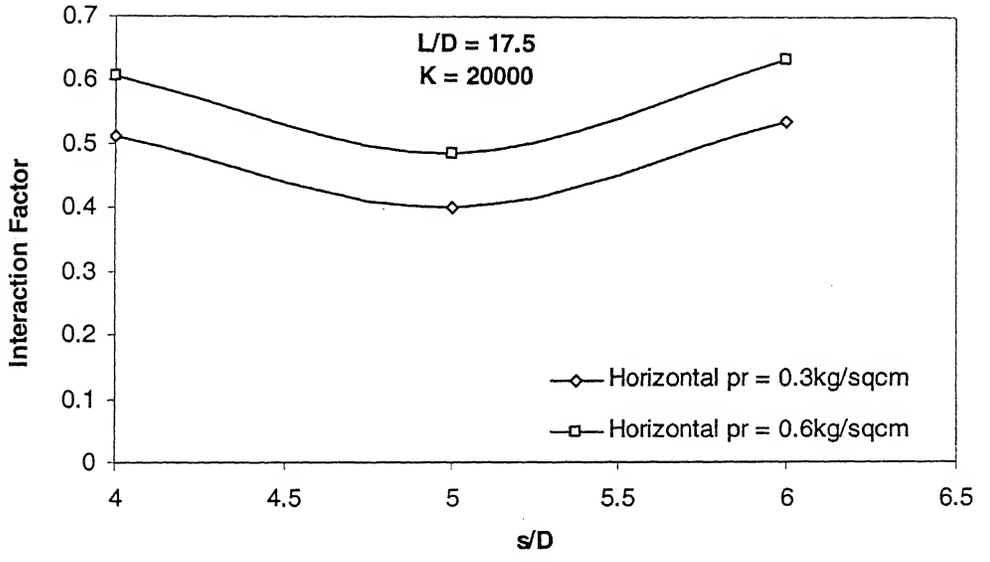

Fig. 6.12. Interaction factor for Horizontal stress condition, L/D = 17.5

Here also the trend of the α in the present condition not matches with the proposed interaction factor by Poulos and Mattes (9171). The reason is that in the present study the horizontal stress of different level is applied on a soil mass.

Chapter - VII

Comparison of DEM and Experimental Results

7.1. General

Discrete Element Method was used in the present study to simulate the present experimental condition and to get the load displacement behaviour of single pile of L/D of 8.93 in clay under various stress condition. The values of total capacity of single pile in σ_V and σ_H test from DEM is not the prime concern as it is a 2-D model and also a very few soil particles are considered here which can not exactly represent the experimental condition. Only the characteristics of the curves, which were determined by DEM, is studied and compared with the experimental curves.

7.2. Load Displacement Characteristics from σ_V Tests

7.2.1. σ_V Tests at Cell pressure of 0.3 kg/cm^2

A normalized load vs. displacement curves were plotted for both DEM and experiment to show the behaviour and trend of the curves for single pile in σ_V test in terms of tip resistance and shaft resistance. The normalized plot for tip resistance and shaft resistance is shown in Fig. 7.1 and Fig. 7.2. It is observed from the plot that experimental results exhibit a definite peak for both tip and shaft resistance. The curves from DEM have a steady increasing trend with displacement for tip resistance but in case of shaft resistance it shows a definite peak. The DEM and experimental curves show a similar trend at displacement of 25% of pile diameter for both tip and shaft resistance.

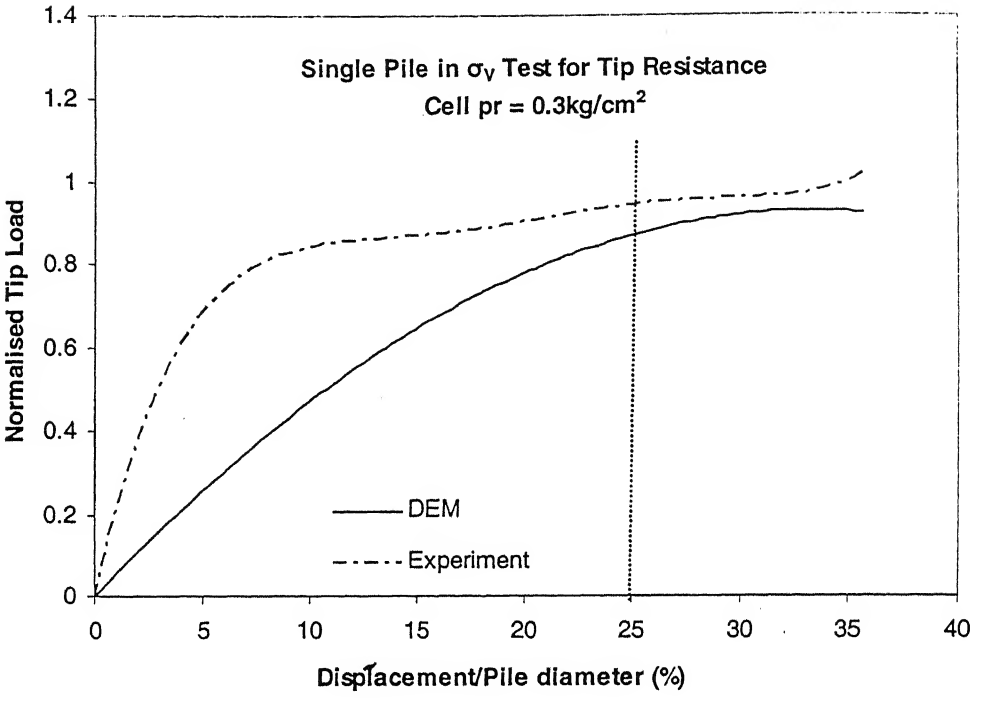

Fig. 7.1. Comparison plot of Tip Resistance (σ_V test, cell pr = 0.3kg/cm^2)

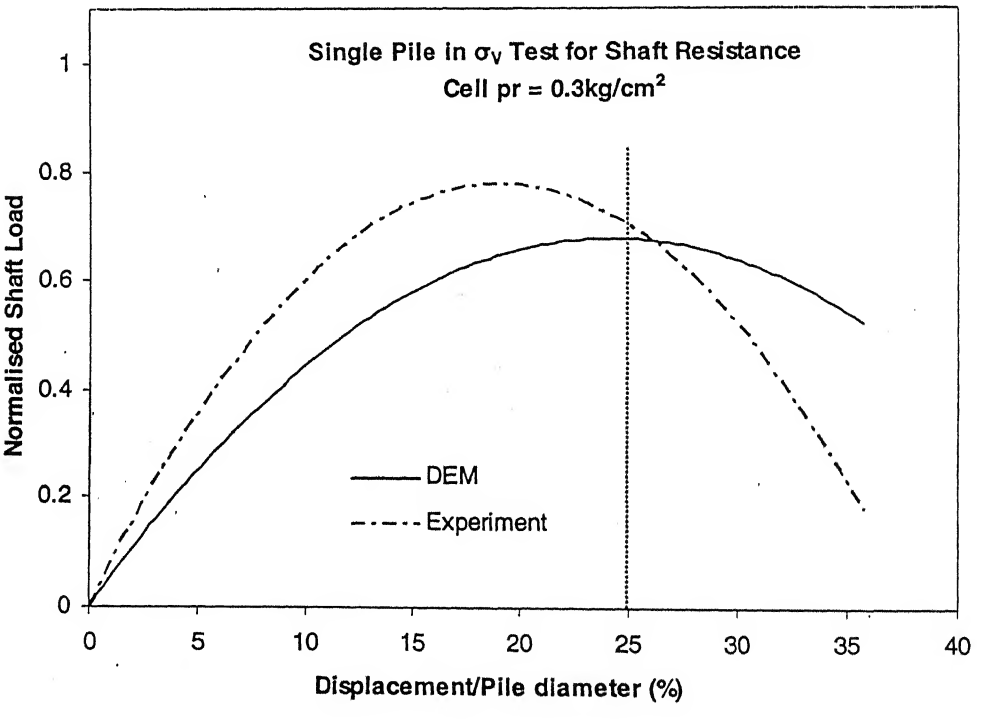

Fig. 7.2. Comparison plot of Shaft Resistance (σ_V test, cell pr = 0.3kg/cm^2)

7.2.2. σ_V Tests at Cell pressure of 0.6kg/cm^2

Similar normalized load displacement plot for tip and shaft resistance in σ_V test at cell pressure of 0.6kg/cm^2 is shown in Fig. 7.3 and Fig. 7.4 respectively.

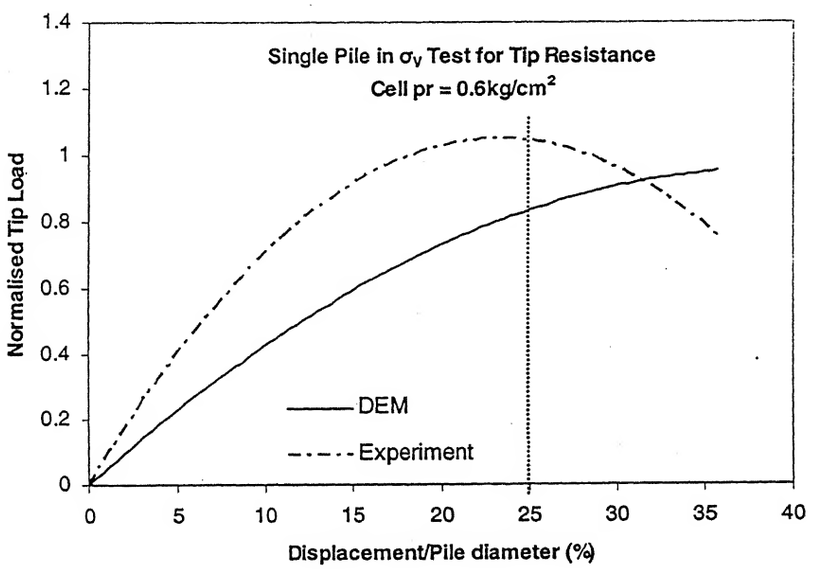

Fig. 7.3. Comparison plot of Tip Resistance (σ_V test, cell pr = 0.6kg/cm^2)

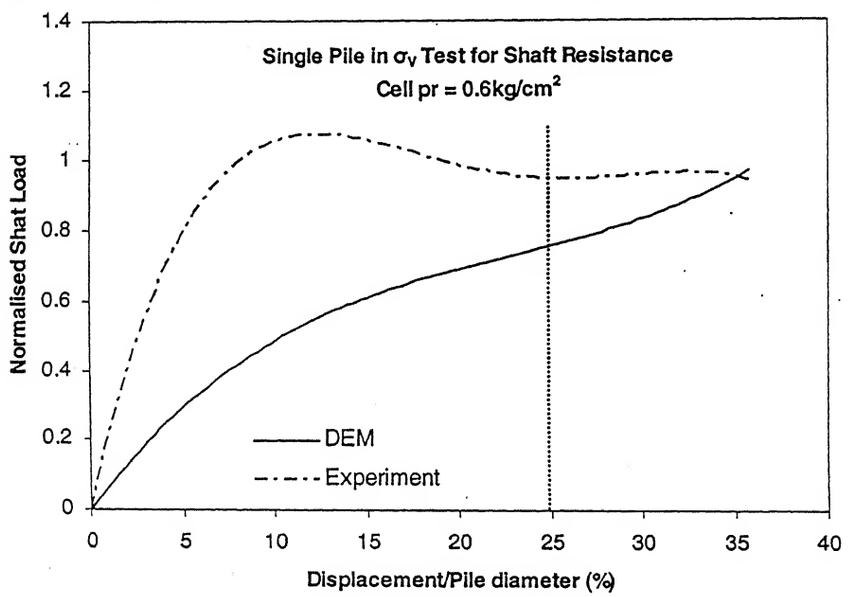

Fig. 7.4. Comparison plot of Shaft Resistance (σ_V test, cell pr = 0.6kg/cm^2)

For both tip and shaft resistance curves from experiment shows a definite peak but curves from DEM shows an increasing trend with displacement. For both case the rate of increase of normalized load is more for experimental curves than the curves from DEM. Here also after displacement of 25% of pile diameter DEM and experimental results follow the same trend.

7.3. Load Displacement Characteristics from σ_H Tests

7.3.1. σ_H Tests at Cell pressure of 0.3kg/cm^2

Normalized load displacement curves for tip and shaft resistance were plotted for single pile in σ_H test at cell pressure of 0.3kg/cm^2 and it is shown in Fig. 7.5 and Fig. 7.6.

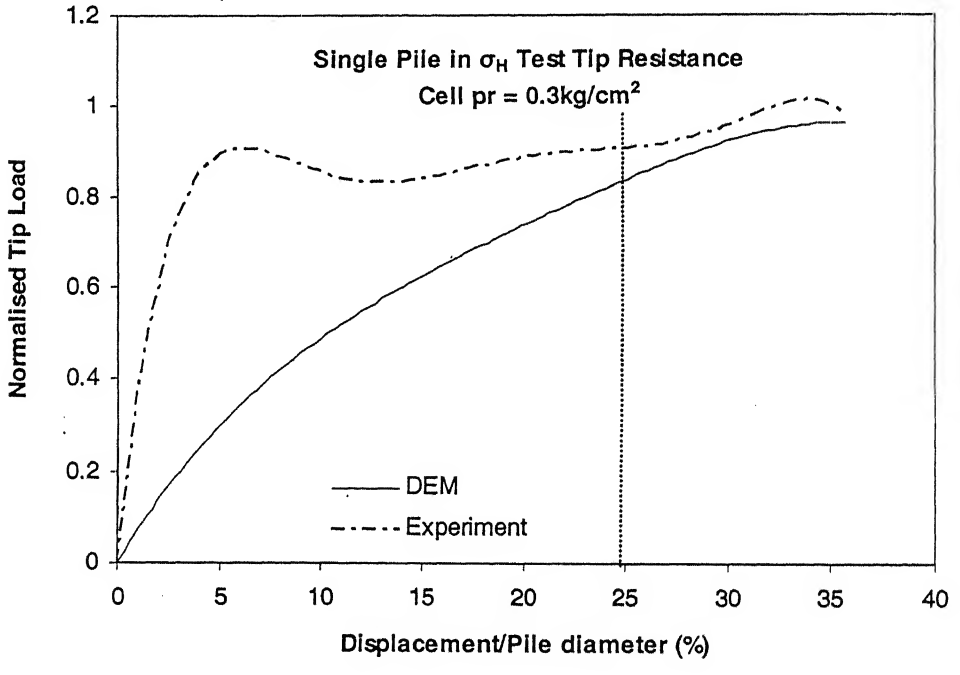

Fig. 7.5. Comparison plot of Tip Resistance (σ_H test, cell pr = 0.3kg/cm^2)

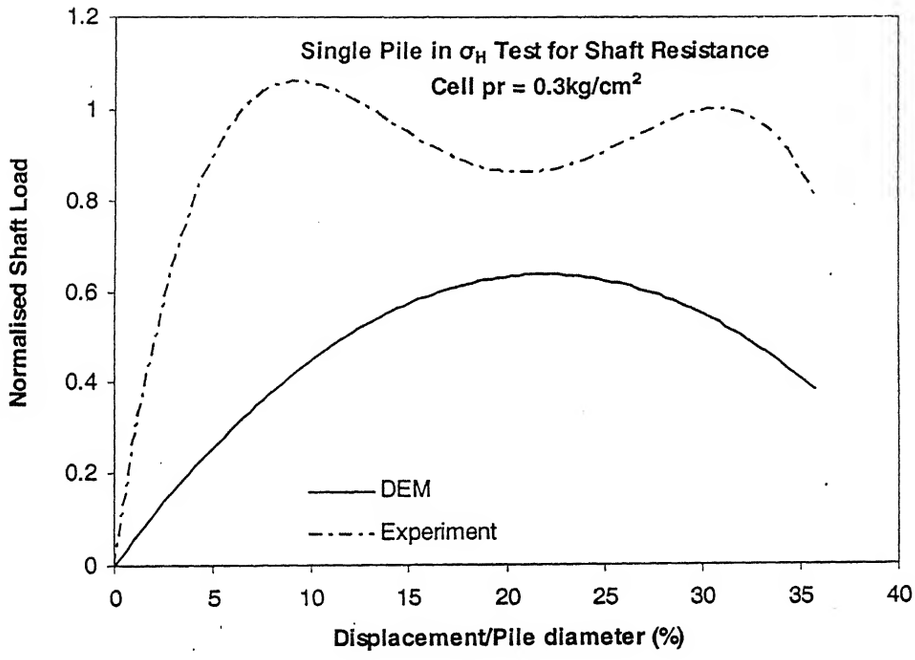

Fig. 7.6. Comparison plot of Shaft Resistance (σ_H test, cell pr = 0.3kg/cm^2)

From the above plot it is observed that the curves from experiment have a peak at displacement of 4 to 5% of pile diameter and after that it becomes almost constant. The curve from DEM has no peak for tip resistance but there is a definite peak for shaft resistance at displacement of 23% of pile diameter. Also the rate of increase is more for experimental curves than curves from DEM. Here for tip resistance both DEM and experimental results shows the similar trend after displacement of 25% of pile diameter.

7.3.2. σ_H Tests at Cell pressure of 0.6kg/cm^2

Normalized load displacement curves for tip and shaft resistance were plotted for single pile in σ_H test at cell pressure of 0.6kg/cm^2 and it is shown in Fig. 7.7 and Fig. 7.8.

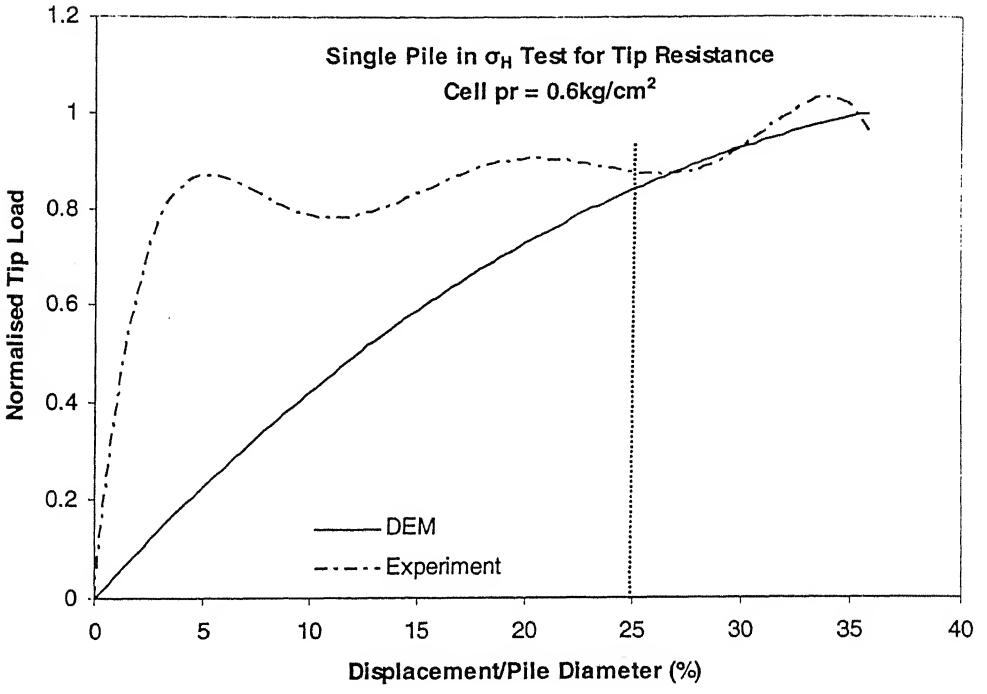

Fig. 7.7. Comparison plot of Tip Resistance (σ_H test, cell pr = 0.6 kg/cm^2)

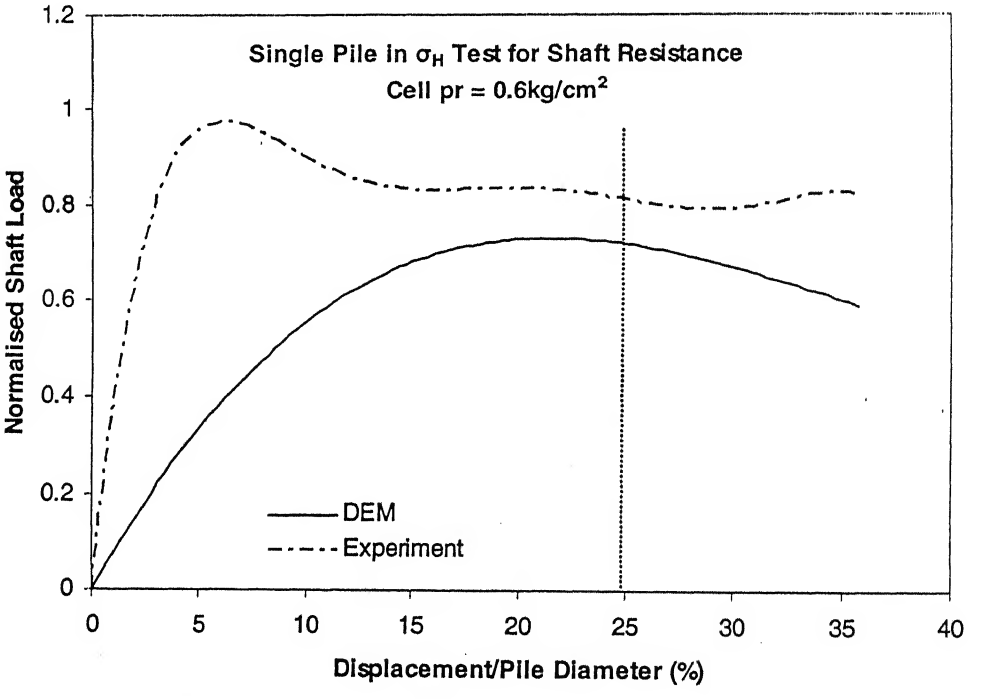

Fig. 7.8. Comparison plot of Shaft Resistance (σ_H test, cell pr = 0.6 kg/cm^2)

The curves in cell pressure of 0.6kg/cm^2 have a similar trend as for cell pressure of 0.3kg/cm^2 in σ_H test.

7.4. Comparison of values obtained from DEM and Experiment

The comparison of the values of total capacity for single pile in both σ_V and σ_H test at both cell pressures is shown in Table 7.1.

Table 7.1. Comparison of values from DEM and Experiment

Methods	Cell Pressure (kg/cm^2)	Vertical Test (σ_V Test)			Horizontal Test (σ_H Test)		
		Tip Resistance q_{pV} (kg)	Shaft Resistance f_{sV} (kg)	Total Resistance q_{tV}(kg)	Tip Resistance q_{pH} (kg)	Shaft Resistance f_{sH} (kg)	Total Resistance q_{tH}(kg)
DEM	0.3	9	6.2	15.2	10.2	5.8	16
	0.6	10	10.5	20.5	11	11.2	22.2
Experiment	0.3	4.4	5	9.4	4.4	7.5	11.9
	0.6	7	11	18	5	8.6	13.6

7.5. Conclusion

Though the load displacement curves of single pile in clay by DEM did not match exactly, the trend in the variation of load versus displacement are quite similar (monotonically increasing). The simulated response with respect to the load displacement curve shows a linear behavior followed by a nonlinear behavior. In all the DEM simulations the tip resistance did not show any peak value in other words the load continued to increase with displacement. However, the DEM and experimental curves show a similar trend at

displacement of 25% of pile diameter for both tip and shaft resistance. The total resistance of single pile as determined by DEM simulation increased with increase in cell pressure under both test conditions namely σ_V test and σ_H test. The total resistance for pile in controlled horizontal stress condition (σ_H test) was more than controlled vertical stress condition (σ_V test) in both sand and clay which almost satisfied the experimental results. Although the simulation results were not spot on, nevertheless it is demonstrated that DEM as a numerical tool hold a lot of promise for direct simulation of cohesive and cohesionless soils.

Chapter VIII

Conclusions

8.1. General

The present experimental study and proposed analysis by Discrete Element Method and a Regression method on behaviour of model piles and pile group under compressive load at different stress condition lead to the following concluding remarks.

8.2. Conclusions from Experimental Results

1. The bearing capacity factor (N_c) value increases with increasing L/D ratio from about 9 upto a maximum of about 11. The adhesion factor (β) increases with increase in horizontal stress level and its value varies from 0.5 to 1.0.

2. The mobilization of total resistance occurs at a pile movement of 4 to 10% of pile diameter for both cell pressure and stress conditions in Marine clay.

3. Total resistance of pile group reaches its ultimate value at a displacement of 4 to 10% of pile diameter at a cell pressure of 0.3kg/cm^2 and 7 to 12% of pile diameter at cell pressure of 0.6kg/cm^2 in both vertical and horizontal stress conditions in Marine clay.

3. The total resistance of 2x1 pile group increases with increases in spacing from 4D to 5D and decreases from 5D to 6D for both L/D and stress conditions.

4. For 2x2 pile group the total resistance increases with increase in pile spacing for both L/D and stress conditions in Marine clay.

5. For single pile, the total resistances from σ_H test are always greater than the values from σ_V test

6. At cell pressure of 0.3kg/cm^2 and L/D= 8.93, the total resistances from σ_V tests are always greater than the values from σ_H tests for all group piles. For L/D = 17.5, the total resistance from σ_H tests is greater than values from σ_V tests for 2x1 pile groups. However reverse trend is observed for 2 x 2 pile groups.

7. At cell pressure of 0.6 kg/ cm^2, the total resistances from σ_H tests are always greater than that obtained from σ_V tests for all pile groups and L/D ratios.

8.3. Conclusions from DEM analysis

1. At the time of installation the magnitude of force induced in y direction at pile walls in clay was greater than sand. The magnitude of side wall force in clay was very large as compared to sand due to the adhesion property of clay. But the force induced in the x direction at pile walls in clay was smaller than in sand.

2. In the relaxation period the rate of load released in y direction at bottom wall for sand was more than clay. For sand the rate of releasing load was 154.94kg/sec but in case of clay this rate was 94.61kg/sec for bottom wall. But for side walls the load releasing in y direction at side walls was more in clay than sand. The average rate of load released at side walls in clay was 30kg/sec whereas in case of sand it was 5.9kg/sec.

3. The tip resistance for sand was more than clay for all cases but the difference between those values was very small. But in case of shaft resistance the values were greater for clay than sand.

4. The total resistance for pile in controlled horizontal stress condition (σ_H test) was more than controlled vertical stress condition (σ_V test) in both sand and clay which almost satisfied the experimental results.

8.4. Conclusions from Regression Analysis

1. The efficiency based on proposed formula by regression analysis for 2x1 pile group increases with increase in spacing from spacing 4D to 5D but it decreases from spacing 5D to 6D for both L/D and stress condition. It may be concluded that for a given length and number of piles in a group, there was a critical value of spacing at which pile and soil inside the piles acts as a one unit; i.e. group action occurs. Hence 5D is the critical spacing up to which group action occurs.

2. It is concluded by the proposed formula for 2x2 pile group, the efficiency increases with increasing pile spacing from 4D to 6D for both L/D and vertical and horizontal stress condition. It may be concluded that group action may occur from spacing 4D to 6D for 2 x 2 pile groups.

3. The value of new proposed interaction factor decreases as s/D increases from 4D to 5D and it increases from 5D to 6D. The trend of the new interaction factor (α) is different from the proposed interaction factor by Poulos and Mattes (9171) due to the vertical and horizontal stress on a clay sample.

8.5. Scope for Further Investigation

Though it was tried to include most of the variables affecting the compressive behaviour of piles and pile groups, even there is lots of more considerations to be taken into account in the present analysis. The present analysis can be modified by taking into account those factors. The scopes of the future works are as follows:

1. In the experiment, the higher value of cell pressure can be taken to get clearer picture of behaviour of pile and pile group under high stress condition in Marine clay.

2. Configuration of pile group can be changed and can used 3x3, 4x4 etc. to get behaviour of those pile group in Marine clay.
3. Spacing of pile may be taken more to understand the behaviour of pile group at different spacing and by those relation one can predict the interaction factor for a lot of spacing in different stressed conditions.
4. Same experiment can be performed in sand to determine the behaviour of pile and pile groups under different stress condition.
5. Only mild steel piles are used in experimental program, concrete piles and timber piles may be tested to account the effect of pile material. Piles of different roughness will lead to differentiate the behaviour response under compression for smooth and rough piles.
6. Suggested DEM analysis can be extended to 3-D analysis for group pile for both sand and clay.

References

1. Anandarajah, A. (1994). "Discrete-element method for simulating behavior of cohesive soil." *Journal of Geotechnical Engineering*, Vol. 120, No. 9, September 1994, pp. 1593-1613.
2. Anandarajah, A. and Yao, M (2003). "Three-dimensional discrete element method of analysis of clays" Journal of Engineering Mechanics, Vol. 129, No. 6, June, pp. 585-596.
3. Asmar, B.N., Langston, P.A., Matchett, A.J., Walters, J.K. (2002). "Validation tests on a discrete element model of vibrating cohesive particle systems" Computers and Chemical Engineering, Vol. 26, pp. 785-802.
4. Azzouz, A.S. and Lutz, D.G. (1986). "Shaft behaviour of a model pile in plastic empire clays." *Journal of the Geotechnical Engineering,* Vol. 112, No.6, April, pp. 389-406.
5. Bengtsson, P.E. (1983). Floating pile in soft, highly plastic clays. *Canadian Geotechnical Journal*, Vol-20, pp-159-168.
6. Bjerrum,L. (1973), "Problems of Soil Mechanics and Construction on Soft Clay", 8th International Conference on Soil Mechanics and Foundation Engineering, Moscow, Vol. 3, pp. 111-159.
7. Blanchet, R. et al (1980). Behaviour of friction piles in soft sensitive clays. *Canadian Geotechnical Journal*, Vol-17, pp-203-224.
8. Bndraratna, A.S. Balasubramanium, P.Phamvan (1992). Development of negative skin friction on driven pile in soft Bangkok clay. *Canadian Geotechnical Journal*, Vol-29, pp-393-404.
9. Bolin, H.W. (1941), "The Pile Efficiency Formula of the Uniform Building Code", Building Standard Monthly, 1, pp. 4-5.

10. Briaud, J.L., and Garland.E., "Loading Rate Method for Pile Response in Clay', Journal of Geotechnical Engineering Division, ASCE, Vol. 111, No. 3, March, 1985, pp. 319-335.

11. Butterfield, R. and Ghosh, N. (1977). The response of single piles in clay to axial load, Proc. 9th ICSMFE, 1, 451-457, Tokyo.

12. Chang, C.S. and Chao, S.J. (1991). "Discrete element method for bearing capacity analysis." Computers and Geotechnics, Vol. 12, Issue. 4. pp. 273-288.

13. Chow, Y.K. (1985). "Torsional Response of Piles in Nonhomogeneous Soil." *Journal of Geotechnical Engineering*, Vol. 111, No. 7, July 1985, pp. 942-947.

14. Chow, Y.K. and Thevendran, V. (1987). "Optimisation of pile groups" Computers and Geotechnique, Vol. 4, Issue. 1, pp. 43-58.

15. Coyle, H.M. and Reese, L.C. (1966). Load transfer for axially loaded piles in clay, ASCE, *Journal of Soil Mechanics & Foundations Division.* SM 2, 1-26.

16. Coyle, H.M. and Sulaiman, I.H. (1967) Skin friction for steel piles in sand. *Journal of Soil Mechanics & Foundations Division,* ASCE, (93), 6, 261-278.

17. Dayal, U. and John H.Allen (1975). The effect of penetration rate on the strength of remoulded clay and sand samples. *Canadian Geotechnical Journal*, Vol-12, pp-336-348.

18. Feld, J. (1943). "Discussion on friction pile foundation", Trans., ASCE, 108, pp. 143-144.

19. Fellenius, B.H., Samson, L. and Bozozuk, M (1978), "Soil disturbance from pile driving in sensitive clay." *Canadian Geotechnical Journal*, Vol. 15, pp. 346-361.

20. Flaate, K. and Selnes, P. (1977). Side friction of piles clay, Proc. 9th ICSMFE, Tokyo,1, 517-522.

21. Fortina, J., Hjiajb, M., Saxce, G. D. (2002). "An improved discrete element method based on a variational formulation of the friction contact law." Computers and Geotechnique, Vol. 29, pp. 609-640.

22. Groger,T., Tuzun, U. and Heyes, D.M. (2003). "Modelling and measuring of cohesion in wet granular materials" Powder Technology, Vol. 133, pp. 203-215.

23. Hakuno, M., Uemura, D. and Yamamoto, T. (1989). "A DEM simulation of under ground structures" Proc. of 1st US conf. on DEM, Golden, CO, US.

24. Hoit, M.I., McVay, M., Hays, C. and Andrade, P.W. (1996). "Nonlinear pile foundation analysis usinf Florida-Pier." Journal of Bridge Engineering, Vol. 1, No. 4, pp. 135-142.

25. Janbu, N. (1976), "Static Bearing Capacity of Friction Piles", Proceedings of the European Conference on Soil Mechanics and Foundation Engineering, Vol. 1.2, pp. 479-488.

26. Jensen, R.P., Edil, T.B., Bosscher, P.J., Plesha, M.E. and Kahla, N.B. (2001). "Effect of particle shape on interface behaviour of DEM-simulated granular materials." The International Journal of Geomechanics, Vol. 1, No. 1, pp. 1-19.

27. Kerisel, J. (1965). Vertical and horizontal bearing capacity of deep foundations in clay. Symp. on bearing capacity and settlement of foundations. Duke University, pp. 45-52.

28. Kraft, L.M., Amerasinghe, S.F. and Focht, J.A (1981). Friction Capacity of Piles Driven into Clay. ASCE, *Journal of the Geotechnical Engineering Division*, Vol. 107, No. 11, November 1981, pp. 1521-1541.

29. Madhav, M.R. and Avirudhan, I.V. (1982). "Measurement and estimation of shaft resistance of piles" M.Tech. thesis, IIT Kanpur, Civil Engineering Dept. India.

30. Madhav, M.R. and Budkowska, B.B. (1986), "Analysis of efficiency of axially loaded pile group." Proc. of 2nd International Symposium on Numerical Models in Geomechanics, pp. 505-510.

31. Madhav, M.R. and Pooroosshasb, H.B. (1985), "Pile group efficiency by the boundary integral method." Communicated to Computers and Geotechnique.

32. Madhav, M.R., Basudhar, P.K. and Kumar, N. (1987). "Prediction of pile group efficiency" M.Tech thesis, IIT Kanpur, Civil Engg Dept. India.

33. Masters, F.M. (1943), "Timber Friction Pile Foundation", Trans., ASCE, 108, pp. 115-173.

34. Mattes, N.S. and Poulos, H.G. (1971), "Model tests on Piles in Clay", Proc. First Australia – New Zealand Conference on Geomechanics, Melbourne. Vol. 1, pp. 254-260.

35. Meyerhof,G.G., (1951), 'The Ultimate Bearing Capacity of Foundations", Geotechnique, London, 2.4, pp. 301-322.

36. Meyerhof,G.G., (1976) " Bearing capacity and Settlement of Pile Foundation". Journal of Geotechnical Engineering Division, ASCE, Vol. 102, No. GT3, 1976, pp. 197-228.

37. Mishra, B.K. (1995). "Study of media mechanics in tumbling mills." Ph.D. thesis. Department of Metallurgical Engineering, Univ. of Utah.

38. Mochtar, I.B. and Edil, T.B. (1988). Shaft resistance of model pile in clay. ASCE, *Journal of Geotechnical Engineering,* Vol. 114, No. 11, 1227-1244.

39. Onate, E. and Rojek, J. (2004). "Combination of discrete element and finite element methods for dynamic analysis of geomechanics problems." Computer Methods in Applied Mechanics and Engineering, Vol. 193, pp. 3087-3128.

40. Poulos, H.G. (1968). "Analysis of the settlements of pile group." Geotechnique, 18, pp. 449-471.

41. Poulos, H.G. (1988). "Modified calculation of pile group settlement interaction." Journal of Geotechnical Engineering, Vol. 114, No. 6, pp. 697-706.

42. Poulos, H.G. and Davis, E.H. (1980), "Pile foundation analysis and design", Wiley, New York, pp. 30-35.

43. Poulos, H.G. and Mattes, N.S. (1969). "The behaviour of axially loaded end bearing piles." Geotechnique, Vol. 19, pp. 285-300.

44. Poulos, H.G. and Mattes, N.S. (1971). "Settlement and load distribution analysis of pile groups." Australian Geomechanics Journal, G1 (1), pp. 18-28.

45. Poulos, H.G., and Davis, E.H. (1968). "The settlement behaviour of single axially loaded incompressible piles and piers." Geotechnique, 18, pp. 351-371.

46. Radhakrishnan, R. et al (1991). Performance of precast driven pile in Marine clay. *Journal of the Geotechnical Engineering Division*, Vol. 117, No. 4, April,1991, pp-637-657.

47. Rajamani, R.K., Mishra, B.K., Songfack, P., Venugopal, R., (1999). "MILLSOFT – a simulation software for tumbling mill design and troubleshooting." Min. Engg., Dec., 41-47.

48. Rao, K.S.S. and Venkatesh, K.H. (1988). A direct assessment of pile-soil interaction coefficients in buried piles. 1st Int. Geotech. Seminer on Deep foundation on bored and auger piles, Belgium, pp-401-407.

49. Rao, K.S.S. and Venkatesh, K.H. (2003). Laboratory investigations on the bearing capacity of buried piles in clay. IGC-2003, 'Geotechnical Engineering for Infrastructural Development'. Roorkee, pp-125-128.

50. Roy, M., Blanchat, R., Tavenas, F. (1981). Behaviour of sensitive clay during driving. *Canadian Geotechnical Journal*, Vol-18, pp-67-85.

51. Sayed, S.M. and Bakeer, R.M. (1992). "Efficiency formula for pile groups." Journal of Geotechnical Engineering, Vol. 118, No. 2, pp. 278-299.

52. Scott, R.F. and Craig, M.J.K (1980). "Computer Modeling of Clay Structure and Mechanics" *Journal of the Geotechnical Engineering Division*, Vol. 106, No. 1, January 1980, pp. 17-33.

53. Seiler, J.F. and Keeney, W.D. (1944), "The efficiency of piles in groups", Wood Preserving News, Vol. 22, No. 11, pp. 109-118.

54. Tang, T.N. (2004). "Triaxial test simulations with discrete element method and hydrostatic boundaries" Journal of Engineering Mechanics, Vol. 130, No. 10, pp. 1188- 1194.

55. Terzaghi, K. and Peck, R.B. (1948), "Soil Mechanics in Engineering Practice", Wiley, New York, pp. 468.

56. Ting, J.M., Corkum, B.T., Kauffman, C.R. and Greco, C. (1989), "Discrete numerical models for soil mechanics." *Journal of the Geotechnical Engineering*, Vol. 115, No. 3, March, pp. 379-398.

57. Ting, J.M. and Corkum, B.T. (1992). "Computational Laboratory for Discrete Element Geomechanics." *Journal of Computing in Civil Engineering*, Vol. 6, No. 2, April 1992, pp. 129-146.

58. Tomlinson, M.J.(1957), The adhesion of piles driven in clay soils, Proc. 4th ICSMFE, 2, 66-71, London.

59. Vijayvergiya, V.N., and Focht, Jr.,J.A., (1972), "A New Way to Predict the Capacity of Piles in Clay", Proceedings, IVth Annual OTC, Houston, Texas, Vol. 2, pp. 865-874.

60. Whitaker,T. and Cooke,R.W., (1965), "Bored Piles with Enlarged Base in London Clay", Proc. 6th International Conference on Soil Mechanics and Foundation Engineering., Vol. 2, pp. 342-346.

61. Whitaker,T. and Cooke,R.W., (1966), "An Investigation of the shaft and base resistance of Large Bored Piles in London Clay", Proc. Symp. Large Bored Piles, ICE, London, pp. 7-49.

62. Williams, G.M.J., and Coleman, R.B., (1965), "The Design of Piles and Cylinder Foundations in Stiff Fissured Clay", Proc. of 6th International Conference on Soil Mechanics and Foundation Engg. Montreal, Vol. 2, Division. (3-6), pp. 347-351.

63. Woodward, R.J., Lundgren, R., and Boitano, J.D. (1961), Pile loading tests in stiff clays, Proc. 5th ICSMFE, 177-184, Paris.

64. Zeewaert,L., (1960), "Reduction of Point Bearing Capacity of Piles because of Negative Friction", Panamerican Conference on SMFE, Mexico, Proceedings, Vol. 3, pp. 1145-1152.